The Metamorphosis of Mosquito Immune and Circulatory Physiology: Comparative Analyses in Larval and Adult *Anopheles gambiae*

By

Garrett Philip League

Dissertation
Submitted to the Faculty of the
Graduate School of Vanderbilt University
in partial fulfillment of the requirements
for the degree of

DOCTOR OF PHILOSOPHY
in

Biological Sciences
May, 2017
Nashville, Tennessee

Approved:

Julián F. Hillyer, Ph.D.

Kenneth C. Catania, Ph.D.

Laurence J. Zwiebel, Ph.D.

Antonis Rokas, Ph.D.

Andrea Page-McCaw, Ph.D.

Dedicated to Jesus Christ, the creator and sustainer of all life (Colossians 1:16-18). “For ‘in him we live and move and have our being’” (The Apostle Paul, quoting from Epimenides of Crete in Acts 17:28). *Soli Deo Gloria!*

ACKNOWLEDGEMENTS

I would like to acknowledge my advisor Dr. Julián Hillyer, who has served as a thoughtful and accessible guide throughout my time in graduate school. I have learned much from his sound advice and attention to detail and I am deeply thankful for his patient mentorship. My committee members, including Drs. Ken Catania, Larry Zwiebel, Antonis Rokas, and Andrea Page-McCaw, provided helpful feedback in shaping my dissertation research, and I am thankful for their time and input. I thank my all labmates, past and present, especially Leah Sigle, Tania Estévez-Lao, Dr. Lisa Brown, Dr. Lillian Shapiro, Yan Yan, Oge Onuh, Valeria Garcia, and former labmate Dr. Jonas King for their support, both personally and professionally. It has been a joy to work with you. I thank my entire family, especially my parents Scott and Amanda, for their counsel and encouragement throughout the years, as well as for the countless prayers and acts of love too numerous to recall, much less list. I reserve my most heartfelt thanks for my wife Kim for being my closest earthly companion during graduate school. I will always treasure this most special season of our lives together and I know that our greatest discoveries are still to come. Finally, in the words of the patriarch Jacob in Genesis 35:3, I thank "the God who answers me in the day of my distress and has been with me wherever I have gone," to whom I offer this work.

TABLE OF CONTENTS

LIST OF TABLES

LIST OF FIGURES

CHAPTER I

INTRODUCTION

Overview

Insects are one of the most abundant, diverse, and successful classes of organisms on Earth. Within the insects, the Nematocera are an epidemiologically important suborder of Diptera (flies) that includes, among others, black flies, biting midges, and mosquitoes. Mosquitoes are responsible for transmitting a number of intractable human diseases which have historically ranked among the deadliest to ever to plague mankind, including dengue fever, lymphatic filariasis, and malaria. Numerous methods have been employed with varying degrees of success to control mosquito populations and the diseases they transmit, including the removal of mosquito breeding sites, the use of chemical insecticides like DDT, as well as a variety of integrated pest management strategies (Patterson, 2016; Ramirez et al., 2009). However, due to the evolution of insecticide resistance and the spread of invasive species, no single control method has proven to be a panacea. More recently, manipulation of the mosquito host immune response has been proposed as another viable means of pest control (Clayton et al., 2014; Ramirez et al., 2009). As host immune responses are a crucial determinant of pathogen viability and transmission, further investigations into the role of mosquito immunity in determining the outcomes of various host-pathogen interactions are urgently needed.

Equipped with a potent innate immune system, mosquitoes have developed an effective series of conserved immune responses that act in concert to limit infections. Mosquitos acquire pathogens from a number of sources, including the microbe-rich aquatic environments of the

immature stages and the infectious blood meals of the adult stage. Upon entering the mosquito hemocoel (body cavity) either via ingestion and subsequent penetration of the midgut or via breaches in the cuticle, pathogens are met with a wide range of cellular and humoral host immune responses (Hillyer, 2010; Hillyer, 2016). In the dynamic environment of the hemocoel, both pathogens and host-derived immune factors are subject to the forces of the open circulatory system, where hemolymph (insect blood) is propelled by the dorsal vessel, the main hemolymph pumping organ in mosquitoes (Glenn et al., 2010). Indeed, the immune and circulatory systems are so intimately intertwined in the hemocoel that they have become functionally integrated such that immune responses preferentially occur at areas of highest hemolymph flow, so as to maximize immune surveillance and pathogen killing efficiency (King and Hillyer, 2012; Sigle and Hillyer, 2016).

Because mosquitoes are holometabolous insects and undergo dramatic morphological, physiological, and environmental changes during the larval to adult transition, we predicted that their circulatory and immune systems, and hence the nature of their interactions, would differ in important respects between the larval and adult life stages. At the outset of my dissertation work, however, no studies had examined circulation-dependent immunity in larvae and little data existed on the relative strength and composition of larval and adult immune responses. In light of this, the overarching goal of my dissertation research was to compare and contrast circulation-based immunity and overall immune competence in larval and adult mosquitoes to determine the extent to which differing larval and adult selection pressures have led to divergent immune responses between the two life stages.

Regarding circulation-dependent immunity, we hypothesized that key structural and functional differences between the larval and adult circulatory systems would result in functional

integration of the larval circulatory and immune systems that reflected the distinct morphology and physiology of the larval stage. Furthermore, since larvae encounter an abundance of microbes in their aquatic environments and survival through the larval stage is essential for reproduction in the adult life stage, we hypothesized that mosquito larvae have evolved powerful innate immune responses that wane in the adult life stage due to immune senescence and other factors. In sum, in this dissertation I document striking differences between the larval and adult circulatory systems, which have led to stage-specific functional integration of the larval circulatory and immune systems. Furthermore, I also present compelling evidence that mosquito larvae display enhanced antibacterial immunity compared to adults.

Mosquito Life Cycle

As holometabolous insects, mosquitoes undergo a complete metamorphosis, which includes four distinct life stages: the aquatic egg, larva, and pupa stages and the terrestrial adult stage (Fig. 1). After a blood meal, adult female mosquitoes lay their eggs in water, where they hatch and develop through four actively feeding larval instars. Each of the four larval instars is punctuated by a molt, or shedding of the cuticle, the fourth and final of which results in pupation. The pupal stage of mosquitoes is a non-feeding stage where the mosquito begins metamorphosis prior to emergence of the imago, or adult insect. Shortly after eclosion, adult mosquitoes mate, imbibe plant nectar, and, in the case of females from anautogenous mosquito species, seek a blood meal, which is required for egg production. It is during a blood meal that the female is at risk of acquiring blood-borne pathogens, which she can transmit to a second host during a subsequent feeding. After feeding, gravid females seek a suitable oviposition site to lay their eggs so that the life cycle of the subsequent mosquito generation can begin.

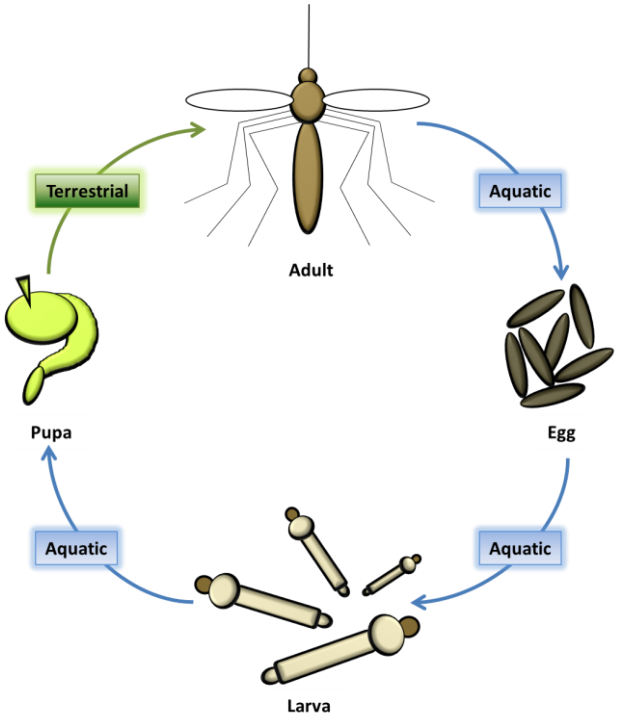

Figure 1. The mosquito life cycle. The mosquito life cycle consists of four general stages that inhabit both aquatic and terrestrial environments. Adult female mosquitoes lay their eggs in water where the eggs hatch and develop through four larval instars. After the fourth instar, larvae pupate and the pupae undergo metamorphosis before emerging from their aquatic habitat as terrestrial adults.

Mosquito Adult Circulatory Physiology

Mosquitoes, like other insects, transport nutrients, wastes, signaling molecules, and immune factors throughout their hemocoel via an open circulatory system, where hemolymph (insect blood) directly bathes the internal tissues and organs. To accomplish the majority of this circulation, adult mosquitoes employ a muscular dorsal vessel, which is a helically coiled tube that runs the length of the insect along the dorsal midline and is subdivided into a thoracic aorta and an abdominal heart (Fig. 2) (Andereck et al., 2010; Glenn et al., 2010). The aorta is a simple, non-contractile tube that conducts hemolymph from the abdomen to the head. By contrast, the heart portion of the dorsal vessel contracts myogenically in a wave-like manner in both the anterograde (toward the head) and retrograde (toward the posterior abdomen) directions. The

heart is also distinguished from the aorta in that it contains incurrent ostia (valves) at the anterior portion of abdominal segments 2-7. During anterograde contraction periods, hemolymph enters the lumen of the dorsal vessel via each of these abdominal ostia and exits the aorta into the head, where it slowly circulates posteriorly. During retrograde contraction periods, however, the abdominal ostia remain closed and hemolymph enters the heart via a single pair of ostia at the thoraco-abdominal junction, exiting the dorsal vessel via a pair of excurrent openings at the posterior terminus of the heart. Although the structure and function of the dorsal vessel has been described in detail in adult mosquitoes, prior to the initiation of my dissertation work little was known regarding the structure and function of the larval circulatory system and how it compared to that of adults. I have addressed this gap in our understanding of the mosquito circulatory system in the comparative larval and adult study presented in Chapter II.

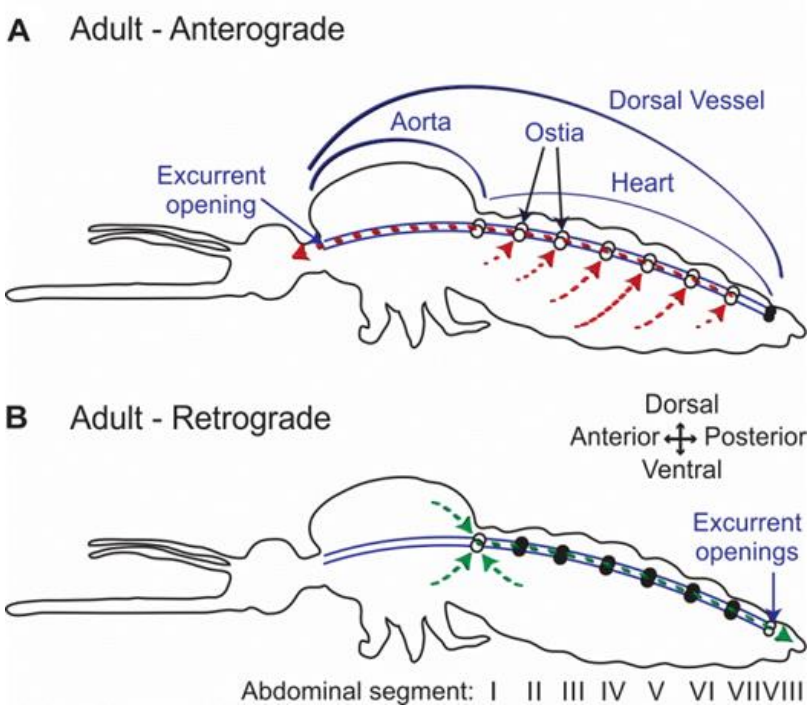

Figure 2. Hemolymph circulation through the dorsal vessel of adult mosquitoes. (A) During periods of anterograde heart contraction, hemolymph enters the heart through 6 paired ostia located at the anterior portions of abdominal segments 2-7 and exits into the head via an anterior excurrent opening of the aorta. (B) During periods of retrograde heart contraction, hemolymph enters a single pair of ostia at the thoraco-abdominal junction and exits into the abdomen via excurrent openings of the posterior terminus of the heart. Figure adapted from (League and Hillyer, 2016).

Mosquito Adult Immunity in the Hemocoel

Mosquitoes, unlike vertebrates, do not have an adaptive immune system, but instead rely on a highly conserved innate immune system to kill pathogens by phagocytosis, lysis, melanization, and other mechanisms (Hillyer, 2016). The mosquito immune system is spatially organized into three major immune compartments, namely, the midgut, the hemocoel, and the salivary glands, as well as conceptually organized into both cellular and humoral immune responses (Hillyer, 2010). Although much research effort has been expended on describing immunity in the midgut (Abraham and Jacobs-Lorena, 2004; Cirimotich et al., 2010; Whitten et al., 2006; Yassine and Osta, 2010), comparatively few studies have been conducted on immunity

in the hemocoel. However, as many pathogens, including *Plasmodium* (the causative agent of malaria), must enter the hemocoel before becoming transmissible to a new host, understanding immunity in the hemocoel is essential to grasping the full picture of the mosquito immune response.

Upon entering the mosquito hemocoel, pathogens are confronted with both cellular and humoral immune factors, which are the two partially overlapping arms of the innate immune system. The cellular immune response consists of the fat body and hemocytes, phagocytic immune cells that represent the first-responders to infection (Hillyer and Strand, 2014). Hemocytes are found as both circulating and sessile (attached to tissues) cells and are categorized into three subpopulations: (1) granulocytes, which are phagocytic cells that make up around 95% of the approximately 1,000-4,000 circulating hemocytes in adults; (2) oenocytoids, which are non-phagocytic phenoloxidase-producing cells; and (3) prohemocytes, which have been suggested to act as pluripotent hemocyte progenitor cells (Strand, 2008) but may simply represent small granulocytes that have recently undergone mitosis (King and Hillyer, 2013). The humoral immune response consists of soluble immune effectors such as phenoloxidase, which is one of the principle enzyme catalysts in melanization, and antimicrobial peptides. Humoral immune responses are initiated upon interaction of host-derived pattern recognition receptors with pathogen-associated molecular patterns, which leads to the activation or repression of extracellular signaling cascades, activation of intracellular signal transduction pathways, which include the Toll, Imd, and JAK-STAT pathways, and the transcription of immunity genes in hemocytes and other tissues.

Mosquito immune responses in the hemocoel are subject to swift hemolymph circulatory currents (Hillyer, 2015; Hillyer, 2016) and because they are so closely linked, the circulatory and

immune systems of adults are functionally integrated and work cooperatively to limit systemic infections (King and Hillyer, 2012; Sigle and Hillyer, 2016). Although other studies have observed immune responses on the heart (Hernández-Martínez et al., 2013; Hillyer et al., 2007; Michel et al., 2005; Schnitger et al., 2007; Yassine et al., 2014; Yassine et al., 2012), neither these studies. nor the studies documenting functional integration in adults, have examined whether these phenomena occur in the larval stage. To address this gap in our knowledge, I examined *Anopheles gambiae* larvae after infection to determine whether immune responses in this life stage are functionally coordinated with their circulatory system, and this study is presented in Chapter III.

Larval Immune Competence Relative to Adults

Anopheles mosquitoes oviposit in small, warm bodies of water that are also natural breeding grounds for bacteria (Laird, 1988), and therefore the risk of bacterial infections must be high during the larval life stage. Because of this, and the fact that mosquitoes must survive the larval stage in order to reproduce, larvae are likely to have evolved more proficient means of neutralizing infections than adults. Although the mosquito adult immune response has been studied in depth, little is known about larval immunity and how larval immune responses compare to those of adults. Differences in the expression patterns of some immunity genes occur across developmental stages (Christophides et al., 2002; Dimopoulos et al., 1997), however no study has functionally described the cellular and humoral antibacterial immune responses of mosquito larvae, let alone placed these responses in the context of adult immunity. If larval and adult immune responses indeed differ in either strength or composition, this would imply that future studies could no longer assume either complete continuity or discontinuity in immune responses across life stages and that metamorphosis has, to some extent, decoupled the larval and

adult immune systems, thus enabling their independent evolution (Moran, 1994). Furthermore, if immune responses differ across life stages, this would have important implications for the creation of stage-specific control measures that are better tailored to the specific immune responses of each life stage.

Because hemocyte numbers decline with adult age (Castillo et al., 2006; Hillyer et al., 2005; King and Hillyer, 2013; Pigeault et al., 2015), increase in response to immune stimuli (Baton et al., 2009; Castillo et al., 2011; Christensen et al., 1989; Coggins et al., 2012; King and Hillyer, 2013), and may also increase in preparation for tissue restructuring during metamorphosis (Castillo et al., 2006; King and Hillyer, 2013), it is likely that mosquito larvae display enhanced antibacterial cellular immune responses compared to adults. Furthermore, as bacteria are also subject to melanization in the hemocoel (Hillyer et al., 2004), and the strength of the melanization response has also been shown to decline with adult age (Christensen et al., 1986; Chun et al., 1995; Cornet et al., 2013; Li et al., 1992), we also expect humoral immunity to be stronger in larvae compared to adults. To test whether *A. gambiae* larvae have a more potent antibacterial immune response compared to differently aged adults, I compared the strength of a range of immune responses between larvae, newly emerged adults and older adults, and present the findings in Chapter IV.

Summary and Preview of Subsequent Chapters

Mosquitoes vector numerous deadly diseases that cause tremendous human suffering worldwide. Understanding how the mosquito circulatory and immune systems work in conjunction to fight pathogens is critical to potentially limiting their transmission to human hosts. Furthermore, because mosquitoes are holometabolous insects, studies of the circulatory and immune systems in adults should be complemented by studies in larvae, as these life stages

differ, yet are inextricably linked to one another. Understanding how larval and adult immunity relate to each other could yield insight into how larval infections prime adults against subsequent infections (Bargielowski and Koella, 2009; Moreno-García et al., 2015), and why larvae tend to evolve resistance to pesticides faster than adults (Koella et al., 2009), as the mechanisms behind both of these phenomena are not fully understood. To being to more fully understand the mosquito larval immune system and how it compares to that of adults, the dissertation work presented in the subsequent chapters describes how the larval and adult circulatory systems are structurally and functionally adapted to meet the unique physiological needs of each life stage, and how these adaptations have led to spatially distinct yet functionally analogous integration of the circulatory and immune systems. Finally, by comparing both cellular and humoral immunity across life stages and adult ages, we show that larvae have more robust immune responses than adults, and that immunity declines with adult age. Taken together, these findings suggest that a holistic approach to the study of mosquito immunity that incorporates both larval and adult life stages yields important insights that could aid in the creation and novel pest and disease control measures.

CHAPTER II

COMPARATIVE STRUCTURAL AND FUNCTIONAL ANALYSIS OF THE LARVAL AND ADULT DORSAL VESSEL AND ITS ROLE IN HEMOLYMPH CIRCULATION IN THE MOSQUITO *ANOPHELES GAMBIAE*

Preface

This chapter provides a detailed comparison of the *Anopheles gambiae* larval and adult circulatory systems and shows that though the heart is structurally similar in both life stages, it differs with respect to both contraction and hemolymph flow dynamics. This work laid the foundation for the study on the coordinated function of the larval circulatory and immune systems presented in Chapter III. I led the experimental effort and conducted the majority of the experiments, and did so by adapting for the larval stage a series of techniques previously applied only to the adult life stage. During the course of this project I mentored Ogechukwu "Oge" Onuh, a School for Science and Math at Vanderbilt high school student, and her contributions during experiments on larval heart contraction and dorsal vessel hemolymph flow rates were incorporated into this chapter. All experiments were designed, analyzed, and written with my advisor, Dr. Julián Hillyer. This chapter is adapted from the final transcript of this work, which was published in the February 1, 2015 issue of *The Journal of Experimental Biology* (volume 218, pages 370-380).

Abstract

Hemolymph circulation in insects is driven primarily by the contractile action of a dorsal vessel, which is divided into an abdominal heart and a thoracic aorta. As holometabolous insects,

mosquitoes undergo striking morphological and physiological changes during metamorphosis. This study presents a comprehensive structural and functional analysis of the larval and adult dorsal vessel in the malaria mosquito *Anopheles gambiae*. Using intravital video imaging we show that, unlike the adult heart, the larval heart contracts exclusively in the anterograde direction and does not undergo heartbeat directional reversals. The larval heart contracts 24% slower than the adult heart, and hemolymph travels across the larval dorsal vessel at a velocity that is 68% slower than what is seen in adults. By fluorescently labeling muscle tissue we show that although the general structure of the heart and its ostia are similar across life stages, the heart-associated alary muscles are significantly less robust in larvae. Furthermore, unlike the adult ostia, which are the entry points for hemolymph into the heart, the larval ostia are almost entirely lacking in incurrent function. Instead, hemolymph enters the larval heart through incurrent openings located at the posterior terminus of the heart. These posterior openings are structurally similar across life stages, but in adults have an opposite, excurrent function. Finally, the larval aorta and heart differ significantly in the arrangement of their cardiomyocytes. In summary, this study provides an in-depth developmental comparison of the circulatory system of larval and adult mosquitoes.

Introduction

Circulation of hemolymph (blood) in the insect open circulatory system is essential for the transport of nutrients, waste, signaling molecules and immune factors throughout the hemocoel (body cavity) (Chapman et al., 2013; Klowden, 2013). Hemolymph circulation is accomplished primarily via the pumping action of a muscular dorsal vessel that lies beneath the dorsal cuticle and runs the length of the body along the dorsal midline. The dorsal vessel consists of two distinct regions: the abdominal heart and the thoracic aorta. The heart is a pulsatile organ

that contains ostia (valves) that allow hemolymph to enter the lumen of the vessel, whereas the aorta serves as a passive conduit for hemolymph propelled into the thorax by the contractile action of the heart.

In adult mosquitoes, intravital imaging has revealed that the heart contracts bidirectionally, propelling hemolymph towards the head (anterograde) and towards the posterior of the abdomen (retrograde) (Andereck et al., 2010; Glenn et al., 2010). During anterograde heart contractions, hemolymph enters the lumen of the dorsal vessel via incurrent ostia located at the anterior portion of abdominal segments 2-7 and exits into the head via an excurrent opening located at the anterior end of the aorta. During retrograde heart contractions, however, hemolymph enters the dorsal vessel via a single pair of ostia located at the thoraco-abdominal junction and exits into the abdominal hemocoel via a pair of excurrent openings located at the posterior terminus of the heart (Glenn et al., 2010).

Studies on heart function and hemolymph flow dynamics in anopheline mosquitoes have yielded important insights into both immunity (King and Hillyer, 2012) and circulation (Andereck et al., 2010; Boppana and Hillyer, 2014; Estévez-Lao et al., 2013; Glenn et al., 2010). However, these studies in *A. gambiae* have focused on the adult life stage without addressing how hemolymph is propelled in the immature stages. As holometabolous insects, mosquitoes undergo dramatic changes en route to adulthood. Mosquitoes lay their eggs in water, where they hatch into larvae, develop through four larval instars, pupate and, finally, emerge into terrestrial environments as airborne adults. Because larvae are adapted to swimming and feeding in aquatic habitats and have yet to undergo the metamorphic changes necessary for flight and reproduction, the larval body plan differs significantly from that of adults. A recent study in the distantly related culicine mosquito, *Aedes aegypti*, compared the ultrastructure of the larval, pupal and

adult heart, and found that the structure and arrangement of the cardiomyocytes is similar across all life stages, with major differences occurring primarily in heart-associated tissues such as the alary muscles (Leódido et al., 2013). However, no mosquito study on the larval stage has coupled structural data on the dorsal vessel with functional data on hemolymph flow. The only study that has ventured into a related area used bright-field light microscopy to compare, at a gross level, larval and adult dorsal vessel structure and heart contractions, but this study did not visualize hemolymph flow or flow mechanics (Jones, 1954).

Although little attention has been given to larval circulation and heart structure in mosquitoes, larval studies in the fellow dipteran *Drosophila melanogaster* have increased our understanding of cardiac function in immature insects while also serving as a model for human cardiac physiology (Babcock et al., 2008; Curtis et al., 1999; Lehmacher et al., 2012; Molina and Cripps, 2001; Piazza and Wessells, 2011; Sláma and Farkas, 2005). Furthermore, as the insect heart and associated tissues are restructured or even destroyed during the pupa to adult transition (King and Hillyer, 2013; Lehmacher et al., 2012; Leódido et al., 2013; Molina and Cripps, 2001; Smits et al., 2000), larval heart structure and circulatory dynamics cannot merely be inferred from observations in adults. Here, we used live imaging techniques to visualize and quantify heart contraction dynamics and hemolymph flow velocity in *A. gambiae* fourth instar larvae and adults. We show that the larval heart contracts exclusively in the anterograde direction, and that heart contraction rates and hemolymph flow velocity are slower in larvae when compared with adults. Furthermore, we present a comprehensive structural comparison of the dorsal vessel in both life stages and highlight differences that may account for the markedly different hemolymph flow patterns observed between larval and adult mosquitoes.

Materials and Methods

Mosquito rearing and maintenance

Anopheles gambiae Giles *sensu stricto* (G3 strain; Diptera: Culicidae) were reared as described (Estévez-Lao et al., 2013). Briefly, eggs were hatched in distilled water and larvae were fed a combination of Koi food and yeast. Upon pupation, mosquitoes were transferred to plastic containers with a marquisette top where adults emerged and were fed a 10% sucrose solution *ad libitum*. All mosquito stages were maintained in an environmental chamber set to 27°C and 75% relative humidity under a 12 h:12 h light:dark photoperiod. All experiments were performed on fourth instar larvae and adult female mosquitoes at 5 days post-eclosion.

Mosquito injection

Larvae were immobilized by removing excess water and were then injected at the mesothorax with either ~0.1 μl PBS (pH 7.0) or 0.008% solids 2 μm diameter red fluorescent (580/605) carboxylate-modified microspheres (Invitrogen, Carlsbad, CA, USA) in PBS. Injured and naïve larvae received a needle wound or no treatment at all, respectively. Larvae were restrained for video recording by placing them in water that was pooled between two stacks of coverslips that were resting on a glass slide (Fig. 1A). This mode of restraint maintains anopheline larvae in their natural horizontal orientation with respect to the water surface. In these experiments, larvae had access to oxygen but in some cases they remained completely submerged during video recording. Thus it is possible that in these cases the restraint method limited the access of larvae to oxygen. However, it is highly unlikely that the restraint method had any effect on the larval heart for two reasons. Firstly, larvae were restrained for only a brief period (~90 s) and their heart rates did not change during the 60 s heart recording. Secondly, anopheline larvae often subject themselves to extensive anoxic conditions due to foraging as well

as their ‘flight’ response, where they swim to the bottom of the larval pool and remain immobile until the perceived threat has disappeared.

Adult mosquitoes were cold-anesthetized prior to injection and restrained dorsal-side up on Sylgard 184 silicone elastomer (Dow Corning Corporation, Midland, MI, USA) plates using a non-invasive method previously described (Fig. 1D) (Andereck et al., 2010; Glenn et al., 2010). After acclimating to room temperature, adults were subjected to the same treatments as the larvae, with injections taking place at the thoracic anepisternal cleft.

Measurement of heart contractions

Immediately after treatment (naïve, injury or injection), 60 s intravital videos of the dorsal abdomen of larvae and adult mosquitoes were recorded under bright-field trans-illumination using a Nikon SMZ1500 stereo microscope (Nikon, Tokyo, Japan) connected to a Hamamatsu ORCA-Flash 2.8 digital CMOS camera (Hamamatsu Photonics, Hamamatsu, Japan) and Nikon Advanced Research NIS-Elements software. Videos were captured at ~20 frames s^{-1} and manually analyzed using NIS-Elements software. Larval heart rates were quantified by visualizing the movement of the dorsal tracheal trunks, a technique previously employed to measure heart rates in *Drosophila* larvae (Dasari and Cooper, 2006). Adult heart rates were quantified by visualizing the direction and frequency of wave-like contractions of cardiac muscle throughout the length of the abdomen (Glenn et al., 2010). Because the heart rate in adult mosquitoes does not differ between anterograde and retrograde contraction periods (Chen and Hillyer, 2013; Estévez-Lao et al., 2013; Glenn et al., 2010; Hillyer et al., 2012), only adult total contraction rates are presented. Four independent trials of 10 individuals per treatment group were conducted. Data were analyzed by two-way ANOVA, using stage and treatment as the variables, followed by Šidák's *post hoc* test.

Graphical representations of individual larval heart contractions were rendered using NIS-Elements software by selecting an area of the heart immediately medial to the longitudinal tracheal trunks and quantifying how the sum light intensity changed as each heart contraction shifted the trachea in and out of the selected area. Graphical representations of individual adult heart contractions were rendered by selecting an area immediately medial to the dorsal diaphragm at the anterior-most region of the abdomen and quantifying changes in sum light intensity as the heart wall moved in and out of the selected area. For visualization ease, all values were multiplied by −1 such that each peak (not valley) signified a contraction.

Measurement of hemolymph flow velocity

Adults and larvae were restrained and injected as described above. For dorsal, intracardiac particle tracking, mosquitoes were injected with ~0.1 µl of 0.008% solids 2 µm diameter red fluorescent microspheres in PBS whereas for ventral, extracardiac particle tracking they were injected with 0.004% solids microspheres. Immediately following injection, adults and larvae were video recorded for 60 s using low-level fluorescence illumination on the SMZ1500 microscope ensemble described above.

Larval videos were acquired through the dorsal and ventral abdomen using either the Hamamatsu ORCA-Flash 2.8 digital CMOS camera or a Photometrics CoolSNAP HQ2 high sensitivity monochrome CCD camera (Roper Scientific, Ottobrunn, Germany) at 20-25 frames s^{-1}. The manual feature of the Object Tracker module of NIS-Elements was used to quantitatively track the trajectory of the neutral density microspheres as they flowed through the dorsal vessel or the ventral hemocoel. Hemolymph flow velocity was calculated from these measurements by dividing the path length of an individually tracked microsphere by the amount of time it was tracked. For each larva assayed, five microspheres were tracked as they travelled

through the heart or through the ventral abdomen. A total of 40 larvae were assayed: 20 were assayed dorsally and 20 were assayed ventrally.

Videos of adult mosquitoes were acquired using the Photometrics CoolSNAP HQ2 camera at 24 frames s^{-1}. A total of 20 adult mosquitoes were assayed, and for each individual 10 microspheres were tracked: five as they travelled in the anterograde direction and five as they travelled in the retrograde direction. All microspheres were tracked for a minimum distance of 500 μm. Particle tracking data were analyzed using the Kruskal-Wallis test, followed Dunn's multiple comparisons *post hoc* test.

Quantification of hemolymph flow into the larval ostia and eighth abdominal segment incurrent opening

Larvae were injected with 0.008% solids 2 μm diameter red fluorescent microspheres in PBS and video recorded for 60 s using low-level fluorescence illumination on the SMZ1500 microscope equipped with the Photometrics CoolSNAP HQ2 camera. The number of fluorescent microspheres entering the dorsal vessel through the incurrent openings of the eighth abdominal segment and the abdominal ostia of segments 2-7 were manually counted. Twenty mosquitoes were assayed and the raw data were analyzed using the Wilcoxon matched pairs test.

Light and fluorescence microscopy of aldehyde-fixed mosquito whole mounts

For fluorescence labeling of larval muscle, whole larvae were first fixed by immersion in 8% formaldehyde (Electron Microscopy Sciences, Hatfield, PA, USA) in PBS for 1 h. The larval thorax and abdomen were then bisected along a coronal plane, cleared of all internal organs, rinsed in PBS, and incubated for 1 h in a solution consisting of 0.3 μmol l^{-1} phalloidin-Alexa Fluor 488 (Invitrogen) and 1% Triton X-100 (Thermo Fisher Scientific, Waltham, MA, USA) in

PBS. After rinsing in PBS, specimens were mounted on glass slides using Aqua-Poly/Mount (Polysciences Inc., Warrington, PA, USA).

For fluorescence labeling of adult muscle, adults were intrathoracically injected with 4% formaldehyde in PBS and allowed to fix for 15 min. Abdomens were bisected along a coronal plane and, after removal of internal organs, placed in 0.5% Tween in PBS for 15 min, rinsed three times briefly in PBS, fixed in 4% formaldehyde for 5 min, and incubated for 1 h in 0.3 μmol l^{-1} phalloidin-Alexa Fluor 488 and 1% Triton in PBS. After rinsing in PBS, adult dorsal abdomens were mounted on a glass slide using Aqua-Poly/Mount. For some adult and larval preparations, cell nuclei were fluorescently labelled by adding Hoechst 33342 (Invitrogen) to the phalloidin-containing solution.

Larval and adult samples were imaged under bright-field and fluorescence illumination using a Nikon 90i compound microscope connected to a Nikon Digital Sight DS-Qi1Mc monochrome digital camera. For the rendering of detailed fluorescence images with extended focal depth, *Z*-stacks of whole mounts were acquired using a linear encoded *Z*-motor and all images in a stack were combined to form a single focused image using the Extended Depth of Focus (EDF) module of NIS-Elements. For three-dimensional rendering, *Z*-stacks were created by acquiring images at 0.5 μm *Z*-intervals for a total *Z*-range of 30 μm. *Z*-stacks were then quantitatively deconvolved using the AQ 3D Blind Deconvolution module of NIS-Elements and rendered using the volume view feature.

Results

The larval and adult heart lie along the dorsal midline, but the larval heart beats exclusively in the anterograde direction

To restrain larvae for video recordings, individuals were placed on a microscope slide in a pool of water between two coverslip stacks (Fig. 1A). Observation of the dorsal abdomen in fourth instar larvae revealed the presence of a dorsal vessel that runs the length of the body and is flanked by dorsal longitudinal tracheal trunks (Fig. 1B). Because of (1) the high visibility of the tracheal trunks under trans-bright-field illumination, (2) their location immediately lateral to either side of the dorsal vessel (which is fairly translucent under bright-field conditions) and (3) their rhythmic movement driven by each dorsal vessel contraction, the dorsal longitudinal tracheal trunks were used as a proxy for monitoring heart contractions. Bright-field intravital video recordings revealed that the larval heart beats at a more or less constant pace and only in the anterograde direction: each contraction originates at the posterior of the abdomen and propagates towards the head in a wave-like fashion (Fig. 1C). Wave-like contractions of the larval heart alternate between periods of systole and diastole to propel hemolymph through the dorsal vessel in a bolus-like fashion. In all the videos recorded during the course of this study, the larval heart was never observed contracting in the retrograde direction.

Visualization of heart contractions in adult mosquitoes was carried out by bright-field trans-illumination of the abdomen using a non-invasive restraint technique described previously (Fig. 1D) (Andereck et al., 2010; Glenn et al., 2010). This method relies on the direct imaging of the heart through the relatively translucent abdominal tergum. Intravital recordings revealed that, as is the case with larvae, the adult heart extends along the dorsal midline of the entire abdomen (Fig. 1E). In contrast to the larval heart, the adult heart undergoes regular heartbeat directional

reversals, beating for longer periods of time in the anterograde direction but switching to the retrograde direction at regular intervals (Fig. 1F). When compared with larvae, the adult heart appears to constrict more narrowly during systole, particularly when contracting in the retrograde direction.

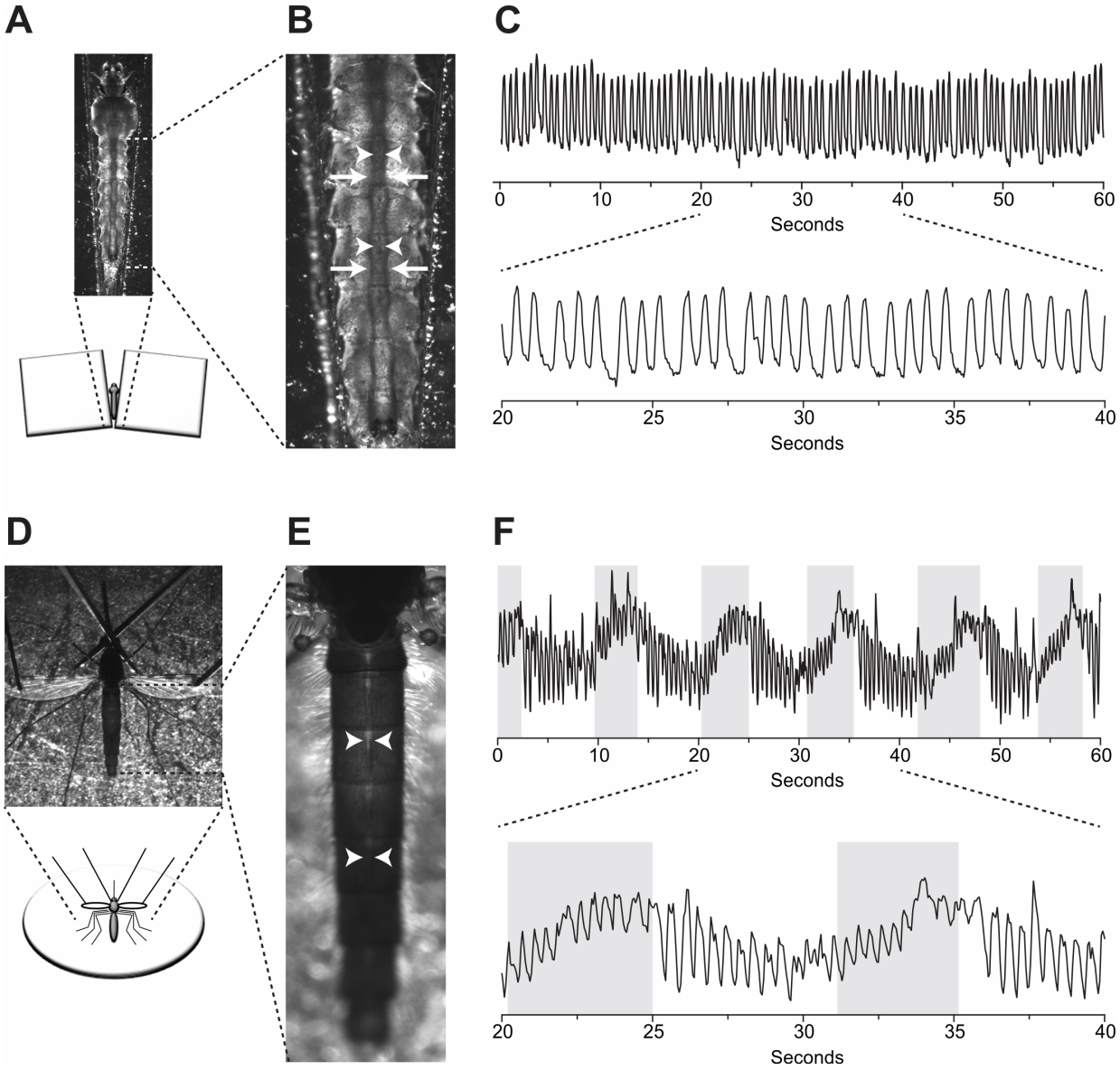

Figure 1. Larval and adult heart contractions in *Anopheles gambiae*. (A) Larval restraint technique for bright-field intravital video recording of heart contractions. Larvae were restrained in water that was pooled between two stacks of coverslips. (B) Bright-field image of the larval abdomen showing that the heart (arrowheads) is located between the dorsal longitudinal tracheal trunks (arrows). (C) Graphical representation of larval heart contractions, where each peak represents a contraction. Contractions from the middle third of the 60 s recording are magnified in the lower graph. All larval contractions propagate in the anterograde direction. (D) Adult restraint technique for bright-field intravital video recording of heart contractions. Adults were cold-anesthetized and pins were placed through non-vascular portions of the wings and over the neck. (E) Bright-field image of the adult abdomen showing the heart (arrowheads). (F) Graphical representation of adult heart contractions, where each peak represents a heart contraction. Contractions from the middle third of the 60 s recording are magnified in the lower graph. Unshaded and shaded areas represent periods of anterograde and retrograde heart contraction, respectively.

The larval heart contracts at a slower rate than the adult heart, but neither is significantly affected by injury or injection

Initial visual observations of larval heart contractions suggested that the resting heart rate of larvae was significantly slower than that of adults. To confirm this, we performed intravital video imaging and measured the larval and adult heart rate in naïve mosquitoes, injured mosquitoes and mosquitoes that had been injected with either phosphate-buffered saline (PBS) or 2 μm diameter microspheres in PBS. Quantification of heart contractions in naïve fourth instar larvae revealed that their heart contracts at an average resting rate of 1.69 Hz compared with 2.21 Hz in adults (Fig. 2). Statistical analysis of the data from all treatment groups confirmed that heart rates differ significantly between the two life stages (Fig. 2; two-way ANOVA, $P<0.0001$). Specifically, the heart rates from each of the four larval groups were significantly lower than the heart rates from the corresponding adult groups (Šidák multiple comparisons test, $P<0.0001$ for all comparisons). Moreover, treatment did not affect larval or adult heart rates (two-way ANOVA, $P=0.6725$), indicating that injury or injection has little or no effect on cardiac physiology. There was also no interaction between the life stage and the treatment, indicating that the life stages were not differentially affected by the injury or injection (two-way ANOVA, $P=0.1029$).

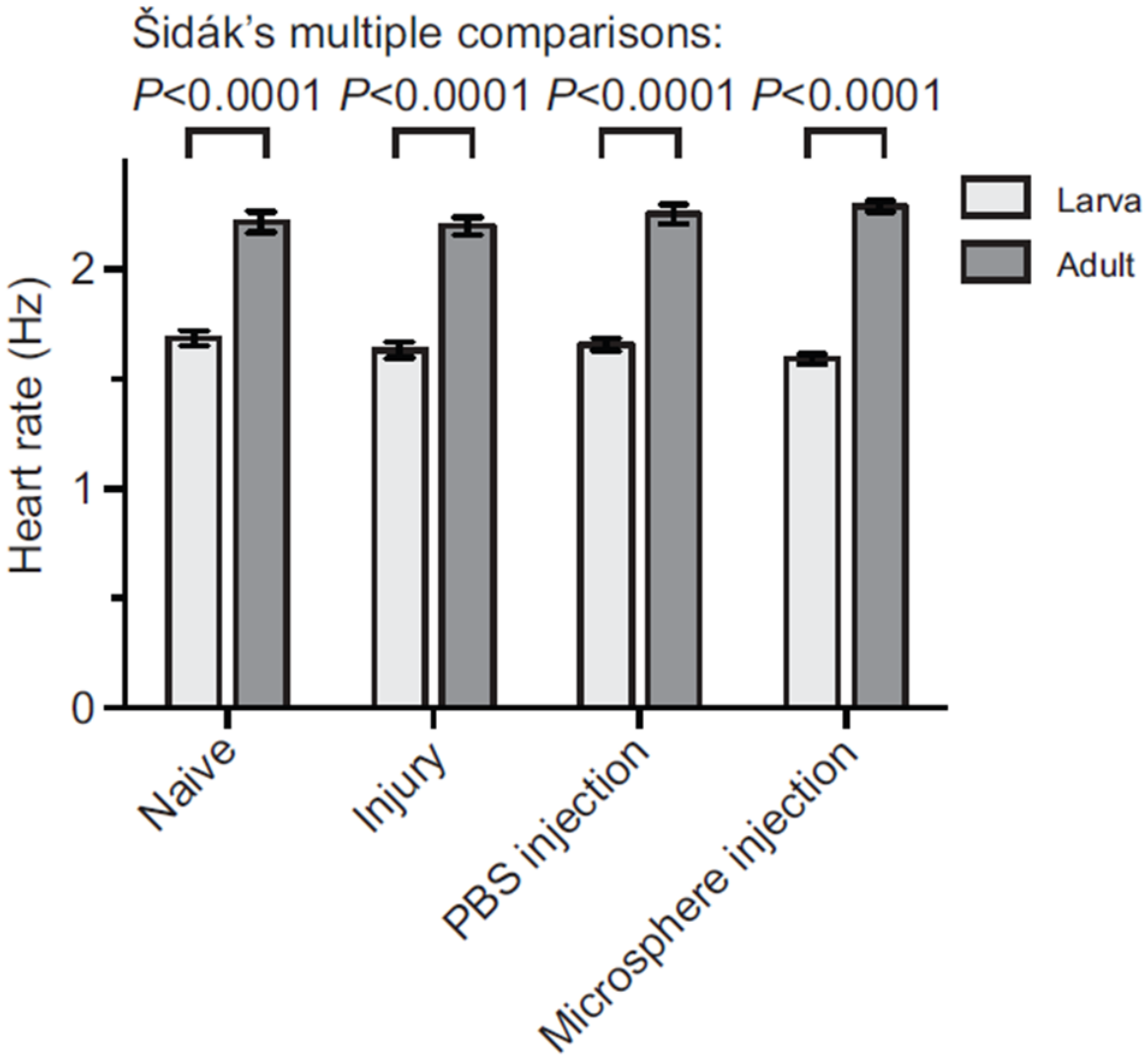

Figure 2. Larval and adult heart contraction rates. Heart contraction rates were quantified in larvae and adults after receiving no treatment (naïve), a needle wound (injury), an injection with PBS, or an injection with 2 μm fluorescent microspheres in PBS. Across all comparisons, larvae displayed lower heart rates than adults (two-way ANOVA, $P<0.0001$), but treatment did not affect heart rates ($P=0.6725$). Whiskers denote the SEM.

Hemolymph flow velocity through the dorsal vessel is significantly slower in larvae compared with adults

Because the larval heart contracts at a slower rate than the adult heart, we hypothesized that larval hemolymph flow velocity inside the dorsal vessel would also be slower. To test this hypothesis, larvae and adults were injected with identical solutions of 2 μm diameter red fluorescent latex microspheres, and the velocity of these microspheres was measured by intravital video imaging under low-level fluorescence illumination (Fig. 3A). Tracking of injected microspheres showed that intracardiac larval hemolymph travels at an average velocity of 2344 μm s^{-1}, whereas intracardiac hemolymph in adults travels in the anterograde and retrograde directions at velocities of 7420 and 7346 μm s^{-1}, respectively (Fig. 3C; Dunn's test, $P<0.0001$ for both comparisons). This indicates that intracardiac hemolymph velocity is ~215% faster in adults when compared with larvae. Consistent with our previous findings (Glenn et al., 2010), hemolymph flow velocity in adults did not differ between periods of anterograde and retrograde flow (Dunn's test, $P>0.9999$). Furthermore, larval hemolymph travelled though the ventral hemocoel in the retrograde direction at an average velocity of 210 μm s^{-1}, which was an order of magnitude slower than intracardiac hemolymph flow and indicated that hemolymph dramatically slows upon exiting the dorsal vessel (Mann-Whitney test, $P<0.0001$; Fig. 3B-D).

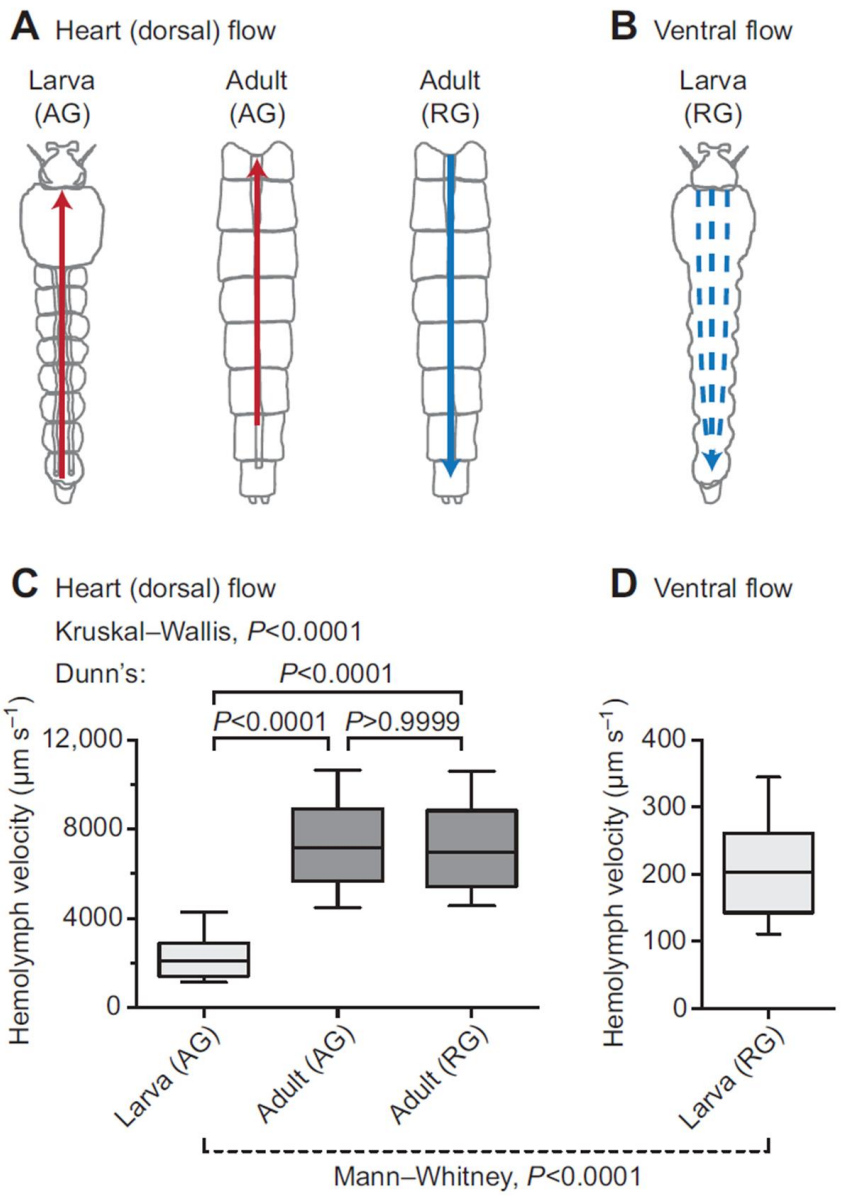

Figure 3. Larval and adult hemolymph flow velocity. (A) Diagrammatic representation (dorsal view; anterior on top) of intracardiac hemolymph flow in larvae (left) and the adult abdomen (middle and right). Hemolymph inside the larval heart is only propelled in the anterograde direction (AG; red arrow) whereas hemolymph is propelled across the adult heart in both anterograde (red arrow) and retrograde (RG; blue arrow) directions. (B) Diagrammatic representation (ventral view) of extracardiac hemolymph flow in the larval ventral abdomen, showing that hemolymph only moves in the retrograde direction (blue arrows). (C) Hemolymph velocity in the heart of larvae and adults, as determined by the tracking of neutral density fluorescent microspheres. Intracardiac (anterograde) hemolymph in larvae travels significantly more slowly than intracardiac (anterograde and retrograde) hemolymph in adults. (D) Extracardiac retrograde hemolymph flow in the ventral abdomen of larvae. In larvae, extracardiac flow is significantly slower than intracardiac flow. For box plots, the centerline marks the median, the box marks 50% of the data, and the whiskers mark 90% of the data.

The larval heart is structurally similar to the adult heart, but its associated abdominal wall musculature and alary muscles differ drastically

The differences observed in larval and adult heart physiology probably result from underlying structural changes that occur during metamorphosis. To uncover these changes, we performed a structural analysis of the musculature associated with the dorsal abdomen of both larvae and adults. Specifically, we treated the dorsal abdomens with Alexa Fluor-conjugated phalloidin, which binds F-actin, and visualized the specimens by fluorescence microscopy.

Muscle staining of the larval abdomen revealed a dorsal vessel consisting of an abdominal heart and a thoracic aorta that spans the length of the body along the dorsal midline (Fig. 4A). The larval heart is nestled within a thin dorsal cavity that is reminiscent of the adult pericardial sinus and is created by massive, segmentally arranged swim muscles that flank the heart and intersect it at nearly 45 deg angles (Fig. 4A-C). Under low magnification, the larval heart was often difficult to distinguish from the surrounding tissues because the fluorescence emitted by the heart, though similar to that of adults, was nearly overwhelmed by that of the surrounding swim muscles (Fig. 4A, B). The larval heart muscle is composed of a single layer of spirally arranged cardiomyocytes which, when viewed from the ventral side, form a clockwise, left-handed helical twist with respect to the lumen of the vessel (Fig. 4C). Three-dimensional rendering of deconvolved *Z*-stacks showed that the larval heart is dorsal and medial to the longitudinal tracheal trunks.

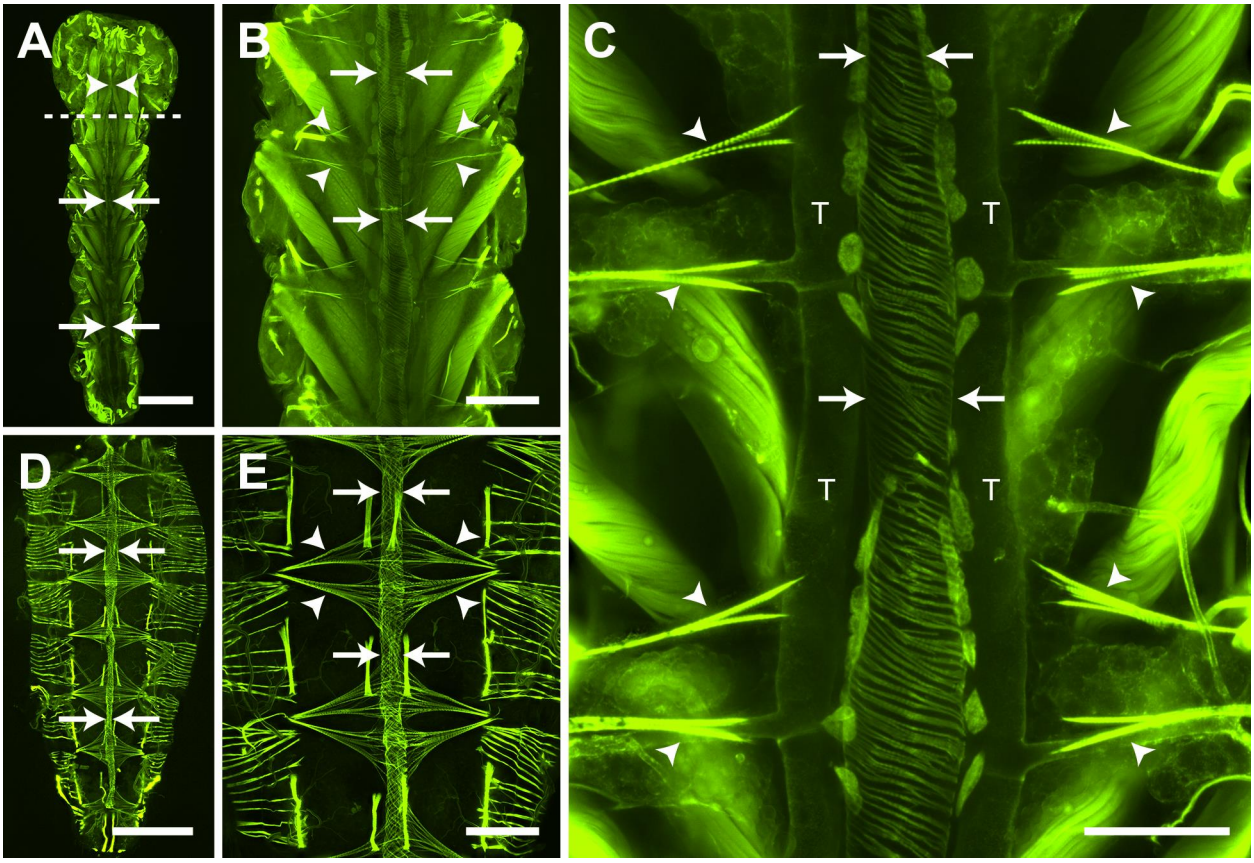

Figure 4. Larval and adult heart structure. All images are fluorescence micrographs of specimens treated with Alexa Fluor conjugated phalloidin, which labels muscles green. (A) Image of the larval dorsal thorax and abdomen showing that the dorsal vessel extends the length of the body along the dorsal midline and is subdivided into an abdominal heart (arrows) and a thoracic aorta (arrowheads). The dashed line delineates the thoraco-abdominal junction. (B) A portion of the larval abdomen illustrated in panel A, magnified to show the heart (arrows) and associated alary muscles (e.g. arrowheads). The larval heart is flanked on either side by large swim muscles that approach the heart at ~45 deg angles. (C) High magnification view of two segments of the larval heart (arrows) showing the spiral arrangement of cardiomyocytes, the dorsal longitudinal tracheal trunks (T) and the alary muscles (arrowheads). Also visible along the surface of the heart are numerous pericardial cells. (D) Adult dorsal abdomen showing the heart (arrows), which runs the length of the abdomen along the dorsal midline. (E) A portion of the adult abdomen magnified to show the heart (arrows) and the extensive alary muscles (arrowheads). All images are oriented with anterior on top. Scale bars: A and D, 500 μm; B and E, 200 μm; C, 100 μm.

Extending towards the dorsal midline from areas near the tergum-pleuron junction at a location that is immediately posterior to each abdominal suture are six complete and three incomplete pairs of bilaterally symmetrical alary muscles (Fig. 4B, C). These muscles attach to

the heart on either side of the abdominal suture and tether it to the dorsal abdominal cuticle. The complete alary muscle pairs are located in abdominal segments 2-7. One incomplete alary muscle pair is located at the thoraco-abdominal junction and the other two are present at the posterior suture where the seventh and eighth abdominal segments are joined. Each alary muscle branches once, and each branch splits again to form two connections at the ventrolateral surface of the heart at a location near the pericardial cells. The points where the alary muscles connect to the heart were usually too tenuous to remain intact in our mounted specimens, but using a different imaging technique other researchers have observed the connection between the alary muscles and the heart of *Aedes aegypti* larvae (Leódido et al., 2013).

Consistent with our video recordings, muscle staining revealed that the larval and adult heart lie in the same location and span the same length along the dorsal midline of the abdomen (Fig. 4). However, comparative analyses revealed a significant disparity in overall abdominal musculature between the larva and adult stages. Specifically, compared with the larval swim muscles, the adult abdomen displays a significantly smaller array of intrasegmental lateral muscle fibers, which are oriented at 90 deg angles with respect to the heart (Fig. 4D, E). In both larvae and adults the structure of the heart varied depending on the contraction state at the time of fixation. However, the spiral arrangement of cardiomyocytes was similar in both life stages (Fig. 4).

Although the alary muscles of larvae and adults share the same point of origin at the body wall, alary muscle connections to the heart are far more extensive in adults when compared with larvae. In adults, each alary muscle branches once and then divides again to form anywhere from 10 to >30 myofiber connections to the heart. So extensive are these connections in adults that the anterior-most connection of one alary muscle extends to the posterior-most connection of the

alary muscle located in the adjacent abdominal segment (Fig. 4D, E). Together, these structures form the basket-like muscular network that comprises the incomplete dorsal diaphragm in adults, a structure that is essentially absent in larvae due to their immature alary muscles.

Larval and adult abdominal ostia are in the same location and display a similar structure

The larval heart contains paired ostia, or valves, at the anterior portion of abdominal segments 2-7. An additional pair of ostia is located at the thoraco-abdominal junction, where the heart joins the aorta (discussed below). The ostia are located on the lateral sides of the heart near the anterior of each abdominal segment (Fig. 5A-C). Near each ostium is the junction of the posterior branch of each alary muscle, and each ostium is flanked ventrally by a pair of large pericardial cells (Fig. 4C; Fig. 5A). The heart muscle near the ostia typically bulges out slightly, giving the periostial regions a slightly wider diameter than other regions of the heart, perhaps due to increased tension created by the attachment of the alary muscles. Each ostium consists of two specialized cardiomyocytes that contain prominent nuclei and form funnel-shaped lips that extend into the lumen of the vessel (Fig. 5B, C).

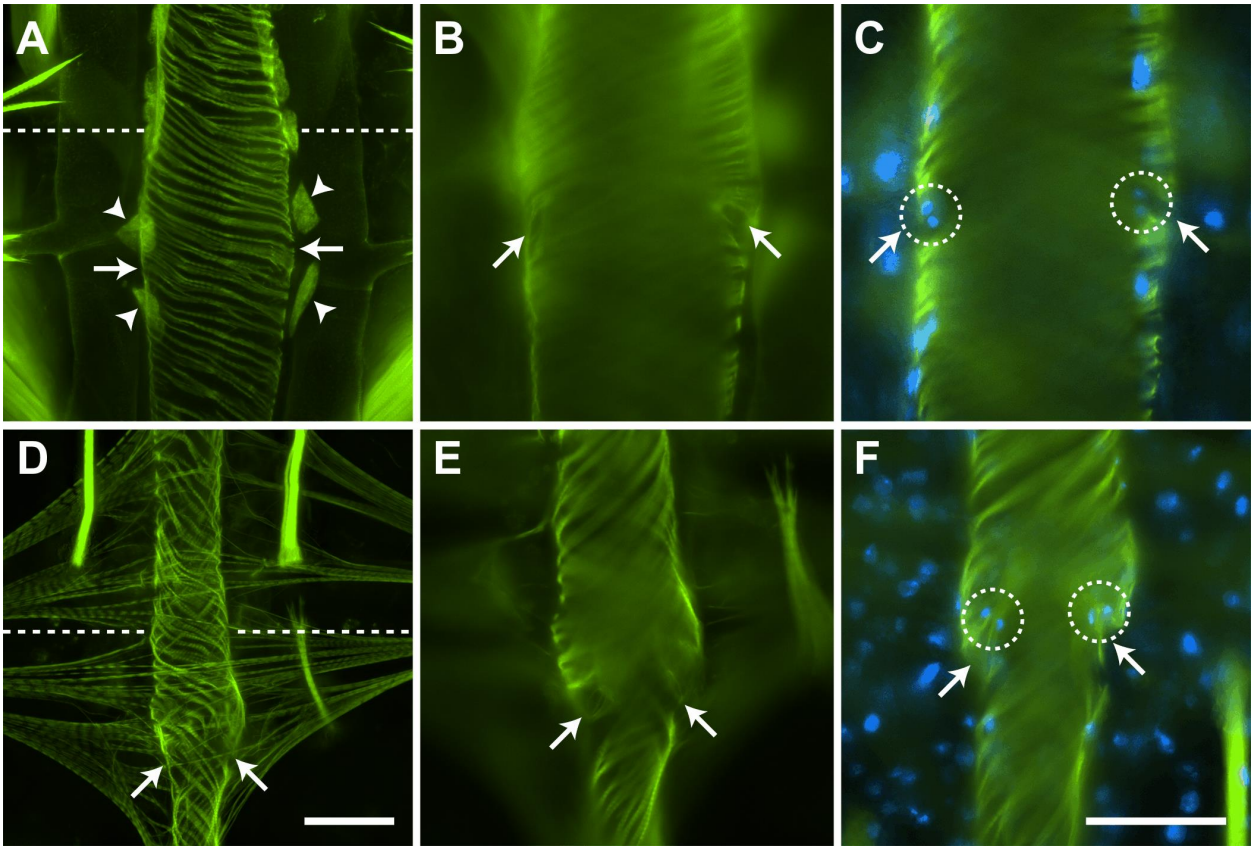

Figure 5. Larval and adult abdominal ostia. Phalloidin stained larval (A-C) and adult (D-F) hearts showing the location and structure of the ostia. (A) Larval ostia (arrows) are located on the lateral sides of the heart in between and dorsal to a pair of enlarged pericardial cells (arrowheads). (B) Ostia (arrows) are oriented towards the anterior of the organism as they extend into the lumen of the vessel. (C) Each ostium (arrows) is composed of a pair of cardiomyocytes (nuclei are labelled blue with Hoechst 33342; circles). (D) Adult ostia (arrows) are located on the lateral sides of the heart near the posterior of each alary muscle pair. Pericardial cells are present but are not labelled. (E) Ostia (arrows) are oriented towards the anterior of the organism as they extend into the lumen of the vessel. (F) Each ostium is composed of two cardiomyocytes (nuclei are labelled blue; circles). Note how the ostia extend into the lumen of the vessel (arrows). All images are oriented with anterior at the top, and the abdominal sutures are marked with a dashed line. Scale bars: A and D, 50 μm; B, C, E and F, 50 μm.

The ostia of adults are also positioned at the anterior portions of abdominal segments 2-7 (Fig. 5D-F), suggesting that all of the larval abdominal ostia are maintained into adulthood. Likewise, adult abdominal ostia form funnel-shaped lips that protrude into the heart lumen in an anterior direction and contain paired nuclei (Fig. 5E, F). Although the muscle that comprises these lips was occasionally observed in larval ostia, it was significantly more prominent in

adults. Furthermore, larval ostial nuclei were typically found closer to the heart wall rather than projecting into the lumen.

Larval hemolymph enters the dorsal vessel primarily through incurrent openings in the eighth abdominal segment and not the abdominal ostia

Intravital video imaging revealed that 2 μm diameter red fluorescent microspheres injected into the larval ventral hemocoel migrate slowly in the retrograde direction, bypass the abdominal ostia and enter the dorsal vessel at the posterior terminus of the heart (Fig. 3B). To gauge the amount of hemolymph that enters the larval heart through the terminal opening in the eighth abdominal segment relative to the ostia located in abdominal segments 2-7, microspheres were injected into the larval thorax and the number of microspheres that entered the dorsal vessel within each abdominal segment over a 60 s time period was quantified. Although microspheres were occasionally observed entering the heart through the abdominal ostia, the vast majority of microspheres (>99%) entered the dorsal vessel through the terminal openings of the heart in the eighth abdominal segment (Wilcoxon matched pairs test, $P<0.0001$; Fig. 6). Even when injecting larvae with higher concentrations of fluorescent microspheres, regardless of the site of injection, the microspheres consistently migrated posteriorly and only entered the dorsal vessel after reaching the eighth abdominal segment.

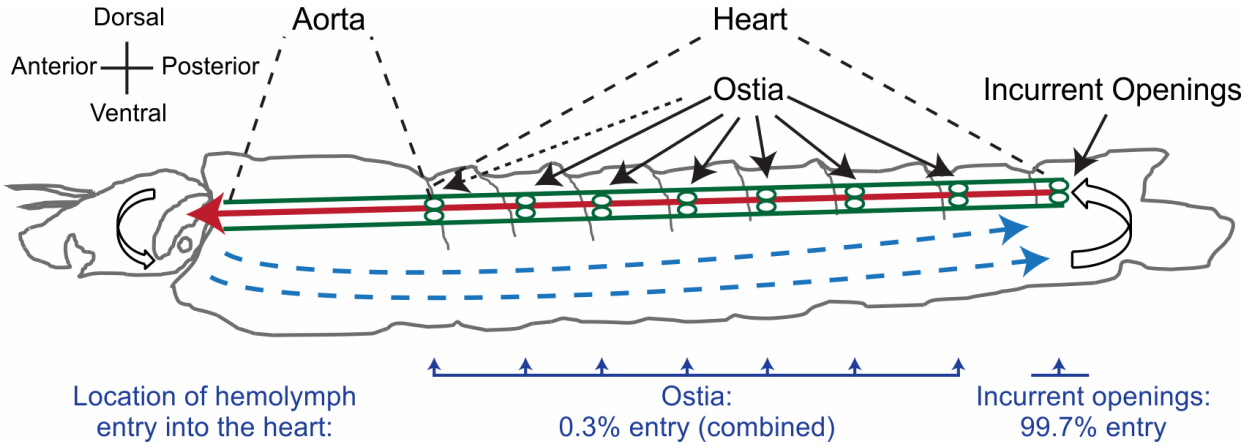

Figure 6. Larval hemolymph flow patterns and entry through the eighth abdominal segment incurrent openings of the heart. Diagrammatic representation (lateral view) of hemolymph flow in larvae. Hemolymph enters the dorsal vessel (green) at the posterior terminus of the heart in the eighth abdominal segment and travels rapidly in the anterograde direction (red arrow) before exiting the aorta near the head. After exiting the aorta, hemolymph flows slowly in the extracardiac hemocoel in the retrograde direction (blue arrows) and then re-enters the dorsal vessel via a pair of incurrent openings at the posterior terminus of the heart. This diagrammatic representation was constructed after visualizing the movement of fluorescent microspheres that had been injected into the hemocoel. The bottom of the image displays the percentage of microspheres that enter the heart through the ostia and the percentage of microspheres that enter the heart through the incurrent openings located at the posterior terminus of the heart (Wilcoxon matched pairs test, $P<0.0001$). The ostia and incurrent openings are labelled with continuous arrows and the thoraco-abdominal ostia are labelled with a dashed arrow.

The larval posterior incurrent openings of the heart are structurally similar to the adult excurrent openings

Examination of the anterior portion of the eighth abdominal segment of phalloidin-treated larvae revealed the structure of the posterior terminus of the heart (Fig. 7A-E). This structure consists of two incurrent openings that allow hemolymph to enter the lumen of the dorsal vessel (Fig. 7C). The cardiomyocytes that form these openings create a laterally oriented figure-of-eight and coalesce at the center of the heart lumen to form a thin but dense structure that protrudes from the heart and attaches to the body wall (Fig. 7A-E). The larval incurrent openings are further supported by two sets of incomplete alary muscles (Fig. 7A, B, D, E), as well as by extensive connections with tracheal tufts that originate near the dorsal longitudinal tracheal

trunks at the posterior of the eighth abdominal segment (Fig. 7D-F). The tracheal tufts are a dense mass of thin trachea that is suspended in the hemolymph and shifts with each heart contraction.

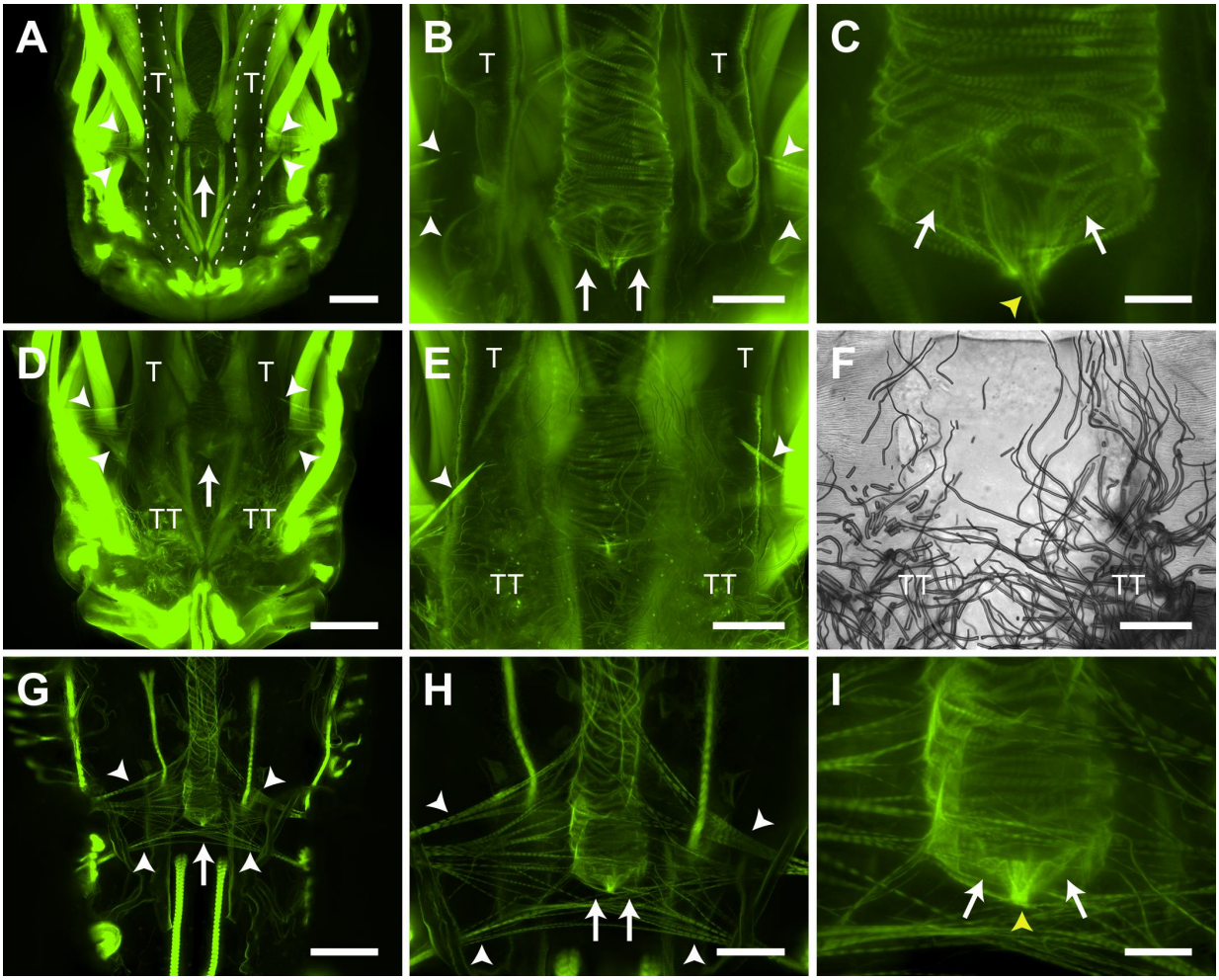

Figure 7. Larval and adult posterior heart structure. (A-C) Image series showing, in increasing magnification, phalloidin staining of the larval posterior incurrent openings of the heart. The posterior terminus of the larval heart ends in the anterior portion of the eighth abdominal segment, lies between the dorsal longitudinal tracheal trunks (T), and is supported by two incomplete pairs of alary muscles (white arrowheads). The posterior terminus of the larval heart contains two incurrent openings (arrows) that contain a muscular tether (yellow arrowhead) that attaches the heart to the abdominal wall. (D-F) Series of fluorescence (D, E) and bright-field (F; same specimen as E) images showing that the posterior terminus of the larval heart is also attached to an extensive network of thin tracheoles called the tracheal tufts (TT), which extend from a location near the posterior base of the dorsal longitudinal tracheal trunks (T). (G-I) Image series showing, in increasing magnification, phalloidin staining of the adult posterior excurrent openings of the heart. The posterior terminus of the adult heart ends in the anterior portion of the eighth abdominal segment and is supported by two incomplete pairs of alary muscles (white arrowheads). The posterior terminus of the adult heart contains two excurrent openings (arrows) that contain a muscular tether (yellow arrowhead) that attaches the heart to the abdominal wall. All images are oriented with anterior at the top. Scale bars: A, D and G, 100 μm; B, E, F and H, 50 μm; C and I, 20 μm.

The posterior terminus of the adult heart is exclusively excurrent (Glenn et al., 2010), and thus serves the opposite function to the one found in larvae. The adult posterior heart shares the same paired openings as the larval posterior heart, as well as a similar point of attachment to the body wall (Fig. 7G-I). Also similar to larvae, the adult posterior terminus of the heart is supported by two sets of incomplete alary muscles, although, as is the case with the other alary muscles, these form more extensive connections to the heart in adults when compared with larvae.

The larval aorta extends from the thoraco-abdominal junction to the base of the head and differs in structure from the heart

Imaging of the larval thoracic musculature after phalloidin staining revealed the presence of a thoracic aorta that extends from the thoraco-abdominal junction to the anterior portion of the thorax (Fig. 8A). The shape of the aorta varies substantially depending on the contraction state of the heart; during contraction, the aorta widens (Fig. 8B, C), while during relaxation the aorta narrows (Fig. 8D). Although no alary muscle attachments were observed supporting the aorta, two prominent trachea that originate from the longitudinal tracheal trunks were seen attached to the anterior portion of the vessel, perhaps providing structural support in addition to meeting oxygen demands (Fig. 8A).

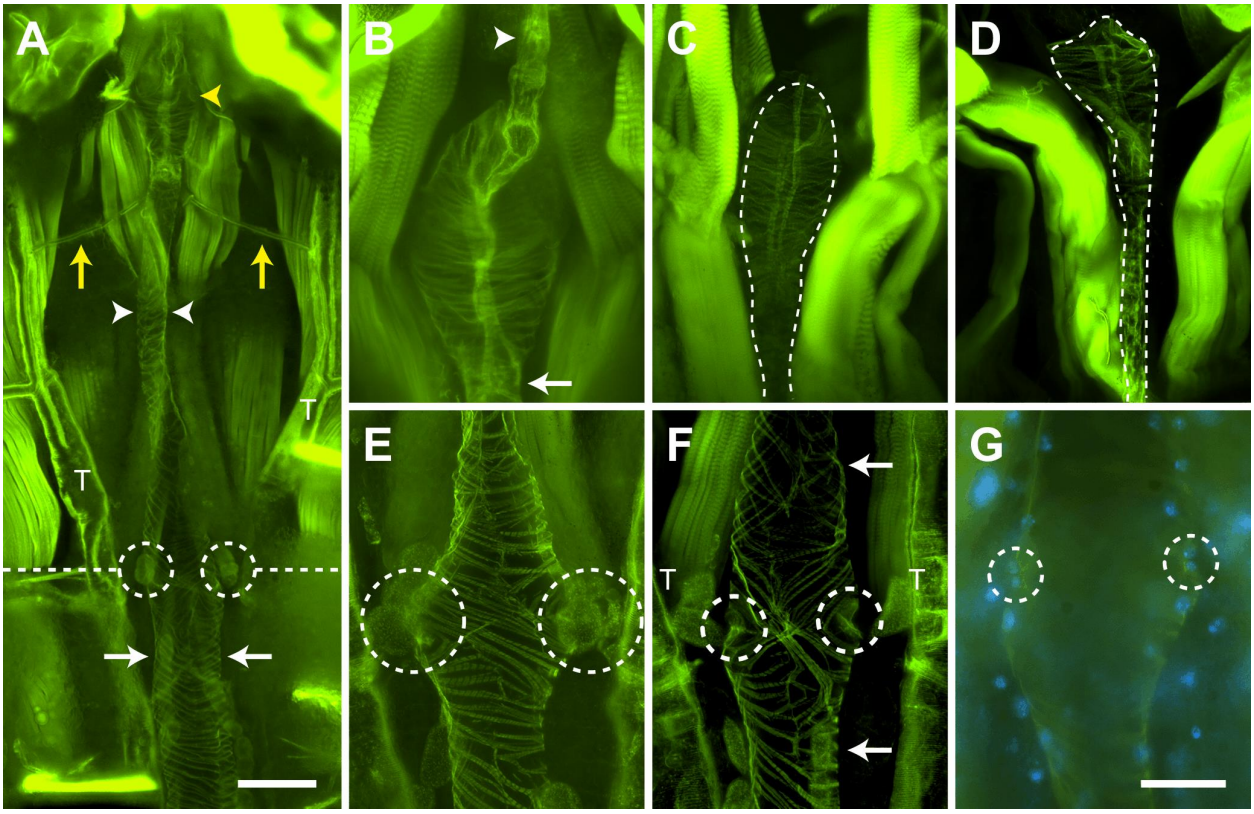

Figure 8. Larval aorta structure. (A) Phalloidin staining of muscle showing the anterior portion of the abdominal heart (arrows), the thoraco-abdominal junction (dashed line), the ostial pair at this junction (circles), the dorsal longitudinal tracheal trunks (T), the thoracic aorta (arrowheads), prominent trachea that attach to the aorta (yellow arrows), and the bulbous chamber of the aorta (yellow arrowhead). (B-D) Series of images showing the anterior bulbous chamber of the aorta. (B) The aorta forms a dense neck region posterior to the bulbous chamber (arrow), which widens significantly into a bulbous chamber before narrowing once again into a thin muscular siphon (arrowhead), where hemolymph passes through prior to emptying into the head. (C, D) The aorta, depending on the contraction state of the heart, varies greatly in shape, widening in response to a heart contraction (C) and narrowing during relaxation (D). (E-G) Series of images showing the structure of the thoraco-abdominal junction. (E) The diamond-shaped thoraco-abdominal junction displays a knot-like arrangement of cardiomyocytes in both left- and right-handed helical orientations and contains two ostia (circles). (F) The regular left-handed helical arrangement of heart cardiomyocytes (bottom arrow) differs from the irregular arrangement of both left- and right-handed helices in aorta cardiomyocytes (top arrow). The ostia at the thoraco-abdominal junction can be seen as invaginations (circles) in the cardiac muscle. (G) Each ostium at the thoraco-abdominal junction contains paired cardiomyocyte nuclei (blue; circles) that lie at the periphery of the heart lumen. All images are oriented with anterior at the top. Scale bars: A, 100 μm; B-G, 50 μm.

At the thoraco-abdominal junction, the heart portion of the larval dorsal vessel forms a diamond-shaped structure reminiscent of the 'conical chamber' described in adult *Drosophila* (Fig. 8A, E-G) (Wasserthal, 2007). The cardiac musculature at the 'conical chamber' forms an irregular knot-like shape consisting of cardiomyocytes in both left- and right-handed helical orientations, which is different from the regular left-handed helical arrangement found throughout the heart (Fig. 8A, E, F). Also in contrast to the cardiomyocytes of the heart, the region of the aorta that is anterior to the thoraco-abdominal junction displays an irregular arrangement of cardiomyocytes that includes longitudinal seams along the dorsal and ventral midlines of the aorta (Fig. 8E, F). These seams form due to the junction of lateral aorta muscles of opposite helical orientation.

Although the aorta proper, unlike the heart, does not contain ostia, a pair of ostia is present at the thoraco-abdominal junction (Fig. 8E-G). As with the abdominal ostia, each thoraco-abdominal ostium is flanked ventrally by pericardial cells and is composed of two specialized cardiomyocytes whose nuclei are found near the perimeter of the vessel wall. Lip-forming muscle projections were difficult to visualize in larvae, although lip-like invaginations typical of abdominal ostia were routinely observed (Fig. 8F). Unlike adults, where the thoraco-abdominal ostia accept extracardiac hemolymph during periods of retrograde heart flow (Glenn et al., 2010), the thoraco-abdominal ostia of larvae were largely inert.

The aorta narrows significantly as it extends from the thoraco-abdominal junction to the anterior of the thorax. As it approaches the anterior portion of the thorax it widens once again to form a bulbous chamber that displays a circular arrangement of cardiomyocytes and can approximate the diameter of the heart. This bulbous chamber, previously described as the 'prothoracic aortic sinus' in *Anopheles quadrimaculatus* (Jones, 1954), begins with a dense neck

region before widening and then tapering off ventrally into a narrow, muscular siphon, which hemolymph passes through just prior to exiting into the head (Fig. 8A, B). Intravital imaging near the base of the head confirmed the presence of the excurrent opening of the aorta, which releases hemolymph into the head where it remains briefly before gradually flowing in the posterior direction. Although hemolymph flow patterns in adults suggest a similar location and function of the adult aorta and anterior excurrent opening, no reliable images of these structures have been obtained (Glenn et al., 2010).

Discussion

The comparative structural and functional data presented herein advance our understanding of the insect circulatory system by providing novel insights into its development across the life stages of the African malaria mosquito, *A. gambiae*. Overall, the larval pattern of unidirectional heart contraction and hemolymph flow reflects a simpler version of the adult circulatory system, a difference in complexity that is probably a function of the more streamlined body plan and overall morphology of the larval life stages. Likewise, the increased complexity of the adult circulatory system may reflect adaptations to the morphology and physiological demands specific to the adult stage, such as those involved in flight, blood feeding, and reproduction.

In this study we found that while the adult heart contracts in both the anterograde and retrograde directions, the larval heart only contracts in an anterograde direction. Unidirectional anterograde heart contraction is a common feature of insect larvae (Dulcis et al., 2001; Gerould, 1924; Jones, 1954; Jones, 1977; Miller et al., 1985; Sláma and Farkas, 2005; Smits et al., 2000). Heartbeat directional reversals, however, have been observed primarily in adult insects from a variety of holometabolous orders, with contraction reversals generally beginning either at the

adult stage or around the time of pupation (Gerould, 1933; Miller, 1997). Although the late-stage larvae of some insects undergo heartbeat reversals prior to pupation (Gerould, 1933; Matsushita et al., 2002; Uchimura et al., 2006), we never observed mosquito larvae, even when nearing pupation, undergoing heartbeat directional reversals. The reason mosquito adults, but not larvae, undergo periodic heartbeat directional reversals remains unknown, but in other insects several environmental and neural stimuli are known to control contraction directionality. For example, the larval heart of *Manduca sexta* contracts only in the anterograde direction whereas the pupal and adult heart periodically reverses contraction direction (Davis et al., 2001). The rhythmicity of adult heartbeat reversals is altered by tactile stimuli, eliminated by the treatment with tetrodotoxin (a neurotoxin), and controlled by specific motor neurons (Dulcis et al., 2001). Neural and hormonal stimuli also modulate the proportional directionality of heart contractions in other insects (Dulcis and Levine, 2005; Dulcis et al., 2005; Kuwasawa et al., 1999), indicating that although the insect heart is myogenic (Chapman et al., 2013; Jones, 1977; Klowden, 2013), contraction dynamics are under partial neural control. In *D. melanogaster*, anterograde heart contractions are thought to be modulated by a putative pacemaker located at the posterior end of the heart (Dulcis and Levine, 2003), whereas retrograde heart contractions are thought to be modulated by a pacemaker located in the conical chamber, which represents the anterior-most region of the heart (Dulcis and Levine, 2005). This conical chamber develops during metamorphosis, and thus is not present in larvae (Curtis et al., 1999; Dulcis and Levine, 2003), suggesting that the larval heart may lack the inherent ability to contract in the retrograde direction. Indeed, the larval heart of most insects appears to lack direct innervation and the formation of an anterior retrograde pacemaker in adults probably coincides with the formation of new neuronal inputs during metamorphosis to coordinate the action of the anterograde and

retrograde pacemakers (Davis et al., 2001; Dulcis et al., 2001; Dulcis and Levine, 2003; Dulcis and Levine, 2004; Dulcis and Levine, 2005). This notion is consistent with the findings of the present study as well as our recent studies that have shown that the adult heart of *A. gambiae* is both innervated and under partial hormonal control, with the identified cardiomyotropic neuropeptides having a stronger effect during periods of anterograde heart contraction (Chen and Hillyer, 2013; Estévez-Lao et al., 2013; Hillyer et al., 2014).

The finding that the larval mosquito heart contracts more slowly than the adult heart is consistent with earlier findings in *A. quadrimaculatus* (Jones, 1954) as well as the increased 'fast forward' phase beating that occurs in *M. sexta* following eclosion (Dulcis et al., 2001; Smits et al., 2000). Similarly, the heart rate of *Drosophila* adults is approximately double that of the third instar larvae (Sláma and Farkas, 2005). We also observed that hemolymph flow velocity was slower in larvae compared with adults, with intracardiac larval hemolymph travelling at less than one-third of the speed of intracardiac hemolymph flow in adults. Because this slower flow velocity correlates with a slower contraction rate in larva when compared with adults, it appears that the more rapid heart rate in adults allows this life stage to propel hemolymph at vastly greater velocities than larvae. Furthermore, as systole appears to constrict the heart of adults to a greater degree than occurs in larvae, the increased reduction in heart luminal volume that presumably accompanies each adult contraction may explain why the developmentally associated increase in intracardiac hemolymph velocity is much greater than the increase in the heart rate (~215% versus ~30%, respectively).

The relative paucity of abdominal body wall musculature in adults compared with larvae indicates a drastic reduction in muscle mass after metamorphosis. However, despite lying in the center of and in close proximity to these abdominal wall muscles, both the larval and adult

hearts: (1) are composed of a thoracic aorta and an abdominal heart; (2) span the same length along the dorsal midline of the abdomen; (3) display the same spiral arrangement of cardiomyocytes; (4) contain the same number of ostia; and (5) retain ostia in the same position and at regular intervals that closely align with the anterior portion of each abdominal segment. Together with the fact that larvae and adults have the same number of abdominal segments, these findings suggest that all portions of the larval heart are maintained following eclosion. In contrast to this high degree of continuity, the adult dorsal vessel in *Drosophila* differs greatly from its larval predecessor in each of the aforementioned areas: (1) unlike adults, the larval aorta spans both thoracic and abdominal segments (T3 to A5) (Curtis et al., 1999; Molina and Cripps, 2001; Wasserthal, 2007); (2) the posterior two segments of the larval heart are lost during metamorphosis (Curtis et al., 1999; Lehmacher et al., 2012; Molina and Cripps, 2001); (3) unlike the regular circular arrangement of adult cardiomyocytes, the larval heart contains a mixture of both circular and helically oriented muscles (Lehmacher et al., 2012); (4) only the first of the three larval ostial pairs are retained into adulthood, with four additional pairs arising during metamorphosis from progenitor cells in the larval aorta (Curtis et al., 1999; Molina and Cripps, 2001; Wasserthal, 2007); and (5) the ostia and the alary muscles of both larvae and adults are not evenly spaced across the abdominal segments. This extensive restructuring of the *Drosophila* dorsal vessel, which is absent in mosquitoes, may be due to the greater disparity between the larval and adult body plans of *Drosophila* when compared with *A. gambiae*, whose larvae and adults, unlike *Drosophila*, both have a distinct head, thorax and abdomen.

In contrast to the relative stability of the heart across mosquito life stages, the supporting alary muscles are grossly under-developed in larvae when compared with adults, an observation recently made across life stages in *A. aegypti* (Leódido et al., 2013) that is also consistent with

structural data from adults of other mosquito species (Martins et al., 2011). This disparity in alary muscle support may partly account for the differences in contraction and hemolymph flow dynamics observed between the two life stages, as alary muscles are believed to not only aid in the relaxation of the heart muscle during diastole (Lehmacher et al., 2012) but also to facilitate the opening and closing of the ostia (Glenn et al., 2010). During our particle-tracking experiments we observed that nearly all of the injected microspheres entered the lumen of the larval dorsal vessel through the posterior incurrent openings of the heart instead of the ostia, a finding that is in agreement with indirect observations in *A. quadrimaculatus* larvae (Jones, 1954). Although larval ostia typically contained lips that were less prominent than those of adults and lay close to the perimeter of the heart, thus resembling ostia in the 'closed' position, the orientation of larval ostia towards the anterior of the insect is consistent with their eventual function in the adult stage as incurrent valves for hemolymph entry into the heart during periods of anterograde heart contractions (Glenn et al., 2010; Jones, 1977). Furthermore, as microspheres occasionally (though rarely) entered the larval heart through the abdominal ostia, we hypothesize that the developmental differences in the mechanics of hemolymph entry into the dorsal vessel are not due to major stage-specific structural differences in the ostia themselves but instead due to differences in the degree of nearby alary muscle support. Indeed, the ostia described here appear to be both developmentally and evolutionarily conserved, as structurally similar ostia have been described in both the larval and adult stages of *A. aegypti* (Leódido et al., 2013) and *Drosophila* (Curtis et al., 1999; Lehmacher et al., 2012; Molina and Cripps, 2001; Wasserthal, 2007).

We have also shown that the function of the posterior terminus of the heart changes with developmental stage: larvae have incurrent openings whereas adults have excurrent openings.

Incurrent function of the posterior larval heart has been inferred from observations in *A. quadrimaculatus* (Jones, 1954), and described in *Drosophila* (Babcock et al., 2008), as well as in some lepidopteran larvae (Locke, 1997; Rao et al., 2009). Each of these insect orders contains several known examples of adults with excurrent posterior heart function, suggesting that the functional change of the posterior terminus of the heart is evolutionarily conserved (Glenn et al., 2010; Wasserthal, 1980; Wasserthal, 1981; Wasserthal, 2007; Wasserthal, 2012). In *A. gambiae*, the posterior end of the heart is structurally similar in both larvae and adults, and the excurrent function that develops following eclosion is a direct result of the onset of retrograde heart contraction periods. The reason the posterior opening of the adult heart does not retain incurrent function even during periods of anterograde heart contractions remains unknown, but it is possible that the high efficiency of the adult abdominal ostia, which are inert in the larvae, has rendered posterior incurrent function unnecessary.

This study also provides the first structural description of the aorta of *A. gambiae*, as this portion of the dorsal vessel has proved difficult to visualize in adults due to its location in the highly sclerotized thorax (Glenn et al., 2010). The aorta differs significantly from the heart in the arrangement of its cardiomyocytes; whereas the heart contains regular, spirally arranged cardiomyocytes that form a left-handed helical twist, the aorta displays muscle cells arranged in both right- and left-handed helices. This distinct arrangement of cardiomyocytes may contribute to the capacity of the aorta for dramatic alterations in its diameter in response to heart contractions. Although similar irregularities in cardiomyocyte orientation have been noted in the heart and aorta of *Drosophila* larvae (Lehmacher et al., 2012), in mosquito larvae we found these irregularities exclusively in the aorta. However, the narrow diameter of the mosquito aorta and its lack of ostia are common features among insect aortas, including that

of *Drosophila* (Chapman et al., 2013; Jones, 1954; Lehmacher et al., 2012; Molina and Cripps, 2001; Wasserthal, 2007).

Hemolymph circulation is an essential yet understudied aspect of insect biology and has been shown to influence thermoregulation, tracheal ventilation and the transport of nutrients, waste, hormones and immune factors (Babcock et al., 2008; Harrison et al., 2012; King and Hillyer, 2012; Klowden, 2013; Nation, 2008; Wasserthal, 1999; Wasserthal, 2003; Wasserthal, 2012). The present study on the circulatory system of *A. gambiae*, a primary disease vector of malaria in sub-Saharan Africa, increases our understanding of key physiological processes in this epidemiologically important mosquito. Specifically, the data presented herein provide novel insights into larval circulatory physiology and describe numerous differences between the larval and adult dorsal vessel, providing a developmental perspective on this organ system. Larvae are a common target in mosquito control strategies (Fillinger and Lindsay, 2011) and many chemical and biological pesticides exert their effect at the larval stage after penetrating the cuticle or midgut and circulating throughout the hemocoel (Favia et al., 2007; Otieno-Ayayo et al., 2008; Paily et al., 2012). Furthermore, numerous mosquito-borne pathogens must complete an obligate migration from the midgut to the salivary glands that involves traversing the hemocoel, where they are subject to hemolymph flow currents (Hillyer et al., 2007). Thus understanding both larval and adult circulatory physiology can yield important insights into current control methods as well as inform the creation of novel ones.

CHAPTER III

FUNCTIONAL INTEGRATION OF THE CIRCULATORY, IMMUNE, AND RESPIRATORY SYSTEMS IN MOSQUITO LARVAE: PATHOGEN KILLING IN THE HEMOCYTE-RICH TRACHEAL TUFTS

Preface

This chapter builds on the findings pertaining to the structure and physiology of the larval circulatory system that are described in Chapter II by identifying the mosquito larval tracheal tufts as the main site of immune activity in larvae. This finding is significant because immune responses at the tracheal tufts occur at the sole region of hemolymph flow into the heart, and thus, it shows the functional integration of the circulatory and immune systems of mosquito larvae. I carried out the experiments presented in this chapter, which involved adapting injection, staining, imaging, and analytic techniques to larvae. All experiments were designed, analyzed, and written with my advisor, Dr. Julián Hillyer. I thank Dr. Patrick Abbot, Dr. Lisa Brown, Leah Sigle, and Tania Estévez-Lao for providing critical feedback during the writing of this manuscript. This chapter is adapted from the final transcript of this work, which was published in September of 2016 in the journal *BMC Biology* (volume 14, article 78).

Abstract

As both larvae and adults, mosquitoes encounter a barrage of immune insults, ranging from microbe-rich communities in larval habitats to ingested blood-borne pathogens in adult blood meals. Given that mosquito adults have evolved an efficient means of eliminating infections in their hemocoel (body cavity) via the coordinated action of their immune and

circulatory systems, the goal of the present study was to determine whether such functional integration is also present in larvae. By fluorescently labeling hemocytes (immune cells), pericardial cells, and the heart, we discovered that fourth instar larvae, unlike adults, contain segmental hemocytes but lack the periostial hemocytes that surround the ostia (heart valves) in abdominal segments 2-7. Instead, larvae contain an abundance of sessile hemocytes at the tracheal tufts, which are respiratory structures that are unique to larvae, are located in the posterior-most abdominal segment, and surround what in larvae are the sole incurrent openings for hemolymph entry into the heart. Injection of fluorescent immune elicitors and bacteria into the larval hemocoel then showed that tracheal tuft hemocytes mount rapid and robust immune responses against foreign insults. Indeed, green fluorescent protein-labeled *Escherichia coli* flowing with the hemolymph rapidly aggregate exclusively at the tracheal tufts, where they are killed within 24 h post-infection via both phagocytosis and melanization. Together, these findings show that the functional integration of the circulatory, respiratory, and immune systems of mosquitoes varies drastically across life stages.

Introduction

Insects have evolved powerful innate immune responses to neutralize infectious agents (Chapman et al., 2013; Hillyer, 2016). Pathogens, including bacteria, viruses, malaria parasites, and fungi, invade the insect hemocoel (body cavity) after ingestion and penetration of the midgut, through breaches in the cuticle, or through the tracheal system. Upon entering the hemocoel, cellular and humoral immune factors kill pathogens by phagocytosis, melanization, lysis, and other mechanisms (Hillyer, 2010; Hillyer, 2016). The primary immune cells that drive these processes are the hemocytes, which are found both circulating with the hemolymph and attached to tissues (sessile) (Hillyer and Strand, 2014; Lavine and Strand, 2002; Strand, 2008).

Immune responses in the hemocoel occur in a dynamic space, where hemocytes, humoral immune factors, and pathogens are propelled through the body by the action of an open circulatory system (Hillyer, 2015; Hillyer, 2016). This circulation is primarily mediated by the contractile action of a muscular dorsal vessel that comprises two distinct regions: the abdominal heart and the thoracic aorta (Chapman et al., 2013; Klowden, 2013). Because circulatory currents move both pathogens and immune components, functional integration is expected to exist between the immune and circulatory systems. Such integration was recently documented in the adult stage of the malaria mosquito *A. gambiae*, where cellular immune responses are rapid and inducible on the surface of the heart (King and Hillyer, 2012). Specifically, in adult mosquitoes, hemolymph enters the lumen of the dorsal vessel via valves, called ostia, which are located in the anterior portion of abdominal segments 2-7 (Glenn et al., 2010; League et al., 2015). A population of sessile hemocytes, called periostial hemocytes, is always present on the surface of the heart in the regions that flank the ostia, where they phagocytose pathogens as they are swept with the hemolymph toward the heart (King and Hillyer, 2012; King and Hillyer, 2013; Sigle and Hillyer, 2016). This initial capture of circulating pathogens induces the migration of additional hemocytes to each periostial region, where they aggregate with the initial population of first responders and amplify the phagocytosis response. Although heart-associated immune aggregations have been observed in multiple mosquito studies (Hernández-Martínez et al., 2013; Hillyer et al., 2007; King and Hillyer, 2012; King and Hillyer, 2013; Michel et al., 2005; Schnitger et al., 2007; Sigle and Hillyer, 2016; Yassine et al., 2014; Yassine et al., 2012), they are not unique to this group of insects. Such aggregations have also been directly or indirectly observed in *Drosophila melanogaster* adults (Akbar et al., 2011; Chambers et al., 2012; Cuttell et al., 2008; Elrod-Erickson et al., 2000; Ghosh et al., 2015; Kocks et al., 2005; Shiratsuchi et al.,

2012; Stone et al., 2012), though these studies did not seek to link immune responses with the functional mechanics of the heart or with hemolymph flow.

To date, no study has examined whether similar interactions between the immune and circulatory systems occur in insect larvae. However, prior to the initiation of this work, several lines of evidence suggested that any such interactions, if they were to exist in mosquito larvae, would differ from what is seen in adults (Glenn et al., 2010; League et al., 2015). First, intracardiac hemolymph in larvae flows solely in the anterograde direction (toward the head), as the larval heart, unlike the adult heart, does not undergo heartbeat directional reversals (Fig. 1). Second, although the ostia of larvae and adults are similar in number, structure, and position, larval ostia are inert and do not serve as incurrent (inflow) valves for hemolymph entry into the heart (Fig. 1A, B). Third, despite sharing a similar structure, the posterior terminus of the larval heart serves as the sole incurrent opening for hemolymph entry into the dorsal vessel, whereas this same posterior terminus in adults only has excurrent (outflow) function (Fig. 1A, C).

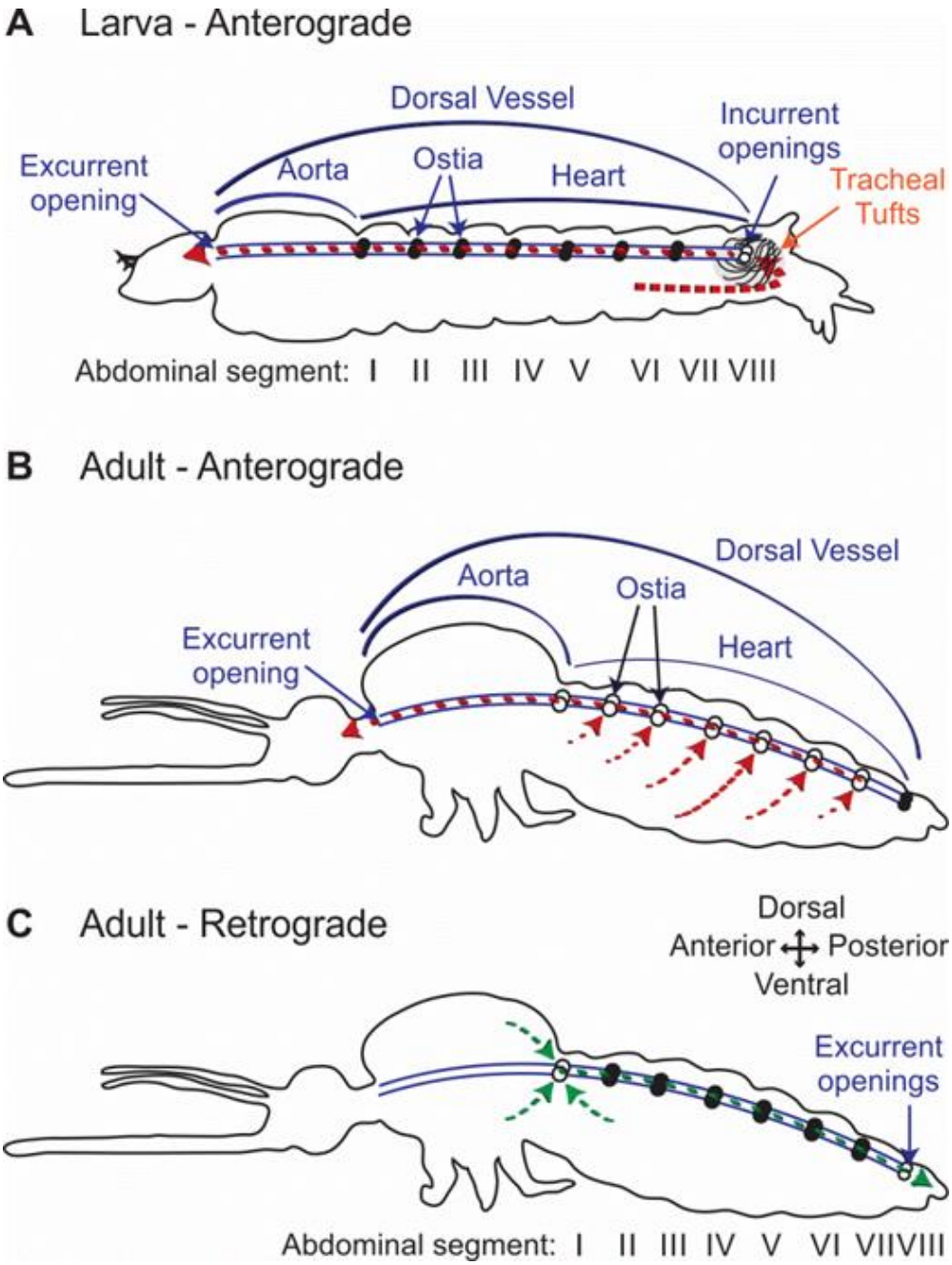

Figure 1. Hemolymph flow through the larval and adult dorsal vessels changes during development. (A) Lateral view of a larva showing the dorsal vessel with ostia. Hemolymph enters the dorsal vessel via a pair of incurrent openings at the posterior heart terminus and exits into the head via an excurrent opening. The larval heart only contracts anterograde. (B) Lateral view of an adult mosquito during an anterograde heart contraction period. Hemolymph enters the dorsal vessel via paired ostia in abdominal segments 2-7 and exits into the head via an excurrent opening. (C) Lateral view of an adult mosquito during a retrograde heart contraction period. Hemolymph enters the dorsal vessel via a pair of ostia at the thoraco-abdominal junction and exits the heart via a pair of excurrent openings at the posterior heart terminus. Illustrations are not drawn to scale. The movement of hemolymph is illustrated using dashed arrows.

In the present study we assessed whether the circulatory and immune systems of mosquito larvae interact during the course of an infection, and describe a pattern that is remarkably different from what is seen in adults. Specifically, we show that, unlike in adults, infection of a mosquito larva does not induce the aggregation of hemocytes and pathogens in the periostial regions of the heart. Instead, infection induces the rapid aggregation and killing of pathogens on the surface of the tracheal tufts, which are respiratory structures that are unique to larvae and associate with the posterior terminus of the heart in the eighth abdominal segment. In a process that is functionally analogous to what is seen in the periostial regions of adults, the tracheal tuft hemocytes of larvae phagocytose pathogens as they near entry into the dorsal vessel, and thus sequester and kill pathogens in the area of the body with the highest hemolymph flow. Taken together, these findings show that the functional integration of the circulatory and immune systems of mosquitoes displays drastic stage-specific differences that reflect the broad changes in body plan that occur during metamorphosis.

Materials and Methods

Mosquito rearing and maintenance

Anopheles gambiae Giles *sensu stricto* (G3 strain; Diptera: Culicidae) were reared as previously described (Estévez-Lao et al., 2013). Briefly, larvae were reared in deionized water and fed a mixture of koi food and baker's yeast. Upon pupation, mosquitoes were transferred to plastic containers with a marquisette net top, and adults were fed a solution of 10 % sucrose *ad libitum*. All life stages were maintained in an environmental chamber set to 27 °C and 75 % relative humidity under a 12 h:12 h, light:dark cycle. Experiments were conducted on fourth instar larvae and adult female mosquitoes at 5 days post-eclosion.

Mosquito injection, inoculation of immune elicitors, and bacterial infection

Mosquito larvae were immobilized by removing excess water and then injected at the lateral center of the mesothorax. Mosquito adults were cold anesthetized and then injected at the thoracic anepisternal cleft. Finely pulled glass capillary tubes were used as needles, and 0.2 µl of the following substances, alone or in combination, were injected: 0.08 % solids 1-µm diameter green fluorescent (505/515) carboxylate-modified microspheres (Invitrogen, Carlsbad, CA, USA) in phosphate-buffered saline (PBS) (pH 7.0), GFP-expressing *E. coli* (modified DH5α) in Luria-Bertani's rich nutrient medium (LB), LB medium, 1 mg/ml pHrodo Red *E. coli* Bio Particles (560/585 nm; Invitrogen) in PBS, or cellular staining solutions (see the next section). For bacterial infections, *E. coli* were grown in LB overnight at 37 °C in a shaking incubator until cultures reached approximately $OD_{600} = 5$, as measured using a BioPhotometer Plus spectrophotometer (Eppendorf AG, Hamburg, Germany).

Staining of hemocytes, pericardial cells, and heart muscle

To fluorescently label hemocytes, live larvae or adults were injected with 67 µM Vybrant CM-DiI or DiO Cell-Labeling Solutions (Invitrogen) in PBS and were incubated at 27 °C and 75 % relative humidity for 20 min or 1 h, respectively. Larvae were then fixed in 16 % paraformaldehyde (Electron Microscopy Sciences, Hatfield, PA, USA) for 1 h and either rinsed briefly in PBS and the whole body mounted directly on a glass slide using Aqua-Poly/Mount (Polysciences Inc., Warrington, PA, USA), or dissected along a coronal plane, rinsed briefly in PBS, and the dorsal abdomen sans the internal organs mounted. Adults were fixed by injecting 16 % paraformaldehyde, and 10 min later the specimens were dissected along a coronal plane, placed in 0.5 % Tween in PBS to reduce surface tension, rinsed briefly in PBS, and the dorsal abdomen sans the internal organs mounted on a glass slide using Aqua-Poly/Mount.

To fluorescently co-stain phagocytic events and hemocytes, larvae were injected with green fluorescent microspheres in PBS, GFP-*E. coli* in LB, or pHrodo Red *E. coli* Bio Particles in PBS and allowed to incubate for 4 h at 27 °C and 75 % relative humidity prior to staining with either CM-DiI or DiO. To co-stain hemocytes and heart muscle, following staining with CM-DiI the larvae were incubated in 16 % formaldehyde for 1 h, dissected, and incubated in 0.7 μM phalloidin-Alexa Fluor 488 (Invitrogen) in PBS on a Pelco R1 Rotary Mixer (Pelco Instruments, Redding, CA, USA) for 1 h. To fluorescently stain pericardial cells, larvae and adults were injected with 0.2 mg/ml Alexa Fluor conjugated IgG 568 nm (Invitrogen) and 0.8 mM Hoechst 33342 nuclear stain (350/461; Invitrogen) in PBS and allowed to incubate for 2 h. To co-stain pericardial cells and hemocytes, larvae were injected with 0.2 mg/ml IgG 488 nm and allowed to incubate for 2 h prior to staining hemocytes with CM-DiI. After staining, specimens were dissected and mounted as described above.

Light and fluorescence microscopy of aldehyde-fixed mosquito specimens

Larval and adult specimens were imaged under bright-field and fluorescence illumination using a Nikon 90i compound microscope connected to a Nikon Digital Sight DS-Qi1Mc monochrome digital camera (Nikon, Tokyo, Japan). For the rendering of detailed fluorescence images with extended focal depth, Z-stacks of whole mounts were acquired using a linear encoded Z-motor, and all images in a stack were combined to form a single focused image using the Extended Depth of Focus (EDF; for image viewing) or Maximum Intensity Projection (for image quantification) modules of Nikon's NIS Elements software. For three-dimensional rendering, Z-stacks were quantitatively deconvolved using the AQ 3D Blind Deconvolution module of NIS Elements and rendered using the volume view feature.

Quantification of fluorescently labeled E. coli and hemocyte fluorescence intensity

GFP-*E. coli* and CM-DiI-labeled hemocyte fluorescence intensity were quantified in abdominal segments 1-8 of larvae using maximum intensity projections of Z-stacks created in NIS Elements software. For abdominal segments 1-7, custom polygonal regions of interest (ROIs) were drawn over the anterior portion of each abdominal segment, encompassing the periostial regions of the heart (Fig. 2). Specifically, these ROIs contained the area in each abdominal segment that lay between the dorsal longitudinal tracheal trunks, and stretched from the abdominal suture to the dorsal abdominal tracheal commissure. For segment 8, two custom ROIs circumscribing each tracheal tuft were constructed. The mean pixel intensity, defined as the average intensity of pixels within a given ROI, was then calculated to compare fluorescence emission across ROIs quantitatively.

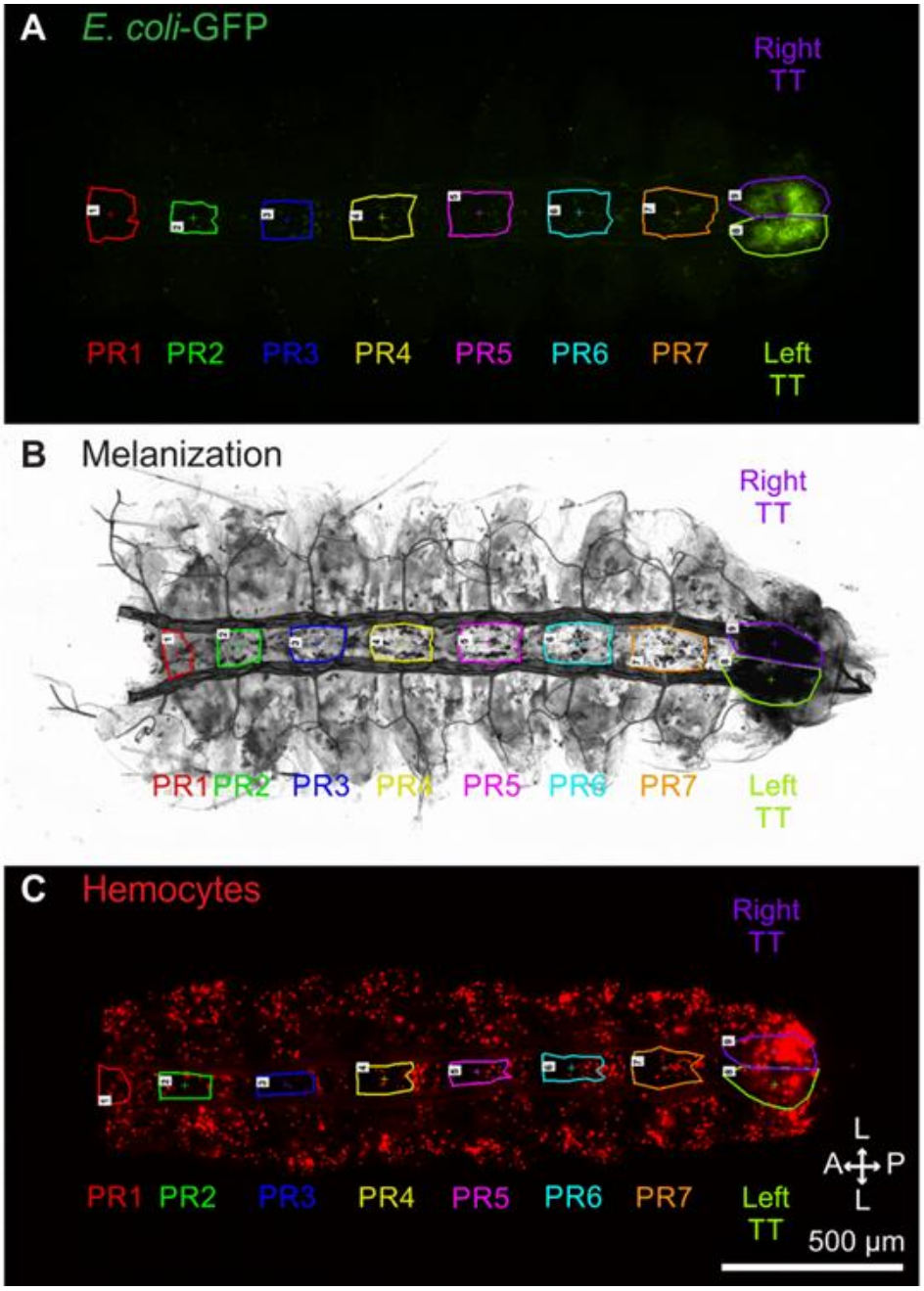

Figure 2. Fluorescence intensity and optical density at the larval periostial regions and tracheal tufts were measured using custom-drawn regions of interest. (A-C) Representative fluorescence and bright-field images of dissected dorsal abdomens from larvae infected with GFP-*E. coli* for 4 h (A) and 24 h (B), and from a naïve larva (C). Images such as these were used to quantify mean fluorescence intensity of GFP-*E. coli* (A) and CM-DiI-stained hemocytes (C), as well as the mean optical density (OD) of melanin deposits (B). Custom regions of interest (ROIs) 1-7 contain each periostial region (PR), delineated as the area in each abdominal segment that lies between the dorsal longitudinal tracheal trunks and stretches from the abdominal suture to the dorsal abdominal tracheal commissure. ROIs 8 and 9 contain the left and right tracheal tufts (TT). Directional arrows: A anterior, P posterior, L lateral.

For GFP-*E. coli* quantification, intensity measurements for any given ROI in the GFP-*E. coli* and injury (injected with LB alone) groups were normalized by subtracting the intensity values from the corresponding ROI from the naïve group, as naïve mosquitoes represent background fluorescence. Three independent trials were conducted at both 4 and 24 h post-treatment, and each trial consisted of at least 10 mosquitoes per group. For CM-DiI-labeled hemocyte quantification, intensity measurements for any given ROI in the CM-DiI-stained naïve, injured, and *E. coli* groups were normalized by subtracting the intensity values from the corresponding ROI of the unstained naïve group. Four and five independent trials consisting of on average 8 and 6 mosquitoes per group were conducted at 4 and 24 h post-treatment, respectively. Because for each mosquito measurements were obtained for all periostial regions and the tracheal tufts (left and right), data were analyzed by repeated measures two-way ANOVA (RM 2 W ANOVA; repeated measures being the nine regions of the body of an individual mosquito), using treatment and ROI as the variables, followed by a Šidák *post hoc* test.

Quantification of melanization in response to E. coli *infection*

Melanization was quantified in abdominal segments 1-8 of larvae using maximum intensity projections created from the bright-field images of the Z-stacks of the same specimens used to measure GFP-*E. coli* fluorescence intensity. These data were analyzed using the same ROI scheme and statistical tests described above. For the melanization analysis, the mean optical pixel density (OD), defined as the average OD of pixels within a given ROI, was calculated to compare melanization across ROIs quantitatively. The OD measurements for any given ROI in the *E. coli* and injured groups were normalized by subtracting the OD values from the corresponding ROI from the naïve group.

Results

Larval sessile hemocytes are segmentally arranged and enriched in the eighth abdominal segment

In adult mosquitoes, sessile hemocytes that are associated with the periostial regions of the heart work in concert with hemolymph flow to clear infections (King and Hillyer, 2012; Sigle and Hillyer, 2016). To determine whether a similar phenomenon occurs in larvae, we initially injected fourth instar larvae and adult mosquitoes with CM-DiI cell labeling solution, which stains hemocytes (King and Hillyer, 2012; King and Hillyer, 2013), and examined the distribution of these cells in the dorsal abdomen by fluorescence microscopy. Analyses of whole and dissected mosquitoes revealed that larvae and adults have a markedly different pattern of sessile hemocyte distribution (Fig. 3). Five-day-old adult females showed a dispersed distribution of hemocytes with no clear segmentation pattern other than the aggregation of hemocytes at the periostial regions of the heart (Fig. 3A, B). In contrast, larvae displayed dense bands of segmentally arranged hemocytes (Fig. 3C, D). These segmental hemocyte bands form continuous rings that encircle each abdominal segment, as this banding is identical in the dorsal and ventral halves of the body (Fig. 3C-H). Furthermore, larvae do not contain the distinct periostial hemocyte aggregates that are typically observed along the heart of adults. Instead, they contain a high concentration of hemocytes in the eighth abdominal segment, a region of the body that contains far fewer hemocytes in adults (Fig. 3B, D).

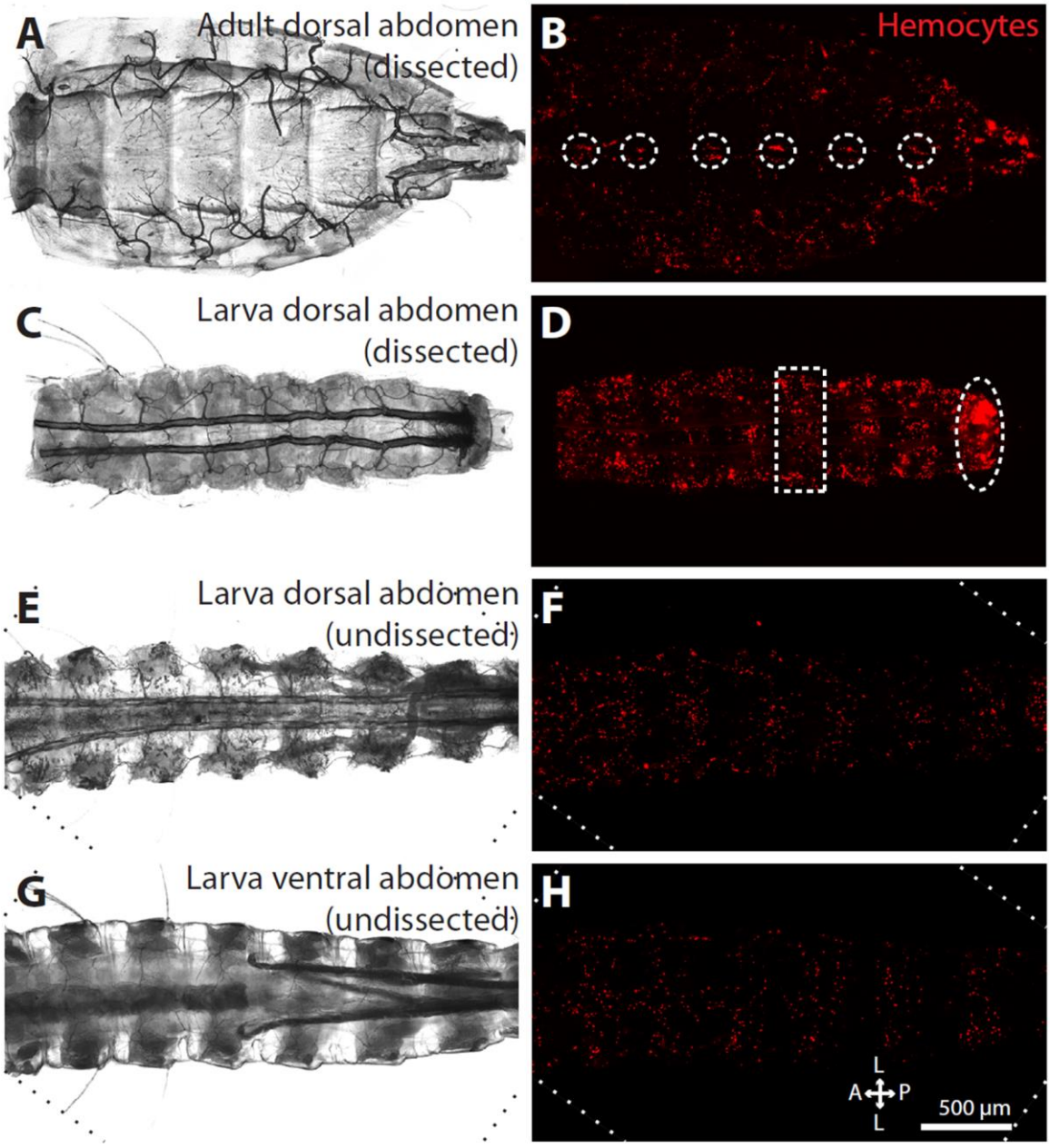

Figure 3. Sessile hemocyte distributions in the abdomen differ between larvae and adults. (A, B) Dissected adult dorsal abdomen under bright-field (A) and fluorescence illumination (B). Hemocytes (CM-DiI; red) form paired aggregates at the periostial regions of the heart (circles). (C, D) Dissected fourth instar larval dorsal abdomen under bright-field (C) and fluorescence illumination (D). Hemocytes form segmental bands in each abdominal segment (e.g., rectangle) and are also concentrated in the eighth abdominal segment (oval). (E-H) Undissected larval abdomen imaged from the dorsal (E, F) and ventral (G, H) views using bright-field (E, G) and fluorescence illumination (F, H). Hemocytes show a segmental banding pattern that encircles the abdomen in each abdominal segment. Diagonal lines in panels E-H denote the edges of rotated images. Directional arrows: A anterior, P posterior, L lateral.

The larval heart lacks periostial hemocytes

To confirm the absence of periostial hemocytes along the larval heart, hemocytes and either the heart or its closely associated pericardial cells, which we used to establish the location of the ostia, were examined by fluorescence microscopy. Injection of larvae with Alexa Fluor conjugated immunoglobulin G (IgG), which labels pericardial cells via their pinocytic function, revealed that the pericardial cells in this life stage flank the heart in a manner that is similar to what is seen in adults (Fig. 4A-D). These cells form seven paired clusters on either side of the ventrolateral surface of the heart, and each paired cluster spans an abdominal suture. In addition, larvae contain an additional paired cluster that has not been documented in adults, which consists of two pericardial cells on either side of the dorsal vessel and spans the thoraco-abdominal junction. With the exception of the pericardial cell clusters located in the eighth abdominal segment, the two posterior-most pairs of pericardial cells within each segmental cluster are larger and are spaced such that a small gap forms between each lateral pair along the anterior-posterior axis (Fig. 4B, D, E) (King and Hillyer, 2012; League et al., 2015). In both life stages, the ostia lie just dorsal to this small gap between the pericardial cells, and in adults, this gap is flanked by periostial hemocytes (King and Hillyer, 2012; League et al., 2015; Sigle and Hillyer, 2016).

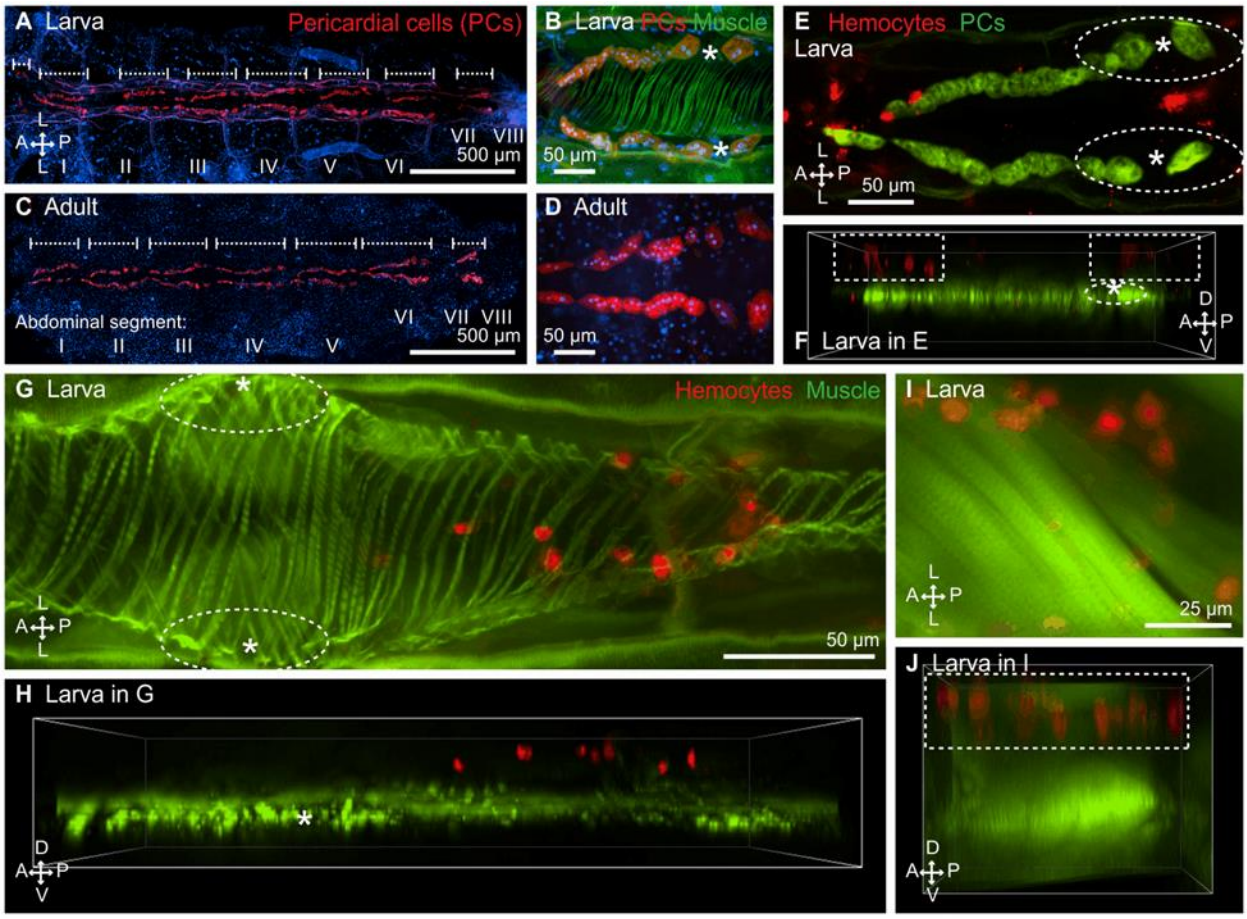

Figure 4. Larvae contain pericardial cells, but lack periostial hemocytes. (A) Dissected larval dorsal abdomen with fluorescently labeled pericardial cells (IgG 568 nm; red). Nuclei were stained blue with Hoechst 33342, and the pericardial cell clusters are delineated by the whiskers. (B) A single set of pericardial cell clusters (red) of a larva, showing the large posterior-most pairs of cells and the gap that forms at a location that is just ventral of each ostium (asterisk) of the heart (phalloidin; green). (C, D) A dissected adult abdomen showing pericardial cell clusters in the same locations as in larvae. Images in panels A and C were assembled by stitching three higher resolution images. (E, F) Co-labeling of pericardial cells (IgG 488 nm; green) and hemocytes (CM-DiI; red) of a larva, displayed both as an Extended Depth of Focus (EDF) image (E) and a three-dimensional (3D) volume view image (F). Segmental hemocyte bands (rectangles) lie dorsal to the pericardial cells, and no hemocytes are present at the periostial regions (oval) that flank the ostia (asterisks). (G, H) EDF (G) and 3D volume view (H) fluorescence images showing that the segmental hemocytes (red) of a larva are dorsal to the heart (green) and distant from the ostia (asterisks). No hemocytes are present at the periostial regions (ovals). (I, J) EDF (I) and 3D volume view (J) fluorescence images of a larva showing that the segmental hemocytes (red; rectangle) lie dorsal to the swim muscles (green). Directional arrows: A anterior, P posterior, D dorsal, V ventral, L lateral.

When the pericardial cells and hemocytes were co-stained, the periostial regions of the larval heart were devoid of hemocytes (Fig. 4E). Though at first glance some of the nearby segmentally arranged hemocytes appeared to occupy the periostial space, 3D deconvolved Z-stacks clearly showed that these segmental hemocytes are attached to the integument that is immediately underneath the cuticle, and thus, these cells lie far dorsal to the ostia, where the periostial hemocytes would be located (Fig. 4F). Staining of heart muscle with Alexa Fluor-conjugated phalloidin, which binds F-actin, in conjunction with hemocyte staining, confirmed this observation by revealing a distinct lack of periostial hemocytes in larvae (Fig. 4G, H). Instead, segmental hemocytes are present on the dorsal integument in a location that is dorsal to both the heart (Fig. 4G, H) and the surrounding swim muscles (Fig. 4I, J).

Larval hemocytes densely populate the eighth abdominal segment tracheal tufts

Qualitative observation of the entire length of mosquito larvae revealed that hemocytes are more abundant in the eighth abdominal segment than in any other region of the body, including the periostial regions (Fig. 3D). In larvae, the eighth abdominal segment is functionally analogous to the periostial regions, as it is the region of the body with the highest hemolymph flow and the only location where hemolymph enters the dorsal vessel (League et al., 2015; Sigle and Hillyer, 2016). However, because the heart is narrow and terminates just posterior to the suture that joins the seventh and eighth abdominal segments (League et al., 2015), the diffuse spatial arrangement of these hemocytes led us to hypothesize that they are largely associated with non-cardiac tissue. A closer examination of the eighth abdominal segment of larvae revealed a dense population of sessile hemocytes that is bound to specialized tracheoles that are arranged into structures collectively referred to as the tracheal tufts (Fig. 5). Recently described in *A. gambiae* larvae (League et al., 2015), the eighth abdominal segment tracheal tufts are a

dense network of thin tracheoles that emanate from the ventral base of the dorsal longitudinal tracheal trunks (Fig. 5A, B; Fig. 6A). Although these tracheoles are predominantly suspended in the hemolymph, some are attached to the posterior terminus of the heart, thus causing them to move with each heartbeat. Furthermore, examination of the exuviae of fourth instar larvae and the dissected dorsal abdomens of pupae and adults showed that the tracheal tufts are unique to larvae and are shed during pupation (Fig. 6).

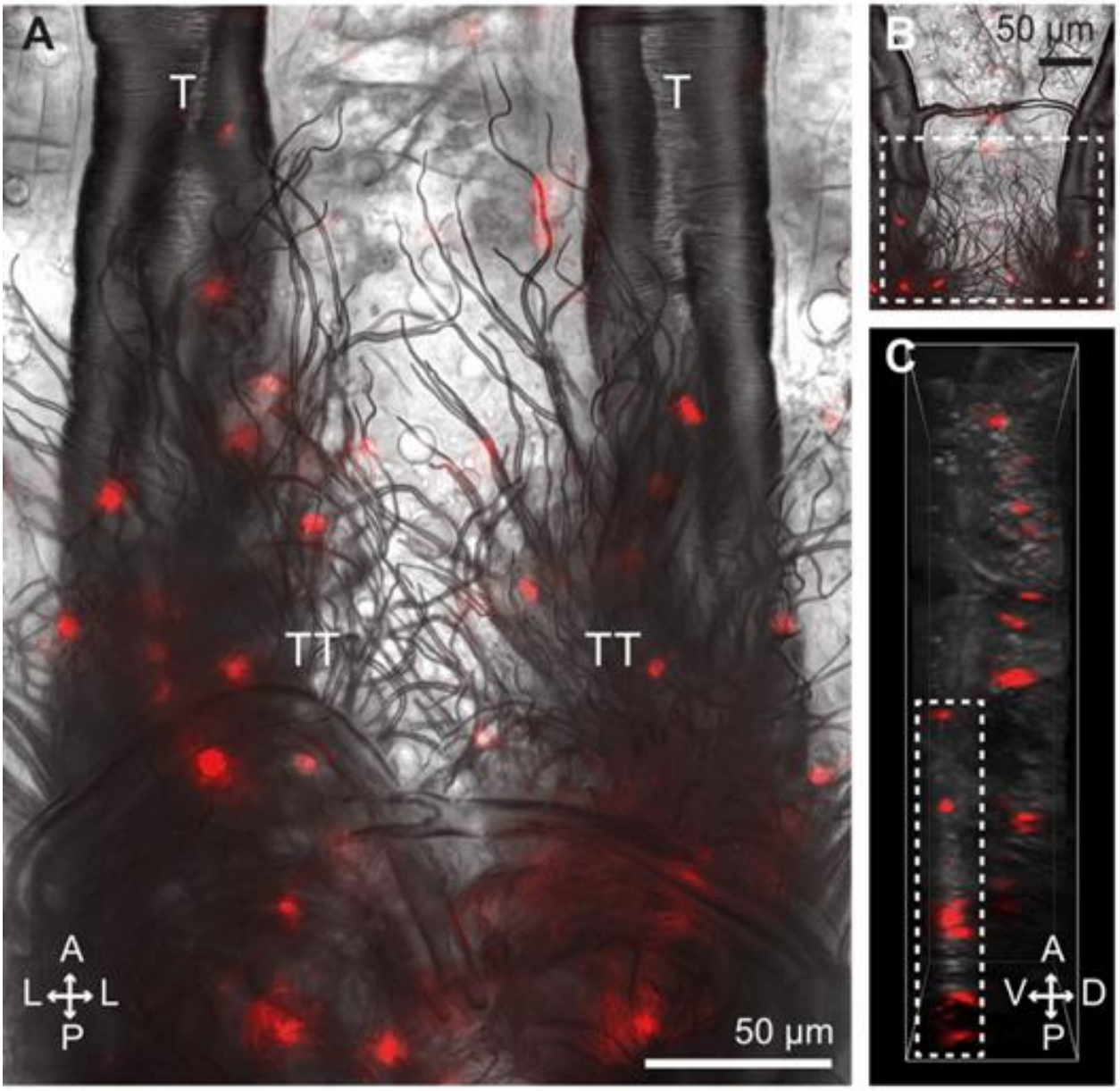

Figure 5. Larval hemocytes associate with the eighth abdominal segment tracheal tufts and are distinct from the segmental hemocyte bands. (A) Posterior portion of the dorsal abdomen of a dissected larva showing the trachea of the seventh and eighth abdominal segments under bright-field and fluorescence illumination. A dense mass of tracheoles known collectively as the tracheal tufts (TT) extend ventrally from the dorsal longitudinal tracheal trunks (T). Hemocytes (CM-DiI; red) bind to the tracheal tufts in high numbers. (B, C) EDF (B) and 3D volume view (C) images of a portion of the seventh and eighth abdominal segments of a larva. Tracheal tuft hemocytes (rectangles) lie ventral to the dorsal segmental hemocytes. Directional arrows: A anterior, P posterior, D dorsal, V ventral, L lateral.

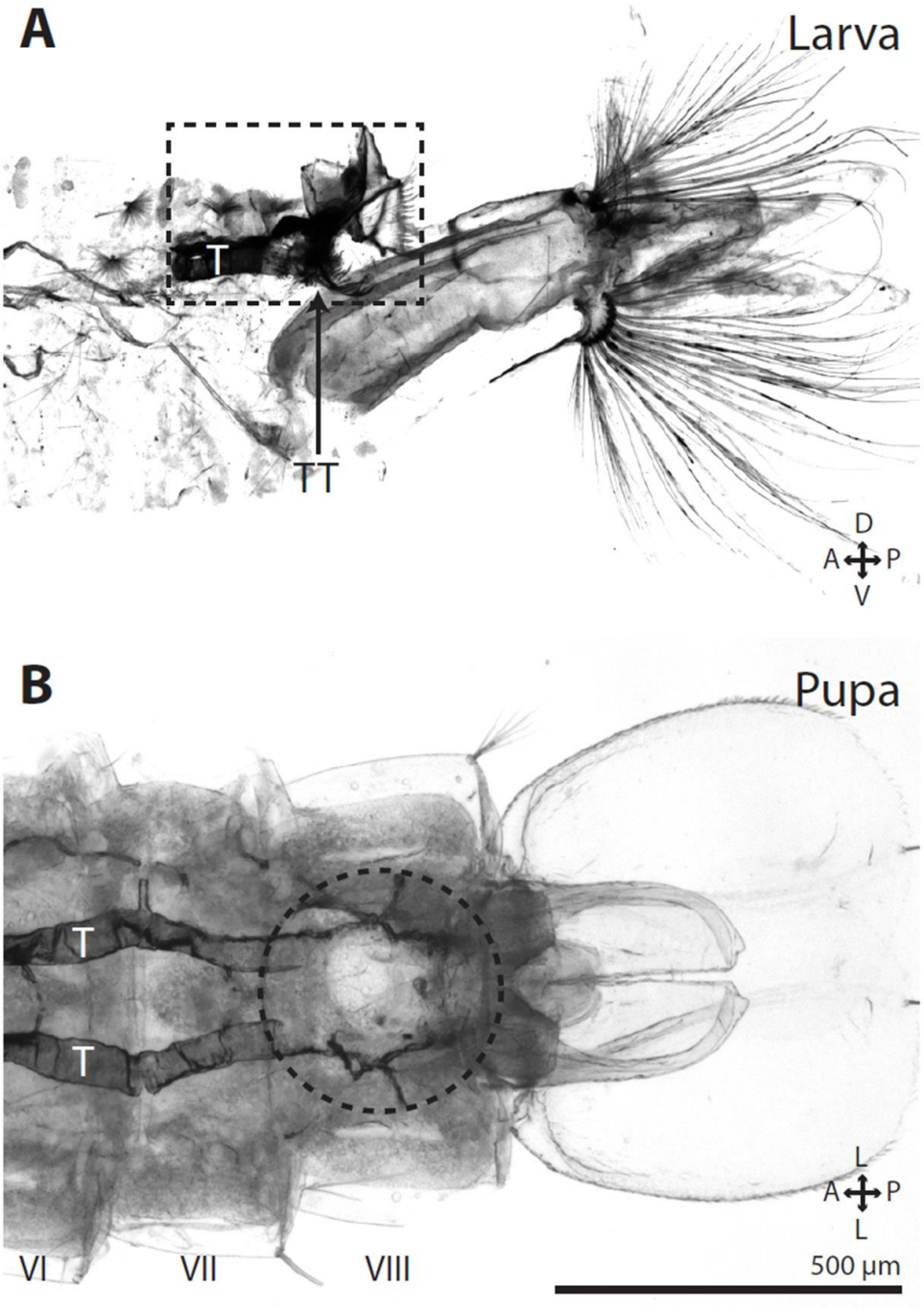

Figure 6. Tracheal tufts are shed in the fourth instar larval exuviae during pupation. (A) Bright-field image of a lateral view of fourth instar larval exuviae showing that the eighth abdominal segment trachea (black rectangle), including the tracheal trunks (T) and the tracheal tufts (TT), are shed during pupation. (B) Bright-field image of a dissected pupal dorsal abdomen, showing the dorsal longitudinal tracheal trunks (T) and the absence of the eighth abdominal segment tracheal tufts (circle). Directional arrows: A anterior, P posterior, D dorsal, V ventral, L lateral.

The tracheal tuft hemocytes comprise a population of cells that is distinct from the segmental hemocytes, as the former are located ventral to the tracheal trunks, whereas the latter are attached to the integument (Fig. 5B, C). In addition to binding the tracheal tuft tracheoles, larval hemocytes often bind to other thin trachea but not to larger trachea, as is evident in the comparative scarcity of hemocytes bound to the dorsal longitudinal tracheal trunks (Fig. 5A, B). A similar phenomenon also occurs in adult mosquitoes; though lacking tracheal tufts and their free-floating tracheoles, hemocytes in adults often bind to thin trachea, and only occasionally bind to the thick trachea, such as those that replace the tracheal tufts in the eighth abdominal segment (Fig. 6). In summary, larvae contain a dense population of hemocytes, called the tracheal tuft hemocytes, in a region of the body that is functionally analogous to the periostial regions of adults.

Larval tracheal tuft hemocytes are phagocytically active

To test whether hemocytes engage in phagocytic immune responses while bound to the tracheal tufts, larvae were challenged with either green fluorescent microspheres, green fluorescent protein-tagged *Escherichia coli* (GFP-*E. coli*), or pHrodo-*E. coli*, and the challenge agent and the hemocytes (labeled *in vivo* with CM-DiI or CM-DiO) were imaged independently or in combination by fluorescence microscopy. Both microspheres and *E. coli* were rapidly phagocytosed by the tracheal tuft hemocytes, with bacterial aggregations at the tracheal tufts beginning within seconds after injection (Fig. 7; Fig. 8A-D). Furthermore, when larvae were challenged with heat-killed *E. coli* bioparticles conjugated to pHrodo (a dye that only fluoresces in acidic environments such as those of a phagolysosome) and 4 h later the hemocytes were labeled, the pHrodo and hemocyte markers co-localized (Fig. 8E-L), further showing that the

tracheal tuft hemocytes mount a rapid and robust phagocytosis response against bacteria that are flowing with the hemolymph.

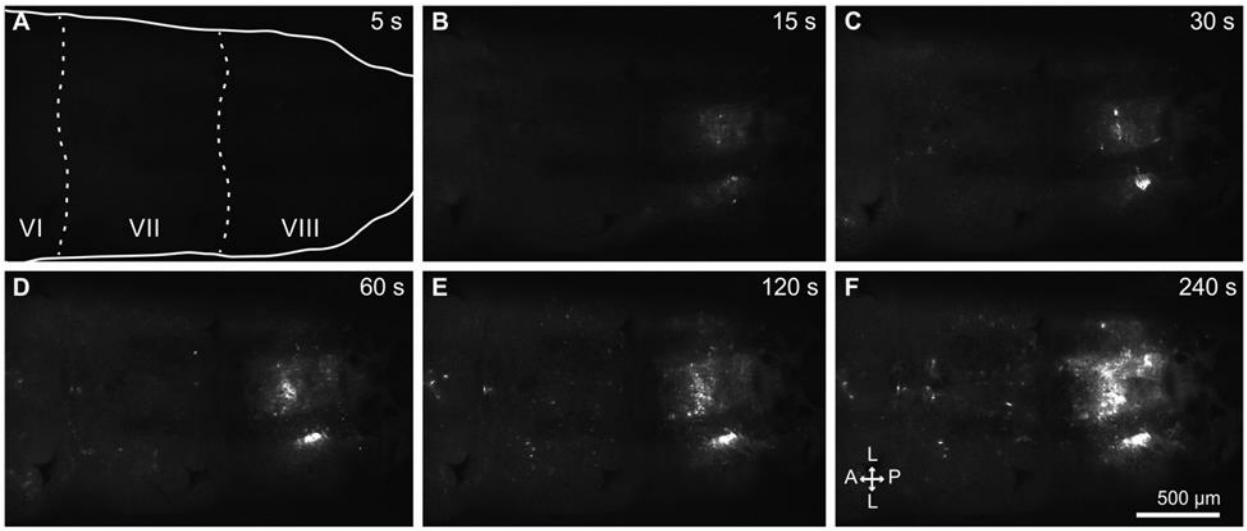

Figure 7. *E. coli* injected into the larval hemocoel rapidly aggregate in the tracheal tufts. (A-F) Still images from an intravital video recorded via fluorescence imaging through the posterior portion of the dorsal cuticle of a larva. GFP-*E. coli* (white) begin to accumulate at the tracheal tufts within 15 s after treatment. The still images shown were extracted at 5, 15, 30, 60, 120, and 240 s post-treatment. The first panel outlines the larva and marks abdominal segments 6-8 (VI-VIII). Directional arrows: A anterior, P posterior, L lateral.

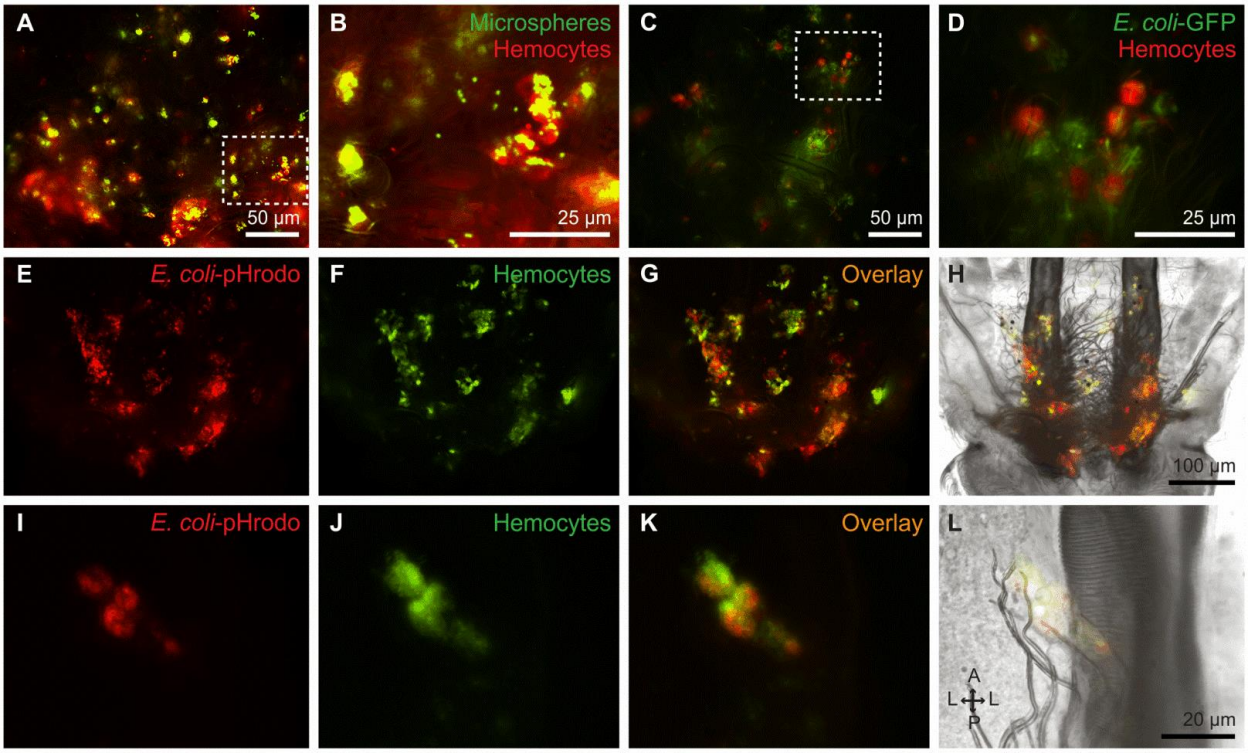

Figure 8. Tracheal tuft hemocytes show high phagocytic activity. (A-D) Fluorescence imaging of the phagocytic activity of tracheal tuft hemocytes (CM-DiI; red) at 4 h post-injection of 1 µm fluorescent microspheres (A, B) or GFP-*E. coli* (C, D; green). Rectangles in A and C are magnified in B and D, respectively. (E-H) Series of fluorescence images (E-G) and bright-field overlay (H) of the tracheal tufts showing the significant overlap of pHrodo-*E. coli* fluorescence (red) and hemocyte fluorescence (DiO; green) at 4 h post-treatment. (I-L) Series of fluorescence images (I-K) and bright-field overlay (L) of a cluster of four tracheal tuft hemocytes (DiO; green) that have phagocytosed pHrodo-*E. coli* (red), showing a significant overlap in fluorescence signal. Directional arrows: A anterior, P posterior, L lateral.

E. coli in the larval hemocoel aggregate in the tracheal tufts, where they are phagocytosed and killed

Injection of both fluorescent microspheres and GFP-*E. coli* into the hemocoel of larvae and adults resulted in patterns of aggregation that mirrored the respective hemocyte distributions in these two life stages: microspheres and *E. coli* aggregated at the periostial regions of the heart in adults and at the eighth abdominal segment tracheal tufts of larvae (Fig. 9; Fig. 10). To quantitatively determine whether pathogen aggregation in larvae was indeed higher at the

tracheal tufts when compared to the periostial regions of the heart, larvae were injected with GFP-*E. coli*, and the fluorescence emitted by these bacteria within the periostial regions and the tracheal tufts was measured at 4 and 24 h post-treatment (Fig. 2).

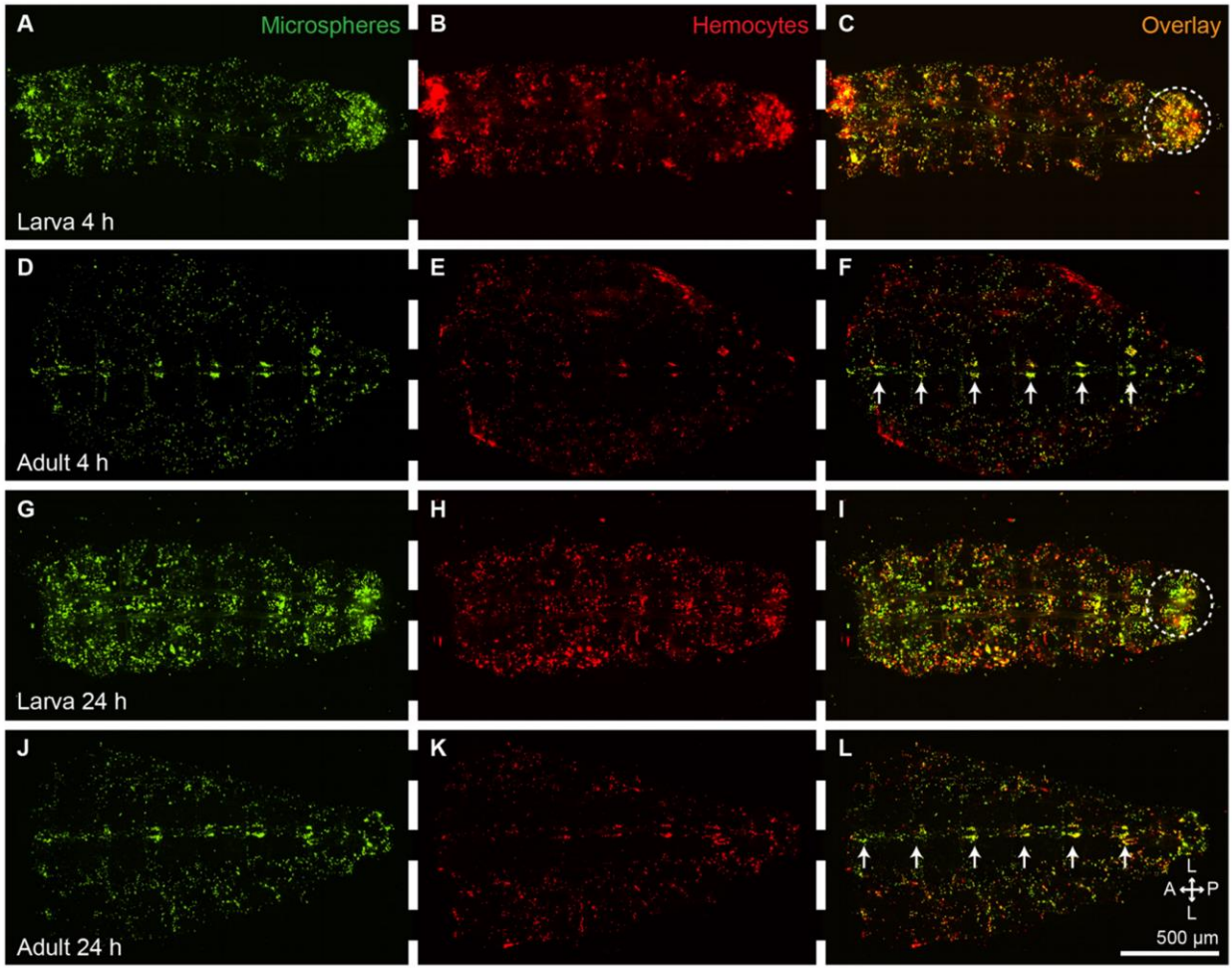

Figure 9. Microspheres injected into larvae and adults aggregate in regions of high hemolymph flow and hemocyte concentration. (A-F) Dissected larval (A-C) and adult (D-F) dorsal abdomens with fluorescently labeled hemocytes (CM-DiI; red) at 4 h after injection with fluorescent microspheres (green). In larvae, microspheres preferentially aggregated in the eighth abdominal segment (A), where there is a high concentration of hemocytes (B, circle in C). In adults, microspheres preferentially aggregated at the periostial regions of the heart (D), where the periostial hemocytes are located (E, arrows in F). (G-L) Dissected larval (G-I) and adult (J-L) dorsal abdomens with fluorescently labeled hemocytes at 24 h after injection with fluorescent microspheres, showing an aggregation pattern identical to that observed at 4 h post-treatment. Directional arrows: A anterior, P posterior, L lateral.

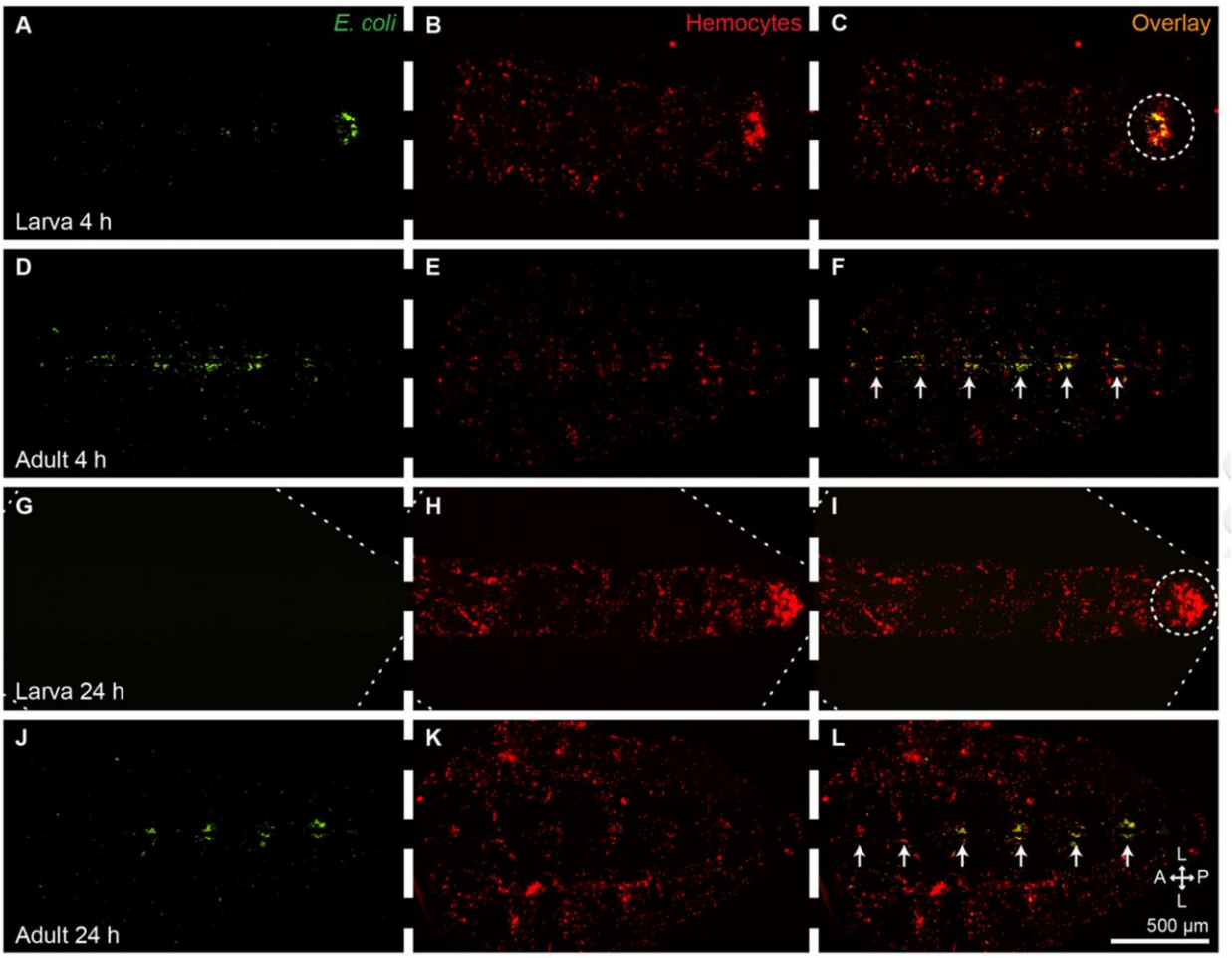

Figure 10. *E. coli* injected into larvae and adults aggregate in regions of high hemolymph flow and hemocyte concentration. (A-F) Dissected larval (A-C) and adult (D-F) dorsal abdomens with fluorescently labeled hemocytes (CM-DiI; red) at 4 h after injection with GFP-*E. coli* (green). In larvae, *E. coli* preferentially aggregated in the eighth abdominal segment (A), where there is a high concentration of hemocytes (B, circles in C). In adults, *E. coli* aggregated at the periostial regions of the heart (D), where the periostial hemocytes are located (E, arrows in F). (G-L) Dissected larval (G-I) and adult (J-L) dorsal abdomens with fluorescently labeled hemocytes at 24 h after injection with GFP-*E. coli*. The aggregation pattern of *E. coli* in adults at 24 h after treatment was similar to that observed at 4 h post-treatment, but in larvae, fluorescence from *E. coli* was not observed anywhere in the body because the infection had been largely cleared. Diagonal lines in panels G-I denote the edges of rotated images. Directional arrows: A anterior, P posterior, L lateral.

At 4 h post-treatment, GFP-*E. coli* formed distinct aggregates in the eighth abdominal segment of infected larvae, and this fluorescence signal was absent in injured (mock-injected) larvae (Fig. 11A-C, G; repeated measures two-way analysis of variance (RM 2 W ANOVA) $P < 0.0001$ for treatment). The strength of the fluorescence signal emitted by GFP-*E. coli*, which is indicative of their abundance, changed depending on the region of the body that was being measured (RM 2 W ANOVA $P < 0.0001$ for segment), and a Šidák multiple comparisons *post hoc* test showed that while there were no significant differences in the fluorescence signals between the different regions of injured larvae ($P > 0.9999$ for all comparisons), there were strong differences in infected larvae. Specifically, there were no significant differences between the GFP signals in the seven periostial regions of infected larvae ($P \geq 0.9926$ for all comparisons), but the GFP signal from the left and right tracheal tufts was significantly higher than the GFP signal of any of the periostial regions ($P < 0.0001$ for all comparisons). Additional pairwise comparisons between injured and infected larvae showed that fluorescence in the periostial regions did not differ between infected and injured larvae (Šidák's $P \geq 0.1069$ for all seven comparisons), but that the fluorescence intensity in the tracheal tufts is significantly higher in the infected larvae when compared to injured larvae (Šidák's $P < 0.0001$ for both comparisons). Finally, although some GFP fluorescence was detected in each of the periostial regions of infected larvae, upon closer examination this fluorescence was not due to pathogen aggregation in those areas but rather due to the uptake of GFP via the pinocytic activity of the pericardial cells and, to a lesser extent, from phagocytosis by the dorsal segmental hemocytes (Fig. 12). Together, these data show that, unlike in adults, bacteria do not aggregate in the periostial regions of larvae, which is as expected given that these

regions are devoid of hemocytes. Instead, infection induces the massive aggregation of bacteria in the hemocyte-rich tracheal tufts.

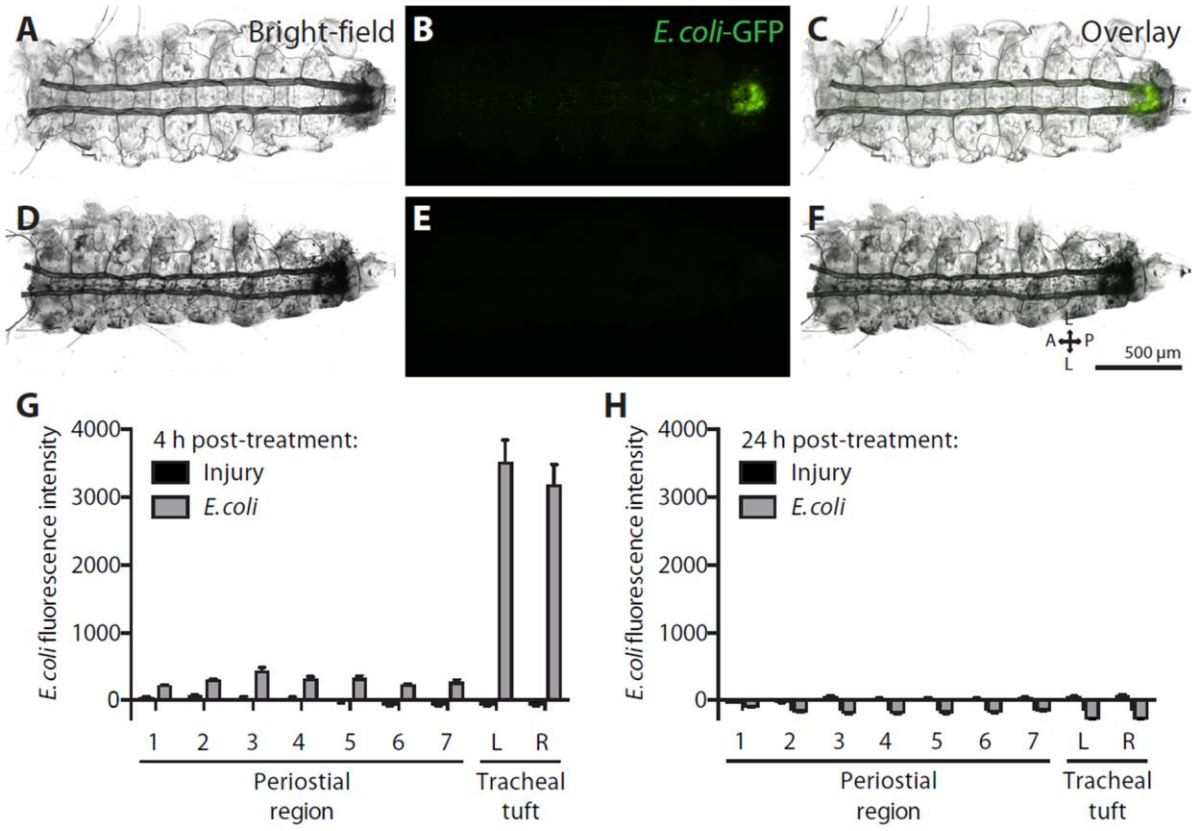

Figure 11. *E. coli* aggregate in the tracheal tufts, where they are rapidly destroyed. (A-F**)** Bright-field (A, D), fluorescence (B, E), and overlay (C, F) images of a dissected dorsal larval abdomen at 4 h (A-C) and 24 h (D-F) post-infection with GFP-*E. coli* (green). At 4 h, the bacteria have aggregated in the eighth abdominal segment, whereas at 24 h little or no fluorescence was observed. (G, H) Mean intensity of fluorescence signal in the periostial regions (1-7) and the left (L) and right (R) tracheal tufts of injured and GFP-*E. coli*-treated larvae at 4 h (G) and 24 h (H) post-treatment. At 4 h, mean intensities from both tracheal tufts of the *E. coli*-treated larvae were significantly higher than those from any region of interest (ROI) in injured larvae ($P < 0.0001$ for all comparisons). At 24 h, with the exception of periostial region 1 ($P = 0.2990$), mean intensities from each ROI were significantly lower in the *E. coli*-treated larvae compared to injured larvae ($P \leq 0.0005$ for all other comparisons). In G and H, whiskers denote the standard error of the mean (SEM). For a graphical presentation of how the ROIs were constructed, Figure 2. Directional arrows: A anterior, P posterior, L lateral.

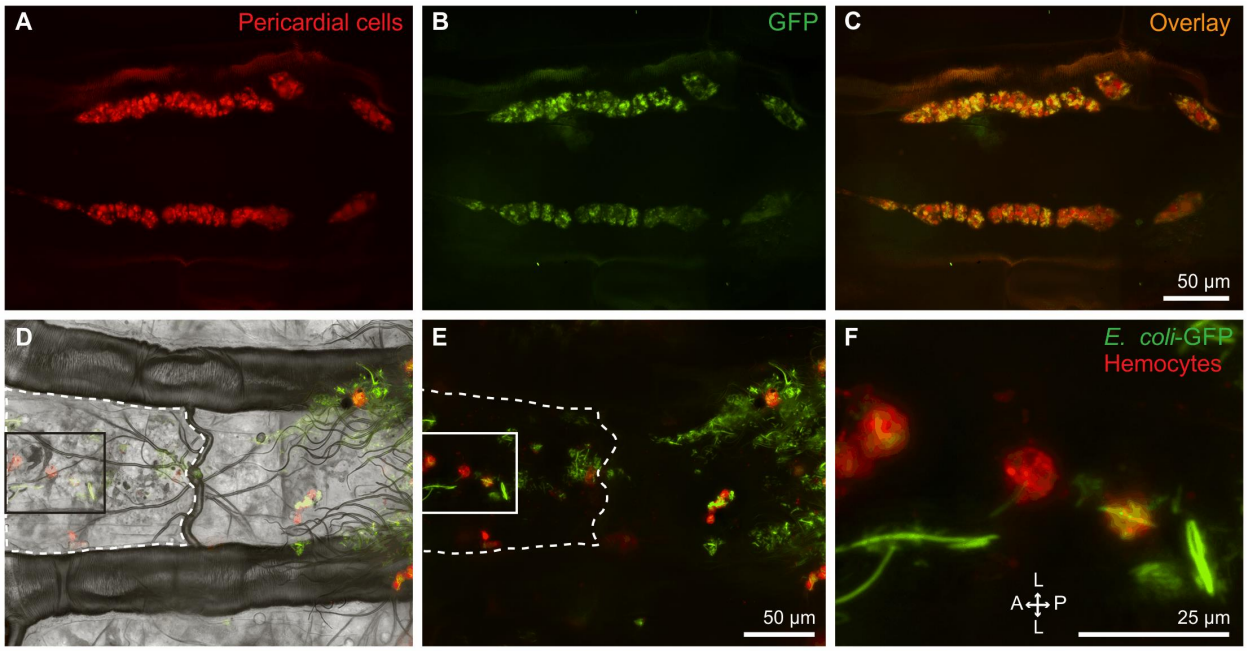

Figure 12. GFP signal from periostial region ROIs of larvae originate from pericardial cells and segmental hemocytes. (A-C) Fluorescence images taken at 4 h post-treatment showing that pericardial cells (A; IgG 568 nm, red) pinocytose GFP (B) that is flowing with the hemolymph following its release from degrading GFP-*E. coli* (overlay of A and B is shown in C). (D-F) Bright-field and fluorescence images of a portion of the seventh and eighth abdominal segments of a dissected larva at 4 h post-injection with GFP-*E. coli* (green), showing that both the tracheal tuft hemocytes and the dorsal segmental hemocytes (CM-DiI; red) engage in phagocytosis. A group of segmental hemocytes (D, E, rectangle) that have phagocytosed *E. coli* within the seventh abdominal segment region of interest (area within dashed outline) is magnified in F. Neither pathogens nor hemocytes were detected within the periostial regions. Directional arrows: A anterior, P posterior, L lateral.

At 24 h post-treatment, little or no GFP-*E. coli* was detected in any specimen, regardless of treatment (Fig. 11D-F, H). Interestingly, the fluorescence signal in infected larvae was significantly lower than that of the injured larvae (RM 2 W ANOVA $P < 0.0001$ for treatment), and a Šidák test that compared the different body regions of infected larvae to the corresponding body regions of injured larvae showed that, with the exception of the first periostial region ($P = 0.2990$), this was the case for all regions of the body ($P \leq 0.0005$ for all other comparisons). Furthermore, there was an interaction between the type of treatment and the segment of the body being assayed (RM 2 W ANOVA $P < 0.0001$), indicating that the differences in the fluorescence

signal emitted in different segments changed with treatment. Visual analysis of the data and a Šidák *post hoc* test showed that this is due to a more pronounced decrease in the fluorescence signal at the tracheal tufts relative to the periostial regions in infected larvae ($P \leq 0.0005$ for all comparisons). Collectively, these findings indicate that larvae mount vigorous and effective antibacterial immune responses that are largely completed within 24 h of infection. These immune responses are strongest at the tracheal tufts, which surround the only incurrent openings of the larval dorsal vessel.

Infection induces a robust melanization immune response at the tracheal tufts

The fluorescence signal emitted by GFP-*E. coli* at 4 h post-treatment is indicative of a vigorous phagocytosis response at the tracheal tufts, and the absence of this fluorescence at 24 h post-treatment is indicative of bacterial clearance. However, the fluorescence signal at 24 h is significantly lower than the fluorescence signal in injury controls, and visual examination of the specimens showed that antibacterial melanization deposits are minor at 4 h post-infection but far more prevalent 20 h later, with these deposits being most abundant at the tracheal tufts. We hypothesized that the negative fluorescence signal seen at 24 h after infection is due to the dampening of fluorescence by dark melanin deposits, and this hypothesis was supported by high magnification fluorescence imaging of the tracheal tufts of infected larvae (Fig. 13).

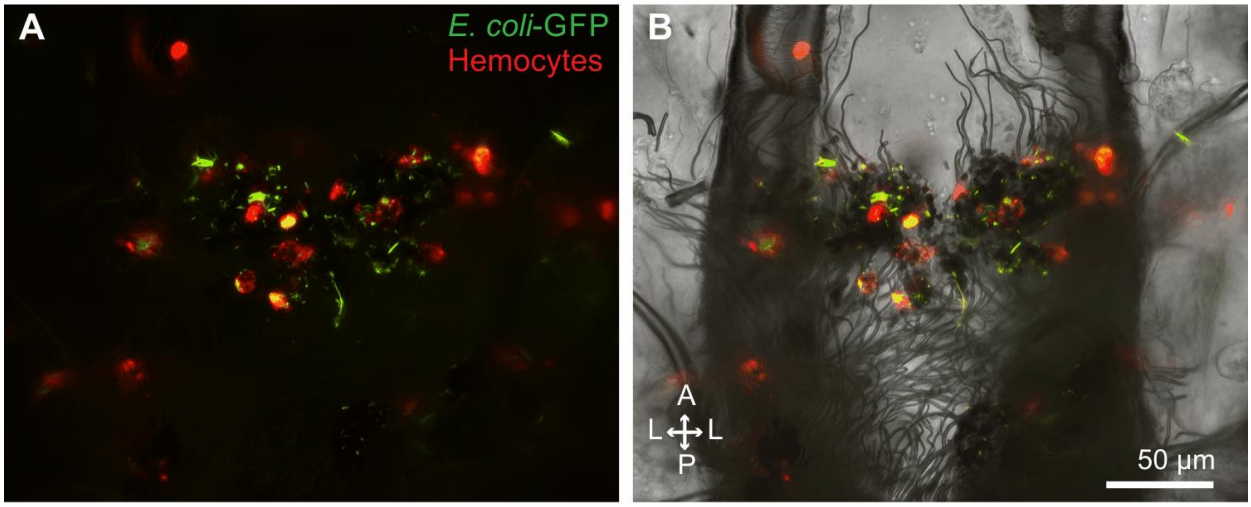

Figure 13. Tracheal tuft hemocytes phagocytose melanized bacteria. (A, B) Fluorescence (A) and bright-field overlay (B) images of tracheal tuft hemocytes (CM-DiI; red) phagocytosing aggregates of melanized (black) GFP-*E. coli* (green) at 4 h post-infection. Notice that melanin deposits dampen the fluorescence signal. Directional arrows: A anterior, P posterior, L lateral.

To quantitatively confirm that a melanization response is indeed taking place, we measured melanin deposition by calculating the mean pixel optical density (OD) in all the periostial regions as well as in the tracheal tufts of the same larvae used to calculate the phagocytosis response (Fig. 2B). In this type of analysis, a higher OD value indicates darker pixels and therefore a stronger melanization response.

At 4 h post-treatment, little or no melanization was visible in either injured or *E. coli*-infected larvae (Fig. 14A, C; RM 2 W ANOVA $P = 0.9969$ for treatment). At 24 h post-treatment, however, melanization remained negligible in injured larvae yet increased dramatically in *E. coli*-infected larvae (Fig. 14B, D; RM 2 W ANOVA $P < 0.0001$ for treatment). With the exception of the first periostial region (Šidák's $P = 0.5972$), the melanization response differed significantly across all pairwise comparisons between injured and infected larvae (Šidák's $P \leq 0.0079$ for all comparisons). Within the infected larvae, melanization was similar in all the periostial regions (Šidák's $P \geq 0.1727$ for all comparisons), but the melanization response

in the tracheal tufts was significantly stronger than in any of the periostial regions (Šidák's $P < 0.0001$ for all comparisons).

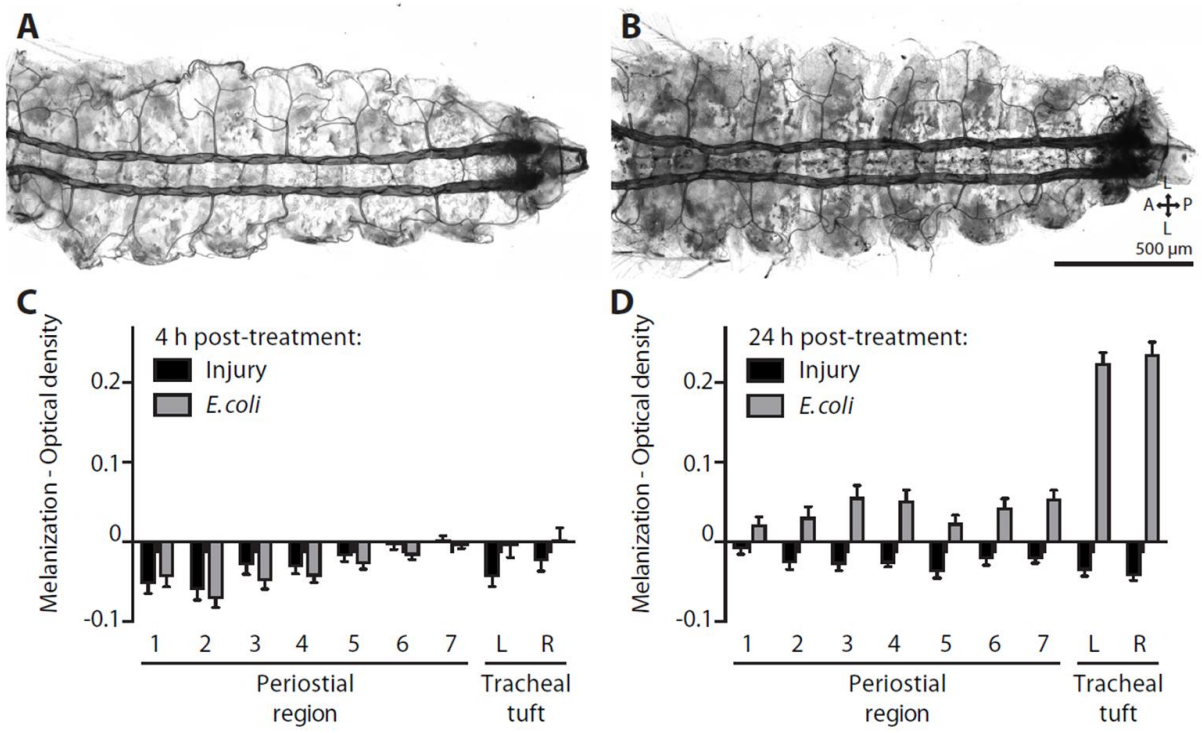

Figure 14. The melanization immune response is concentrated in the tracheal tufts. (A, B) Bright-field image of a dissected larval dorsal abdomen at 4 h (A) and 24 h (B) post-treatment with GFP-*E. coli*. At 4 h there is little or no visible melanization, whereas at 24 h widespread melanization is observed, including the uptake of melanin by the pericardial cells and an enrichment of melanin deposits in the tracheal tufts. (C, D) Melanization, as measured by mean pixel optical density (OD), in the periostial regions (1-7) and the left (L) and right (R) tracheal tufts of injured and GFP-*E. coli*-treated larvae at 4 h (C) and 24 h (D) post-treatment. At 4 h, OD values are similar in injured and *E*. coli-treated larvae ($P = 0.9969$), whereas at 24 h mean OD for all pairwise comparisons was significantly higher in infected larvae when compared to injured larvae ($P \leq 0.0079$ for all other comparisons). In C and D, whiskers denote the SEM. For a graphical presentation of how the ROIs were constructed, see Figure 2B. Directional arrows*:* A anterior, *P* posterior, L lateral.

Because the periostial regions of larvae are devoid of hemocytes, we scrutinized the location of melanin deposits in these regions using a combination of fluorescence and bright-field microscopy, and found that melanin accumulates at the periostial regions of infected larvae

because of the pinocytic activity of pericardial cells (Fig. 14B; Fig. 2B). At the tracheal tufts, however, melanin accumulation is much more pronounced, and this is primarily due to the accumulation and phagocytosis of melanized bacteria by the tracheal tuft hemocytes (Fig. 11; Fig. 14B, D; Fig. 13). Together, these data demonstrate a robust antibacterial melanization response in larvae, with much of the resultant melanin being deposited at the tracheal tufts, near the sole incurrent openings of the dorsal vessel.

Hemocytes are more prevalent in the tracheal tufts but do not aggregate upon infection

In adult mosquitoes, infection induces the migration of circulating hemocytes, whereby many exit circulation and bind to the initial population of sessile hemocytes present at the periostial regions of the heart (King and Hillyer, 2012; Sigle and Hillyer, 2016). To test whether pathogen accumulation in the eighth abdominal segment tracheal tufts of larvae is accompanied by further hemocyte aggregation in this region, naïve, injured and *E. coli*-infected larvae were incubated for 4 or 24 h, the hemocytes were stained *in vivo* with CM-DiI, and the fluorescence signal emitted by the hemocytes was measured (Fig. 15; Fig. 2C).

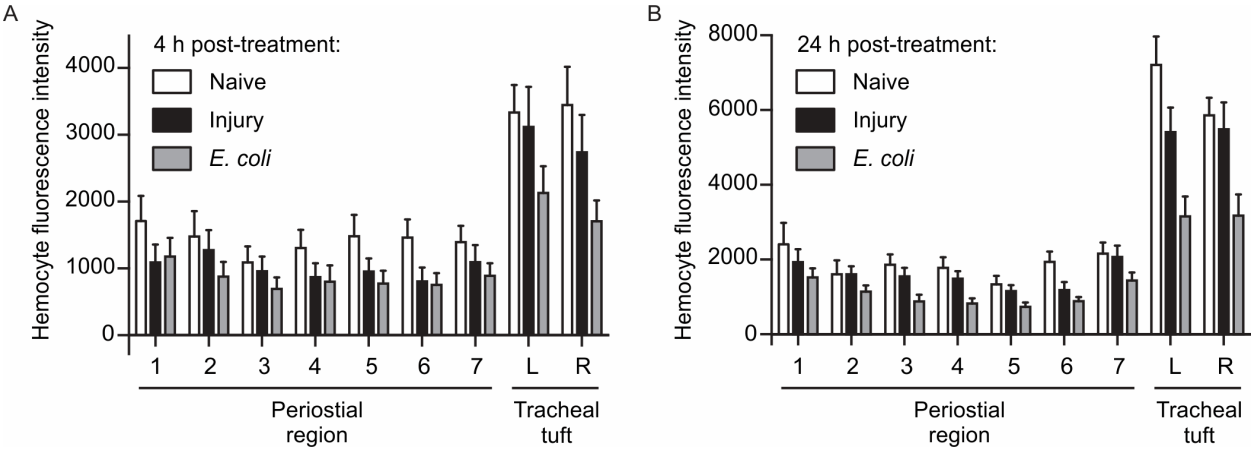

Figure 15. Hemocytes are more abundant in the tracheal tufts, but do not increase in response to *E. coli* infection. (A) Mean intensity of CM-DiI-stained hemocytes in the periostial regions (1-7) and the left (L) and right (R) tracheal tufts of naïve, injured, and GFP-*E. coli*-treated larvae at 4 h post-treatment. Hemocyte intensity was not significantly affected by treatment (RM 2 W ANOVA $P = 0.1123$) but was significantly higher in the tracheal tufts compared to the periostial regions in all three groups (Šidák's $P \leq 0.0312$ for 39 out of 42 comparisons). (B) Mean intensity of CM-DiI stained hemocytes in the periostial regions and tracheal tufts of naïve, injured, and GFP-*E. coli*-treated larvae at 24 h post-treatment. Hemocyte intensity was significantly affected by treatment (RM 2 W ANOVA P=0.0012), with hemocyte intensities from GFP-*E. coli*-treated larvae being significantly lower than those of both naïve and injured larvae (Šidák's $P < 0.0001$ for all comparisons). Hemocyte intensity was significantly higher in the tracheal tufts compared to the periostial regions in all three groups (Šidák's $P \leq 0.0003$ for all comparisons). Whiskers denote the SEM. For a graphical presentation of how the ROIs were constructed, see Figure 2C.

At 4 h post-treatment, there was no difference in the fluorescence signal emitted by hemocytes in naïve, injured, and infected mosquitoes (Fig. 15A; RM 2 W ANOVA $P = 0.1123$ for treatment). However, there was a significant difference between the regions of the body being measured (RM 2 W ANOVA $P < 0.0001$). Specifically, for naïve, injured, and infected mosquitoes, the fluorescence intensities of the two tracheal tufts were significantly higher than the fluorescence intensities in the corresponding periostial regions (Šidák's $P \leq 0.0312$ for 39 out of 42 comparisons). This indicates that hemocytes are absent from the periostial regions of infected larvae (any signal emanates from segmental hemocytes) but are abundant at the tracheal

tufts. This also indicates that at 4 h post-infection the relative number of tracheal tuft hemocytes in infected larvae is similar to that found in naïve and injured larvae.

At 24 h post-treatment, hemocyte intensity was significantly different between naïve, injured, and infected larvae (Fig. 15B; RM 2 W ANOVA P=0.0012). There was also a significant difference between the regions of the body being measured (RM 2 W ANOVA $P < 0.0001$), as the fluorescence signal in the tracheal tufts remained elevated relative to the periostial regions (Šidák's $P \leq 0.0003$ for all comparisons). Furthermore, there was a significant interaction between the region of the body and the treatment (RM 2 W ANOVA $P < 0.0001$ for interaction), indicating that the distribution of fluorescence signal in the different body regions changes depending on the infection status of the larva. Specifically, the fluorescence signal emitted by segmental hemocytes was similar between the periostial ROIs of naïve, injured, and infected larvae (Šidák's $P \geq 0.1528$ for all comparisons), but the signal in the tracheal tufts was lower in infected larvae when compared to naïve and injured larvae (Šidák's $P < 0.0001$ for all comparisons).

Taken together, these results suggest that although hemocytes are more abundant at the tracheal tufts, infection does not recruit circulating hemocytes to the periostial regions or to the tracheal tufts. At 24 h post-treatment, hemocyte fluorescence in the tracheal tufts of infected larvae was lower than that of naïve and injured larvae, but visual analysis of these specimens strongly suggests that this is not due to a reduction in the hemocyte population but rather due to melanization-induced dampening of the fluorescence signal (Fig. 11H; Fig. 14D; Fig. 2B and Fig. 13).

Discussion

Mosquitoes undergo a dramatic metamorphosis as they transition from an aquatic environment during the larval and pupal stages to terrestrial and aerial environments during the adult stage. In the present study, we show that the changes in circulatory and respiratory physiology that occur during the larval-to-adult transition are accompanied by stage-specific interactions between the circulatory, immune, and respiratory systems (Fig. 16). These systems are functionally integrated such that structures once thought to act solely in oxygen dissemination have been co-opted by the immune system to act as both a sieve to sequester circulating pathogens and as an ideal staging ground for mounting cellular and humoral immune responses at the sole entry points for hemolymph into the heart.

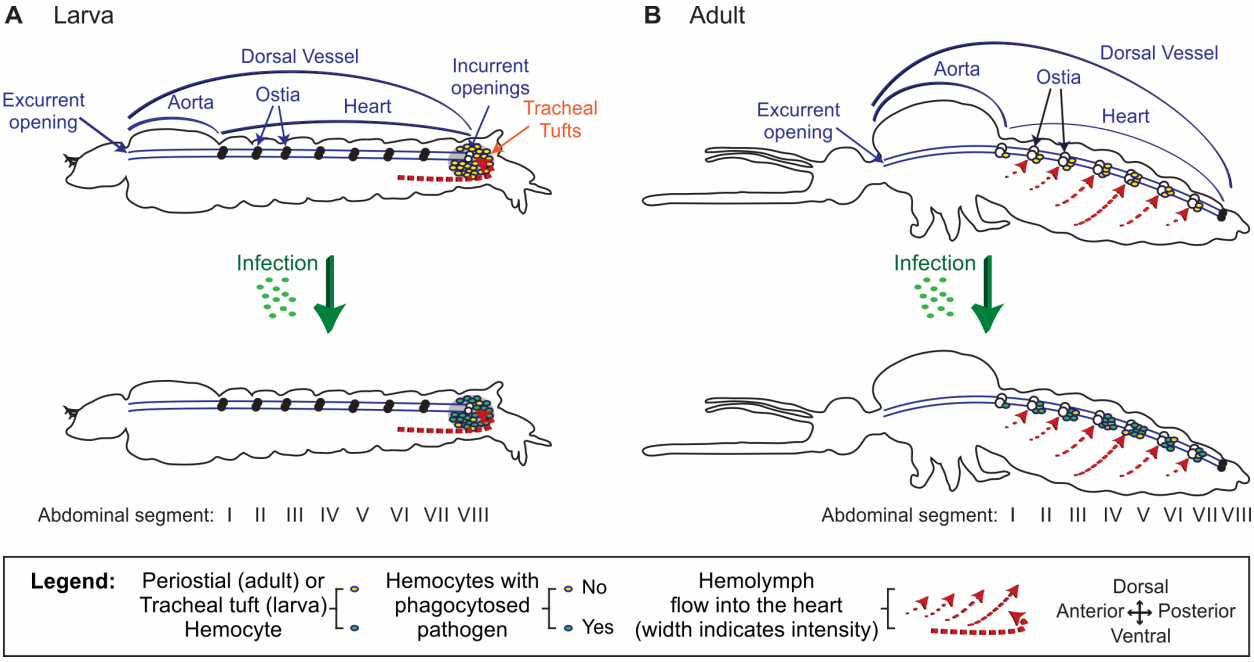

Figure 16. The circulatory and immune systems of mosquito larvae and adults are functionally integrated. (A) In larvae, hemolymph enters the heart via the posterior incurrent openings of the heart. At this location, tracheal tuft hemocytes phagocytose and kill pathogens as they flow with the hemolymph while en route to the heart. Infection does not induce the migration of hemocytes to the tracheal tufts. (B) In adults, hemolymph enters the heart via ostia located in abdominal segments 2-7. At these locations, periostial hemocytes phagocytose and kill pathogens as they flow with the hemolymph while en route to the heart. Infection induces the migration of additional hemocytes to the periostial regions, where they amplify the phagocytosis response. Illustrations are not drawn to scale.

A major finding in this study is that bacteria aggregate and are killed by hemocytes that are attached to the tracheal tufts of mosquito larvae, which are structures that surround the only incurrent openings of the heart. This represents an immune strategy where pathogen sequestration and killing occurs in the areas of the body that receive the highest amount of hemolymph flow. These locations are ideal for mounting immune responses, as they increase the probability of hemocytes encountering circulating pathogens and facilitate the rapid dissemination of hemocyte-produced humoral immune factors. Immune responses at the tracheal tufts are functionally, though not spatially, analogous to the immune responses that occur in the periostial regions of adult mosquitoes (King and Hillyer, 2012; King and Hillyer, 2013; Sigle and

Hillyer, 2016), as in both life stages pathogens and hemocytes associate with the entry points for hemolymph into the heart. Similar aggregations of pathogens at the periostial regions have also been observed in adult *Drosophila*, though these aggregations have not been linked to hemolymph flow or the structural mechanics of the heart, and have not been scrutinized at the cellular level (Elrod-Erickson et al., 2000; Horn et al., 2014). Furthermore, although melanotic nodules and melanized bacteria accumulate on the surface of the heart of lepidopteran larvae (Bao et al., 2011; Pereira et al., 2015), these melanin deposits are diffused along the length of the heart and do not associate specifically with the periostial regions (the tracheal tufts were not examined). Thus, it remains unclear whether these melanization responses in larval Lepidoptera are modulated by hemolymph flow.

A difference between the immune response at the periostial regions of adult mosquitoes and the immune response at the tracheal tufts of larvae is that infection induces the migration of additional hemocytes to the former but not the latter. The reason for this is unclear, but it may be due to the kinetics of the antibacterial immune response in these two life stages. In adults, we have observed bacteria at the periostial regions as far as 12 days post-infection (the last time point that was studied) (King and Hillyer, 2012), and other studies have documented the presence of bacteria in the hemocoel days or weeks after infection (Gorman and Paskewitz, 2000; Hillyer et al., 2005). In larvae, however, our method measuring fluorescence pixel intensity could not detect any bacteria at 24 h post-infection, and higher magnification observation of larval tissues detected few bacteria. Another possibility for the lack of an infection-induced increase in the number of hemocytes in the tracheal tufts is that, unlike in adults, larval hemocytes do not increase in number following immune stimulation or alter their adherence properties upon infection, as occurs in adults after blood feeding or immune

stimulation (Bryant and Michel, 2014; Bryant and Michel, 2016; Castillo et al., 2011; Christensen et al., 1989; King and Hillyer, 2012; King and Hillyer, 2013; Sigle and Hillyer, 2016). However, as these properties have yet to be tested in larval hemocytes, we presently hypothesize that the basal number of hemocytes at the tracheal tufts, in combination with the activity of other sessile and circulating hemocytes, is sufficient to rapidly clear systemic infections. This immune proficiency may in part be facilitated by the streamlined circulatory system of larvae, which contains a single pair of incurrent heart openings (League et al., 2015), as opposed to that of adults, which contains seven pairs of incurrent ostia (Glenn et al., 2010).

In adult mosquitoes, the primary cause of pathogen death at the periostial regions is phagocytosis (King and Hillyer, 2012; Sigle and Hillyer, 2016), and our data show that this immune response is also prominent at the tracheal tufts of mosquito larvae. This response begins within seconds of infection, which is similar to the speed of the phagocytosis response by the periostial, non-cardiac sessile, and circulating hemocytes of adult mosquitoes (Hillyer and Christensen, 2002; Hillyer et al., 2003a; Hillyer et al., 2003b; Hillyer et al., 2004; Hillyer and Strand, 2014; King and Hillyer, 2012; Sigle and Hillyer, 2016). Furthermore, much like in adult mosquitoes (Hillyer, 2016; Hillyer et al., 2003a; Hillyer et al., 2003b; King and Hillyer, 2012), melanization of bacteria is prevalent in larvae. Our observation that melanin deposits are predominant at the tracheal tufts suggests that hemolymph flow drives the accumulation of melanized bacteria at these respiratory structures, and some of the melanized bacteria are phagocytosed by hemocytes. These observations also provide a functional explanation for the spatial distribution of the melanization response against vertically transmitted *Elizabethkingia meningoseptica* that has been observed in *A. gambiae* larvae (Akhouayri et al., 2013), which also occurs in the eighth abdominal segment. Furthermore, our findings provide a new host-immunity

perspective on a previous report linking parasitoid wasp development to the tracheal tufts of *Heliothis virescens* caterpillars, where the authors suggest that the trapping of *Toxoneuron nigriceps* eggs in the tracheal tufts is advantageous for the development of the parasite because it places them in an environment that is rich in oxygen (Rao et al., 2009). Although the authors note that the propensity of the eggs to aggregate near the tracheal tufts is due to the natural flow of hemolymph, it is possible that the host immune response at the tracheal tufts outweighs any respiration-related benefits gained by the wasp eggs.

Our discovery that a high concentration of immunologically active hemocytes is associated with the eighth abdominal segment tracheal tufts of *A. gambiae* larvae represents the first description of this unique population of sessile hemocytes in Diptera. Populations of hemocytes in the posterior abdominal segments have been observed in other dipteran larvae, such as *Drosophila* (Babcock et al., 2008; Honti et al., 2014; Kurucz et al., 2007; Lanot et al., 2001; Makhijani et al., 2011; Márkus et al., 2009; Shrestha and Gateff, 1982b; Stofanko et al., 2008; Welman et al., 2010; Zettervall et al., 2004), *Calliphora* sp. (Arvy, 1953; Crossley, 1964; Zachary and Hoffmann, 1973), and *Musca* sp. (Arvy, 1953; Arvy, 1954). However, unlike the tracheal tuft-bound sessile hemocytes we describe in mosquito larvae, the posterior hemocytes described in other Diptera have not been documented as a hot spot of phagocytic activity during systemic infections or described as being associated with tracheal tufts.

Mosquito larvae are metapneustic, meaning they breathe through a single pair of posterior spiracles (Clements, 1992). Air enters these spiracles and is transported the length of the body by a pair of large dorsal longitudinal tracheal trunks. As they traverse the body, these tracheal trunks branch into a series of smaller segmental branches, which branch into increasingly smaller trachea, finally terminating as thin-walled tracheoles that directly oxygenate

the tissues to which they are permanently attached. However, the tracheoles that comprise the eighth abdominal segment tracheal tufts differ from other tracheoles in that, aside from some attachments to the posterior terminus of the heart, they float freely in the hemolymph instead of being attached to tissues (League et al., 2015).

Tracheal tufts, which have also been referred to as the "tracheole plexus" or "tracheal lungs," have been observed in the larvae of the mosquitoes *A. aegypti* (Christophers, 1960), *Culex* sp. (Imms, 1907; Raschke, 1887), *Anopheles maculipennis* (Imms, 1907; Wigglesworth, 1949), and *Anopheles quadrimaculatus* (Jones, 1954), as well as in the larvae of other dipterans (Dell, 1905; Imms, 1907; Vaney, 1902), but not in *Drosophila*, as our own experiments have confirmed. However, the tracheal tufts have been most comprehensively described in the lepidopteran *Calpodes ethlius* (Locke, 1997). Because of their obvious role in the oxygenation of hemolymph and their close association with hemocytes, the tracheal tufts were originally hypothesized to act as a "lung" for hemocytes. However, given that circulating and sessile hemocytes persist following eclosion and the tracheal tufts do not, we hypothesize that the tracheal tufts are not necessary for the direct oxygenation of hemocytes and instead function in the dissolution of oxygen into the hemolymph. This is supported by our observation that hemolymph flow is highest at the tracheal tufts (League et al., 2015), and thus, the contractile action of the heart disseminates newly dissolved oxygen to other parts of the body. More relevant to immune defense, we hypothesize that hemocytes associate with the tracheal tufts because, in a process analogous to the function of periostial hemocytes (King and Hillyer, 2012; King and Hillyer, 2013; Sigle and Hillyer, 2016), the attachment of immune cells to structures that surround the only incurrent opening of the heart places them in an ideal location to survey the hemolymph for foreign invaders. Additionally, we observed that hemocytes, both in

larvae and adults, have a propensity for binding to thin trachea, and we hypothesize that this also confers an immunological advantage, because the sites for gas exchange are also locations where pathogens often invade the hemocoel (Bukhari et al., 2010; Clark et al., 1968; Engelhard et al., 1994; Franz et al., 2015; King and Hillyer, 2013; Lacey et al., 1988; Miranpuri and Khachatourians, 1991; Romoser et al., 2004; Scholte et al., 2004).

To our knowledge, this study contains the first description of segmentally arranged sessile hemocytes in larval mosquitoes. These segmentally arranged cells are phagocytic, but infection does not induce the aggregation of hemocytes or the dense aggregation of pathogens within these locations. Because of their immune competence and their sheer abundance in the larval stage, this newly discovered population of sessile hemocytes represents a formidable immune reservoir. A similar arrangement of hemocytes, referred to as the segmentally arranged sessile hemocyte islets or patches, has been documented in *Drosophila* (Honti et al., 2014; Lanot et al., 2001; Makhijani et al., 2011; Moreira et al., 2013; Narita et al., 2004; Stofanko et al., 2008; Zettervall et al., 2004), as well as in other Diptera, such as the larger *Calliphora* flies (Crossley, 1964). In *Drosophila*, larval segmental hemocytes detach at the onset of pupation to engage in tissue remodeling (Lanot et al., 2001; Stofanko et al., 2008; Tepass et al., 1994) and in order to encapsulate parasitoid wasp eggs (Márkus et al., 2009; Zettervall et al., 2004). In adult mosquitoes, segmentally arranged hemocytes participate in the consumption of autolysing larval swim muscles during the first couple of days post-eclosion, and then dissipate (King and Hillyer, 2013). Our finding that these cells also contribute to bacterial clearance points to an even broader role for these sessile hemocytes in larval insect immune responses.

A. gambiae is a major vector of malaria in sub-Saharan Africa, and as such, understanding the innate immune defenses of this mosquito against invading pathogens is crucial

to the development of novel pest and disease control programs. In spite of this, the host immune response in larvae has received scant attention compared to the adult stage, a significant oversight considering that larvae are often a major target in pest control efforts (Fillinger and Lindsay, 2011; Tusting et al., 2013), and many common bacterial and fungal pesticides are seeded into mosquito breeding sites where they exert their effects in the hemocoel of larvae (Bukhari et al., 2011; Capone et al., 2013; Federici et al., 2003; Otieno-Ayayo et al., 2008). The present study uncovers an immune strategy that mosquito larvae use in combating microbial infections, which relies on the coordinated action of their circulatory, immune, and respiratory systems to sequester and kill pathogens present in the hemocoel.

CHAPTER IV

ANOPHELES GAMBIAE LARVAE MOUNT STRONGER IMMUNE RESPONSES AGAINST BACTERIAL INFECTION THAN ADULTS: EVIDENCE OF ADAPTIVE DECOUPLING IN MOSQUITOES

Preface

This chapter explores the relative strength and composition of larval and adult immune responses, as our previous comparative data on larval and adult circulation and immunity (Chapters II and III) show that differences exist in immune parameters between these life stages. I oversaw all of the work, and conducted, in whole or in part, all of the experiments. I carried out this work with Tania Estévez-Lao, who synthetized cDNA and ran the qPCR analyses, Yan Yan, who contributed to experiments on sessile hemocyte quantification, and Valeria Garcia-Lopez, a School for Science and Math at Vanderbilt high school student, who participated in the *in vivo E. coli* killing experiments. All experiments were designed, analyzed, and written with my advisor, Dr. Julián Hillyer, and, as of this writing, the manuscript from which this chapter is adapted has been submitted for publication.

Abstract

The immune system of adult mosquitoes has received significant attention because of the ability of females to ingest blood meals and vector disease-causing pathogens. However, few studies have focused on the immune system of larvae, which we hypothesize is highly robust due to the high density and diversity of microorganisms that larvae encounter in their aquatic environments, and the strong selection pressures at work in the larval stage to ensure survival to

reproductive maturity. Here, we surveyed a broad range of cellular and humoral immune parameters in larvae of the malaria mosquito, Anopheles gambiae, and compared their potency to that of newly-emerged adults and older adults. We found that larvae kill bacteria in their hemocoel with equal or greater efficiency compared to newly-emerged adults, and that antibacterial ability declines further with adult age, indicative of senescence. This phenotype correlates with more circulating hemocytes and a differing spatial arrangement of sessile hemocytes in larvae relative to adults, as well as with the individual hemocytes of adults carrying a greater phagocytic burden. The hemolymph of larvae also possesses markedly stronger antibacterial lytic and melanization activity than the hemolymph of adults. Finally, infection induces a stronger transcriptional upregulation of immunity genes in larvae than in adults, including differences in the immunity genes that are regulated. These results demonstrate that immunity is strongest in larvae and declines after metamorphosis and with adult age, and suggest that adaptive decoupling, or the independent evolution of larval and adult traits made possible by metamorphosis, has occurred in the mosquito lineage.

Introduction

Mosquitoes face the threat of infection during all stages of their holometabolous life cycle. These threats arise from numerous sources, including the microbe-rich aquatic environments where larvae reside and the infected blood meals that adults ingest. To combat pathogens that invade their hemocoel (body cavity), mosquitoes have evolved a diverse array of cellular and humoral immune responses (Hillyer, 2010). These responses begin when pathogen-associated molecular patterns are recognized by host-derived pattern recognition receptors. This recognition triggers the amplification or repression of extracellular signaling cascades, the initiation of intracellular signal transduction pathways, and, ultimately, the activation or

expression of immune effectors. These immune effectors, together with the circulating and sessile hemocytes (insect blood cells) that produce many of them, kill pathogens via phagocytosis, lysis, melanization, and other mechanisms (Hillyer, 2016; Hillyer and Strand, 2014).

Despite the critical importance of immune responses for survival, the vast majority of what we know about the mosquito immune system comes exclusively from experiments conducted on adult females, as this stage and sex is responsible for the transmission of blood-borne pathogens such as those that cause dengue (Blair and Olson, 2014; Cheng et al., 2016; Sim et al., 2014), lymphatic filariasis (Bartholomay, 2014; Erickson et al., 2009), and malaria (Clayton et al., 2014; Severo and Levashina, 2014). Recently, we described the functional integration of the circulatory and immune systems of mosquito larvae, whereby pathogens are phagocytosed and melanized by tracheal tuft hemocytes that surround the sole entry point of hemolymph (insect blood) into the heart (League and Hillyer, 2016). However, few other studies have described immune responses in larvae. Most of these studies have focused on uninfected larvae by assaying the developmental expression of immunity genes (Christophides et al., 2002; Costa-da-Silva et al., 2014; Estevez-Lao and Hillyer, 2014; Gupta et al., 2009; Koutsos et al., 2007; Li et al., 2005; Müller et al., 1999; Neira Oviedo et al., 2009; Suwanchaichinda and Kanost, 2009; Ursic Bedoya et al., 2005; Venancio et al., 2009; Vizioli et al., 2000; Vizioli et al., 2001a; Volz et al., 2005), or by describing hemocyte subpopulations (Castillo et al., 2006; Wang et al., 2011b). A minority of studies describing immune response in larvae assessed immune gene expression or protein levels in infected larvae (Biron et al., 2005; Dimopoulos et al., 1997; Meredith et al., 2008; Richman et al., 1996; Shin et al., 2005), and prior to our recently published work (League and Hillyer, 2016), to our knowledge only one study had described a larval

immune response: the encapsulation of the aquatic fungus, Lagenidium giganteum, by Aedes aegypti (Brey et al., 1988).

Although the immune system of mosquito larvae remains largely unexplored, two general lines of reasoning led us to hypothesize that larvae have evolved more proficient means of neutralizing infections than adults. First, by virtue of inhabiting aquatic environments that are rife with microorganisms, mosquito larvae are under constant threat of infection, whereas adults are less likely to encounter pathogens in their terrestrial and aerial habitats. Second, larvae have yet to fulfill any of their reproductive potential, and hence, strong selection pressures must be at work on the larval immune system to increase the probability of their survival to reproductive maturity (Hamilton, 1966; Koella et al., 2009; Monaghan et al., 2008). As a corollary to this, as mosquito adults age and fulfill their reproductive potential, investment in the immune system is expected to wane in order to reallocate resources to other adult processes, such as reproduction (Hurd et al., 2005; Pompon and Levashina, 2015; Rono et al., 2010). If larval and adult immune responses indeed differ in either strength or composition, this would imply that future studies could no longer assume complete continuity in immune responses across life stages, and that metamorphosis has, to some extent, decoupled the larval and adult immune systems, thus enabling their independent evolution (Fellous and Lazzaro, 2011; Moran, 1994). Furthermore, if immune responses differ across life stages, this would have important implications for the creation of stage-specific control measures that are better tailored to the specific immune responses of each life stage.

To test the hypothesis that larvae display stronger immune responses compared to adults, and to gain a better mechanistic understanding of the larval response to infection, we conducted a series of comparative analyses of immune responses in larval and adult Anopheles gambiae. We

show that mosquito larvae are more proficient than adults in killing bacteria, and that this correlates with stronger cellular and humoral immune responses in larvae compared to adults. Furthermore, we uncovered evidence of immune senescence within the adult stage, as the antimicrobial immune response of adults declines over the first five days of life.

Materials and Methods

Mosquito rearing and maintenance

Anopheles gambiae Giles *sensu stricto* (G3 strain) were reared and maintained at 27°C and 75% relative humidity in an environmental chamber set to a 12 h: 12 h light:dark cycle. Larvae were reared in plastic tubs containing deionized water and fed a combination of koi food and baker's yeast. The resulting pupae were separated from the larvae and placed into plastic containers with marquisette tops, and adults that emerged were fed a 10% sucrose solution. All experiments were performed on fourth instar larvae and adult female mosquitoes at 1 and 5 days post-emergence.

Mosquito injection and bacterial infection

Mosquito larvae were immobilized by removal of excess water and injected at the mesothorax (League et al., 2015). Mosquito adults were cold anesthetized and injected at the thoracic anepisternal cleft. For all experiments involving bacterial injection, a Nanoject II Auto-Nanoliter Injector (Drummond Scientific Company, Broomall, PA, USA) was used to inject 69 nl of the following: live, tetracycline resistant, GFP-expressing *E. coli* (modified DH5α; GFP-*E. coli*) in Luria-Bertani's rich nutrient medium (LB), heat-killed GFP-*E. coli*, heat-killed *Micrococcus luteus*, heat-killed *Enterobacter* sp. isolate Ag1 (Jiang et al., 2012; Wang et al.,

2011a), or LB medium alone. For all experiments involving cellular staining solutions (see below), approximately 0.2 µl of a solution was injected using an aspirator.

Bacteria were grown overnight in a 37°C (or 27°C for *Enterobacter*) shaking incubator until they reached an optical density of approximately OD_{600} = 5, as measured in a BioPhotometer plus spectrophotometer (Eppendorf AG, Hamburg, Germany). For experiments using live GFP-*E. coli*, live bacteria were injected at either OD_{600} = 5, which we refer to as the high dose, or diluted with LB medium to OD_{600} = 1, which we refer to as the low dose. Unless otherwise stated, all experiments were carried out at the high dose. The absolute doses of the bacterial inoculums were determined by performing serial dilutions of the GFP-*E. coli* cultures and spreading them on LB agar plates. These plates were grown overnight at 37°C, the number of resulting colony forming units (CFUs) were counted, and the doses were calculated. Low doses of *E. coli* (OD_{600} = 1) ranged from 1,932 to 33,741 (average = 18,061) and high doses (OD_{600} = 5) ranged from 53,889 to 77,970 (average = 65,171). For experiments using heat-killed bacteria, 50 µl of bacterial culture was incubated at 95°C for 10 min on an IncuBlock heating block (Denville Scientific, Holliston, MA, USA), and injected after cooling. Plating of the heat-killed cultures, which resulted in no CFUs, confirmed that all bacteria were dead.

Measurement of in vivo bacteria killing efficiency

Mosquito larvae, 1-day-old adults, and 5-day-old adults were injected with either low or high doses of GFP-*E. coli*. After 24 h, mosquitoes were homogenized in phosphate buffered saline (PBS; pH 7.0) and a dilution was spread on LB agar plates containing tetracycline. After overnight incubation at 37°C, the resulting CFUs in each plate were screened for GFP fluorescence, and were counted to calculate infection intensities. Four independent trials, each paired for both mosquito age (including stage) and *E. coli* dose, were conducted. Each trial

consisted of approximately 10 mosquitoes per group, and the data were combined and analyzed using the Kruskal-Wallis test, followed by Dunn's multiple comparisons *post hoc* test.

Quantification of circulating hemocytes

For each mosquito, an incision was made across the lateral and ventral portions of the suture that joins the 7th and 8th abdominal segment of naïve, injured (LB-injected), and *E. coli*-infected larvae, 1-day-old adults, and 5-day-old adults at 24 h post-treatment. A finely pulled glass capillary needle was then inserted into the thorax, approximately 200 µl of Schneider's *Drosophila* medium was perfused through the mosquito, and the diluted hemolymph was collected within two 1 cm diameter etched rings on a Rite-On glass slide (Gold Seal; Portsmouth, NH, USA) (King and Hillyer, 2013). After allowing the hemocytes to adhere to the slide for 20 min, cells were fixed and stained using Hema 3 (Fisher Scientific, Pittsburgh, PA, USA), and, after drying, mounted with coverslips using Poly-Mount (Polysciences, Warrington, PA, USA) (Coggins et al., 2012; Hillyer et al., 2005). The total number of hemocytes was then counted under bright-field conditions at 40x magnification using either a Nikon 90i compound microscope (Nikon, Tokyo, Japan) or an Olympus BH-2 microscope (Olympus, Tokyo, Japan). Three independent trials consisting of approximately 5 individuals per treatment group were conducted (N=14-16 per group). Data were analyzed by two-way ANOVA, using age (including stage) and treatment as variables, followed by Šidák's *post hoc* test.

Quantification of sessile hemocytes associated with the dorsal abdomen

The hemocytes from naïve, injured, and *E. coli*-challenged larvae, 1-day-old adults, and 5-day-old adults were fluorescently labelled *in vivo* at 24 h post-treatment by injecting live animals with 67 µM of Vybrant CM-DiI Cell-Labeling Solution (Invitrogen, Carlsbad, CA, USA) and 1.08 mM Hoechst 33342 nuclear stain (350/461; Invitrogen) in PBS, and incubating

them at 27°C and 75% relative humidity for 20 min (King and Hillyer, 2012; League and Hillyer, 2016). Larvae were fixed for 5-10 min by immersion in 4% paraformaldehyde (Electron Microscopy Sciences, Hatfield, PA, USA) and then dissected along a coronal plane. Specimens were rinsed in PBS, and the dorsal abdomens, sans the internal organs, were mounted on a glass slide using Aqua-Poly/Mount (Polysciences Inc., Warrington, PA, USA). Adults were fixed for 5-10 min by injection of 4% paraformaldehyde and then dissected along a coronal plane. Specimens were placed in 0.5% Tween in PBS, rinsed briefly in PBS, and the dorsal abdomens, sans the internal organs, were mounted on a glass slide using Aqua-Poly/Mount.

Dissected larval and adult dorsal abdomens were imaged under bright-field and fluorescence illumination using a Nikon 90i microscope connected to a Nikon Digital Sight DS-Qi1 Mc monochrome digital camera and Nikon's Advanced Research NIS Elements software. To render images with extended focal depth, Z-stacks of specimens were acquired using a linear encoded Z-motor, and all images within a stack were combined to form a single focused image using either NIS Elements' Maximum Intensity Projection (for quantification) or Extended Depth of Focus (EDF; for viewing) modules.

Sessile hemocytes attached to the dorsal abdominal wall were quantified by two methods. In the first method, custom polygonal regions of interest (ROI) were drawn on the maximum intensity projections to delineate the dorsal and lateral portions of abdominal segments 2-8, as was done previously for the periostial regions and tracheal tufts of larvae (League and Hillyer, 2016), and the mean pixel intensities of CM-DiI fluorescence within the ROIs were measured and recorded for each abdominal segment as well as for the entire dorsal and lateral abdomen (Fig. 1). For each specimen, background fluorescence was removed by subtracting the intensity values from the abdominal segments of each group's corresponding unstained naïve specimens.

In the second method, EDF images were used to manually count the sessile hemocytes within abdominal segments 4, 5 and 6, with these hemocytes categorized as being bound to one of three tissues: (1) the cuticular integument, (2) the heart (periostial hemocytes), or (3) the trachea. Data were analyzed by two-way ANOVA, using age (including stage) and treatment as variables, followed by Šidák's *post hoc* test.

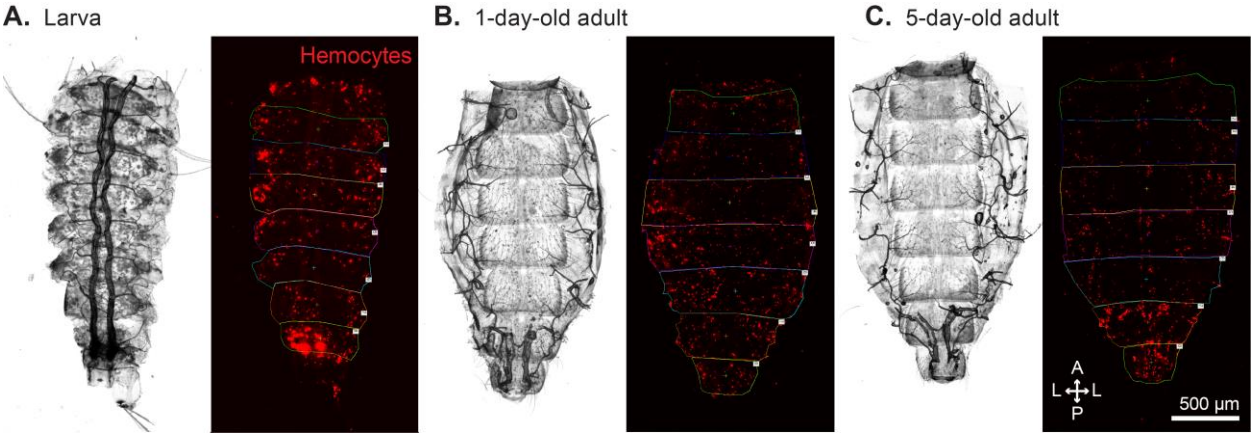

Figure 1. Fluorescence emitted by sessile hemocytes in larvae and adults was measured using custom-drawn regions of interest. Representative images of dissected larva (A), 1-day-old adult (B) and 5-day-old adult (C) dorsal and lateral abdomens imaged under bright-field and fluorescence illumination at 24 h post-infection with E. coli. Hemocytes were stained with CM-DiI (red). Seven custom regions of interest (ROIs), encompassing abdominal segments 2-8, were used to quantify mean fluorescence intensity of CM-DiI stained hemocytes. ROIs delineated the dorsal (tergum) and lateral (pleuron) abdominal cuticle that lies between the abdominal sutures of adjoining abdominal segments. Directional arrows: A, anterior; P, posterior; L, lateral.

Quantification of phagocytosis by circulating hemocytes

Larvae, 1-day-old adults, and 5-day-old adults were injected with *E. coli*, and 1 h later, hemocytes were perfused as described above, except that each mosquito was perfused with approximately 50 µl of Schneider's medium and all the perfusate was collected onto a single etched ring. After allowing the hemocytes to adhere to the slide for 20 min, cells were fixed for 5 min by adding 50 µl of PBS containing 4% formaldehyde and 0.03 mM Hoechst 33342 nuclear

stain. After removal of the fixation and staining solution, slides were mounted with coverslips using Aqua-Poly/Mount. Specimens were then examined under 100x magnification using simultaneous DIC and fluorescence illumination on a Nikon 90i microscope. For each mosquito, the number of bacteria that had been phagocytosed by each of the first 100 hemocytes viewed was counted. These values were used to calculate two parameters: (1) the phagocytic index, which is defined as the percentage of cells that engage in phagocytosis; and (2) the phagocytic capacity, which is defined as the average number of phagocytosed bacteria per hemocyte (Coggins et al., 2012). Three independent trials consisting of 10 individuals per age were conducted. Data were analyzed by the Kruskal-Wallis test, followed by Dunn's *post hoc* test.

Quantification of antimicrobial hemolymph activity

Using a hemolymph extraction method we adapted from a protocol used for *Drosophila* larvae and adults (Musselman et al., 2011), hemolymph was extracted at 24 h after treatment from larvae, 1-day-old adults, and 5-day-old adults that were naïve, injured, or treated with heat-killed *E. coli*, *M. luteus*, or *Enterobacter* sp. Briefly, an incision approximately 5 mm in length was made into the bottom of a 0.6 ml microfuge tube using a feather blade, and freshly wounded larvae or adults were placed inside. This tube was then inserted into a 1.5 ml microfuge tube, which was centrifuged to collect the hemolymph. For each larval collection, up to ten individuals were placed on a Kimwipe to remove all external water before placing the larvae on the inner rim of the 0.6 ml tube. An insect pin was used to puncture the thorax of each larva and the tubes were centrifuged for 10 sec in a mini centrifuge. This resulted in the collection of 1-2 µl of hemolymph. For each adult collection, 20-30 individuals were cold-anesthetized and an insect pin was used to puncture the lateral thorax. The mosquitoes were then placed in the 0.6 ml tube

and centrifuged at 2,152 rcf for 5 min at 4°C. This resulted in the collection of 1-2 µl of hemolymph. Immediately after collection, hemolymph was stored in a -20°C freezer until use.

Antimicrobial activity of hemolymph was measured via a zone of inhibition assay that we adapted from protocols developed for bumblebee workers (Moret and Schmid-Hempel, 2000) and mealworm beetle larvae (Haine et al., 2008). Briefly, a 2 ml *M. luteus* culture was grown overnight in LB broth at 37°C in a shaking incubator until it reached approximately OD_{600} = 10. The entire *M. luteus* culture was then added to 20 ml of sterile, liquid 1% LB agar that was maintained at 55°C by immersion in a water bath. The solution was mixed, and 5 ml of the *M. luteus*-LB agar solution was poured into 9 cm diameter Petri dish plates. After solidifying, equidistant holes were created in the agar 1.5 cm from the outer edge of the Petri dish by piercing and suctioning using a 1 mm tip sterile glass Pasteur pipette. Each hole was then loaded with 1 µl of hemolymph and, once the hemolymph had been absorbed by the agar, the plates were placed upside down in a 37°C incubator for 16 h. Plates were then scanned at 1200 pixels per inch using an Epson Perfection V600 scanner (Epson America, Inc., Long Beach, CA), and images were analyzed using ImageJ software (Schneider et al., 2012). For each sample, the diameters of the individual zones of bacterial growth inhibition were measured three times at different locations, and the average of these diameters was used to calculate the areas of the zones of inhibition. Five independent trials for each of the three bacterial treatments were conducted, each consisting of 2-3 larval and 1-2 adult pooled hemolymph samples per treatment group (naïve, injured, and treated with heat-killed bacteria; N=12-15 and N=5-6 for larval and adult groups, respectively). The data were combined and analyzed by two-way ANOVA, using age (including stage) and treatment as variables, followed by Šidák's *post hoc* test.

Quantification of the phenoloxidase activity of hemolymph

Using the method described for the zone of inhibition assay, hemolymph was extracted from naïve, injured, and *E. coli*-infected larvae, 1-day-old adults, and 5-day-old adults at 24 h post-treatment. Because we noted that using PBS as a solvent causes auto-oxidation of DOPA, and hence darkening that is not caused by phenoloxidase activity, all experiments utilized sterile water as the diluent, and not PBS. After adding 1 µl of extracted hemolymph to 50 µl of water, 10 µl of the diluted hemolymph solution (or water alone in the case of the negative control) was added to a cuvette containing 90 µl of one of the following three solutions: (1) 4 mg/mL 3,4-Dihydroxy-L-phenylalanine (L-Dopa; Sigma); (2) 20 mg/mL Sodium Diethyldithiocarbamate Trihydrate (DETC; Fisher Scientific) and 4 mg/mL L-DOPA; or (3) water alone. Absorbance readings were measured at 490 nm every 5 min for 30 min using a BioPhotometer plus spectrophotometer. Five independent trials were conducted, each consisting of 1 larval or adult sample per treatment group. The data were combined and analyzed by repeated measures two-way ANOVA, using age (including stage) and treatment as variables, followed by Šidák's *post hoc* test.

Quantification of immunity gene expression by qPCR

Total RNA was extracted from the whole body of approximately forty larvae, twenty 1-day-old adults and twenty 5-day-old adults that were naïve, or had been injected 24 h earlier with LB (injury), or GFP-*E. coli*. RNA was purified after homogenization in TRIzol reagent (Invitrogen), and repurified using the PureLink Micro-to-Midi Total RNA Purification System (Invitrogen). For each sample, 5 µg of RNA was treated with RQ1 RNase-Free DNAse I (Promega, Madison, WI, USA) to remove any contaminating genomic DNA, and then used as template for cDNA synthesis using an Oligo$(dT)_{20}$ primer and the SuperScript III First-Strand

Synthesis System for RT-PCR (Invitrogen). Real-time quantitative PCR was performed using Power SYBR Green PCR Master Mix (Applied Biosystems, Foster City, CA) on a Bio Rad CFX Connect Real-Time PCR Detection System (Hercules, CA, USA). Relative quantification of mRNA levels was performed using the $2^{-\Delta\Delta C}{}_T$ method (Livak and Schmittgen, 2001), and mRNA levels were calculated relative to the naïve groups of each mosquito age. In all experiments, ribosomal protein gene *RPS7* was used as the reference gene, and the ribosomal protein gene *RPS17* was used as a control. Primer sequences are listed in Appendix A. Melting curve analyses after RT-PCR confirmed that the cDNAs used in the experiments were free of genomic DNA contamination and that only the gene of interest was amplified. Three independent trials were conducted, and each trial was analyzed in duplicate. Data is presented as the average fold-change relative to the naïve group of a given life stage or adult age. Data for each gene were analyzed separately by age (stage) using the Kruskal-Wallis test, followed by Dunn's *post hoc* test.

Results

Larvae and newly-emerged adult mosquitoes kill bacteria in their hemocoels more efficiently than older adult mosquitoes

To begin to test whether larval and adult mosquitoes have different immune proficiencies, we infected larvae and differently aged adults with either low (OD600 = 1) or high (OD600 = 5) doses of E. coli, and measured their bacterial load 24 h later. We found that, for both doses, bacterial killing proficiency differed significantly between the larval and adult stages (Fig. 2; Kruskal-Wallis $P<0.0001$ for both doses). Specifically, at 24 h following a low dose infection, the bacterial load in fourth instar larvae, 1-day-old (newly-emerged) adults, and 5-day-old adults had decreased by 94%, 86% and 22%, respectively. At 24 h following a high dose

infection, bacterial load had decreased by 85% and 81% in fourth instar larvae and newly-emerged adults, respectively, but increased by 81% in older adults. Statistical analysis of the data revealed that larvae killed significantly more bacteria than 1-day-old and 5-day-old adults following the low dose infection (Dunn's test P=0.0179 and P<0.0001, respectively), but when infected with the high dose, larvae were only more proficient at killing bacteria than 5-day-old adults (P<0.0001). Taken together, these experiments show that larvae and 1-day-old adults display a stronger ability to combat systemic hemocoel infections than 5-day-old adults, and that the difference of the response is more pronounced at higher infection intensities.

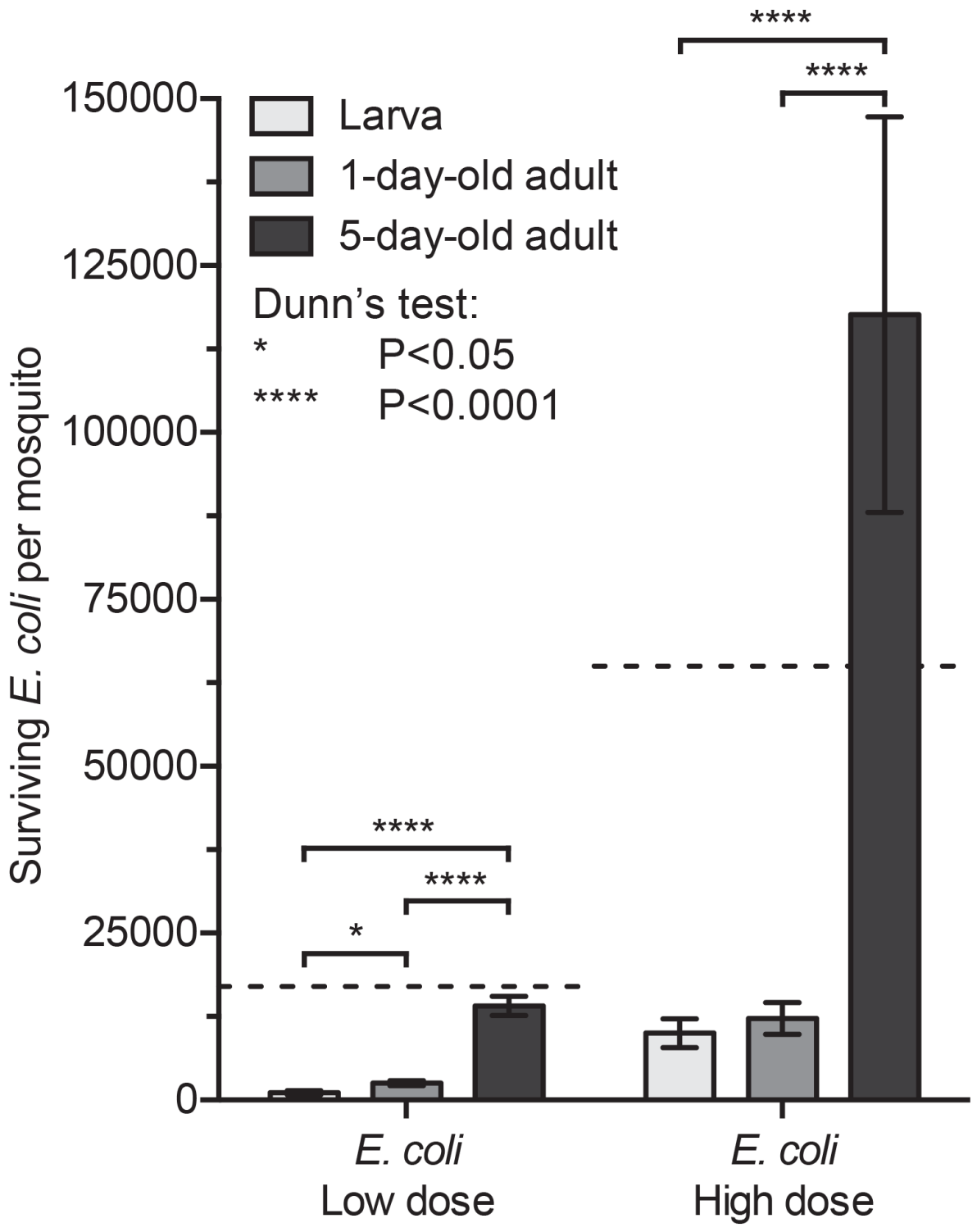

Figure 2. Larvae kill *E. coli* in their hemocoels more efficiently than adults. Average number of *E. coli* in the hemocoel (+/- SEM) of larvae, 1-day-old adults, and 5-day-old adults at 24 h following infection with either a low dose (average = 18,061) or a high dose (average = 65,171) of *E. coli*. Data for each dose were analyzed by the Kruskal-Wallis test, followed by Dunn's multiple comparisons *post hoc* test.

Larvae contain more circulating hemocytes than both newly-emerged and older adults, and larval hemocytes increase in abundance following infection

Because hemocytes are the first cellular responders to infection and kill pathogens via phagocytosis and the production of humoral immune factors (Hillyer and Strand, 2014; Strand, 2008), we hypothesized that the developmental differences we observed in the killing of *E. coli* could be due to differences in the number of circulating hemocytes available to quell the infection. To test this, we counted the circulating hemocytes in naïve, injured (injected with sterile LB broth), and *E. coli*-infected larvae, 1-day-old adults and 5-day-old adults at 24 h after treatment.

The number of circulating hemocytes changed significantly with mosquito life stage and age (Fig. 3; two-way ANOVA $P<0.0001$). Specifically, naïve larvae contain more circulating hemocytes (2,553) than either 1-day-old adults (1,561) or 5-day-old adults (1,097), and a similar age-related pattern was observed for both injured and infected mosquitoes (Šidák's multiple comparisons *post hoc* test $P\leq0.0061$ for all comparisons). Treatment also had a significant effect in the number of circulating hemocytes (two-way ANOVA $P=0.0053$), and this was due to an infection-induced increase in the number of circulating hemocytes in infected larvae compared to naïve larvae (Šidák's $P=0.0327$), which is an effect that was not seen in either 1-day-old adults or 5-day-old adults (Šidák's $P=0.2492$ and $P=0.4774$, respectively). Together, these data show that the number of circulating hemocytes declines following the larva to adult transition, and that this number continues to decline as mosquitoes age.

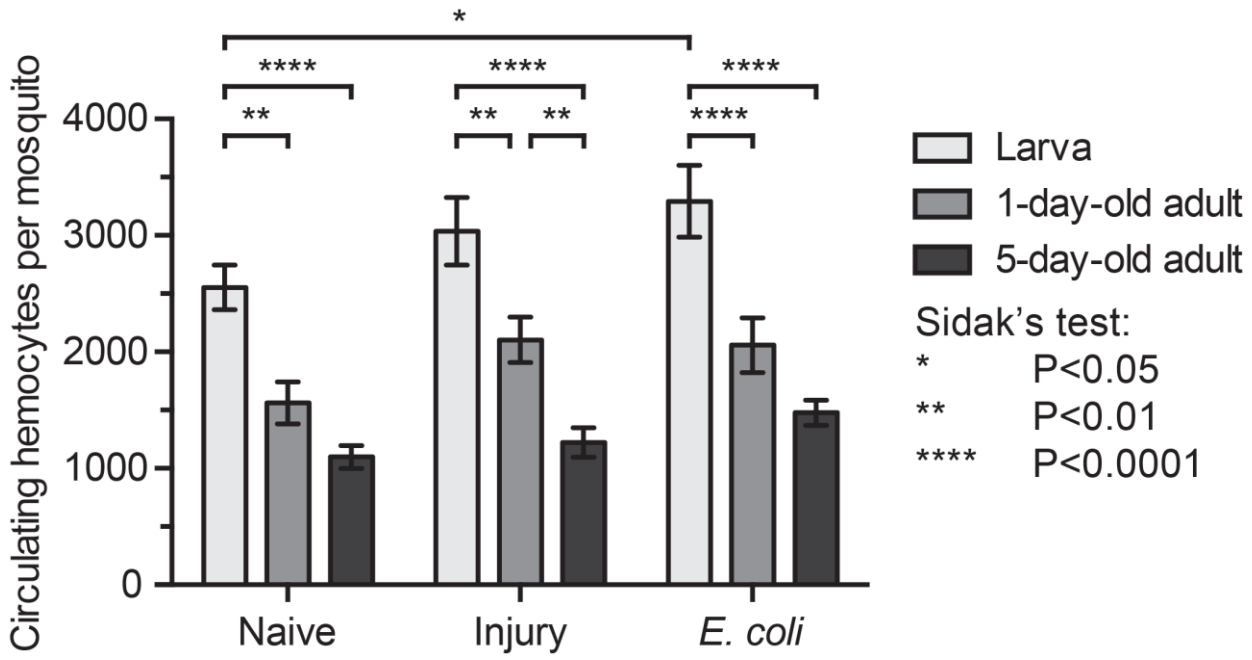

Figure 3. Larvae contain more circulating hemocytes than adults. Average number of circulating hemocytes (+/- SEM) in naïve, injured, or *E. coli*-infected (high dose) larvae, 1-day-old adults, and 5-day-old adults at 24 h post-treatment. Data were analyzed by two-way ANOVA, followed by Šidák's multiple comparisons *post hoc* test.

The spatial arrangement of sessile hemocytes differs between larvae and differently aged adults, and sessile hemocytes increase after infection in newly-emerged adults

We have previously shown that, regardless of the age of an adult mosquito, 75% of hemocytes circulate with the hemolymph whereas 25% are sessile, or attached to tissues (King and Hillyer, 2013). Furthermore, the majority of sessile hemocytes are present on the dorsal abdominal wall or the tissues associated with it (King and Hillyer, 2013). Thus, to compare the sessile hemocyte populations of larvae and adults, we labeled hemocytes *in vivo* using CM-DiI and quantified fluorescence intensity in the dorsal abdomen (Fig. 1).

Spatially, sessile hemocytes in larvae and one-day-old adults are arranged in segmental bands that encircle each abdominal segment, but hemocytes do not retain this clear segmental pattern in 5-day-old adults due to fewer hemocytes on the dorsal tergum (Fig. 4A-F).

Furthermore, hemocytes in larvae are distinctly aggregated at the 8th segment tracheal tufts that surround the posterior opening of the heart (Fig. 4A), a phenotype not observed in adults. Instead, in adults, hemocytes are aggregated in the periostial regions of the heart (Fig. 4B, C, E, F), although this phenotype is less distinct in 1-day-old adults due to more surrounding hemocytes on the dorsal cuticle. Measurements of CM-DiI fluorescence intensity in the dorsal (tergum) and lateral (pleuron) surfaces of the abdomen did not detect differences in the abundance of sessile hemocytes between naïve and injured larvae, 1-day-old and 5-day-old adults (Fig. 4G). However, *E. coli* infection caused a significant increase in hemocyte intensity in 1-day-old adults relative to both injured 1-day-old adults and infected 5-day-old adults (Fig. 4G; Šidák's P=0.0311 and P=0.0220, respectively). When hemocyte intensity was analyzed for each abdominal segment (instead of the entire abdomen), we found that the infection-induced increase in sessile hemocytes of 1-day-old adults was due to strong increases in hemocyte intensity in segments 4, 5 and 6 (Fig. 4H-J), and to a lesser extent in the other abdominal segments (Fig. 5). In larvae, the fluorescence intensity of hemocytes was significantly elevated in the 8th abdominal segment due to their strong association with the tracheal tufts, which is a phenotype not observed in adults (Fig. 4K).

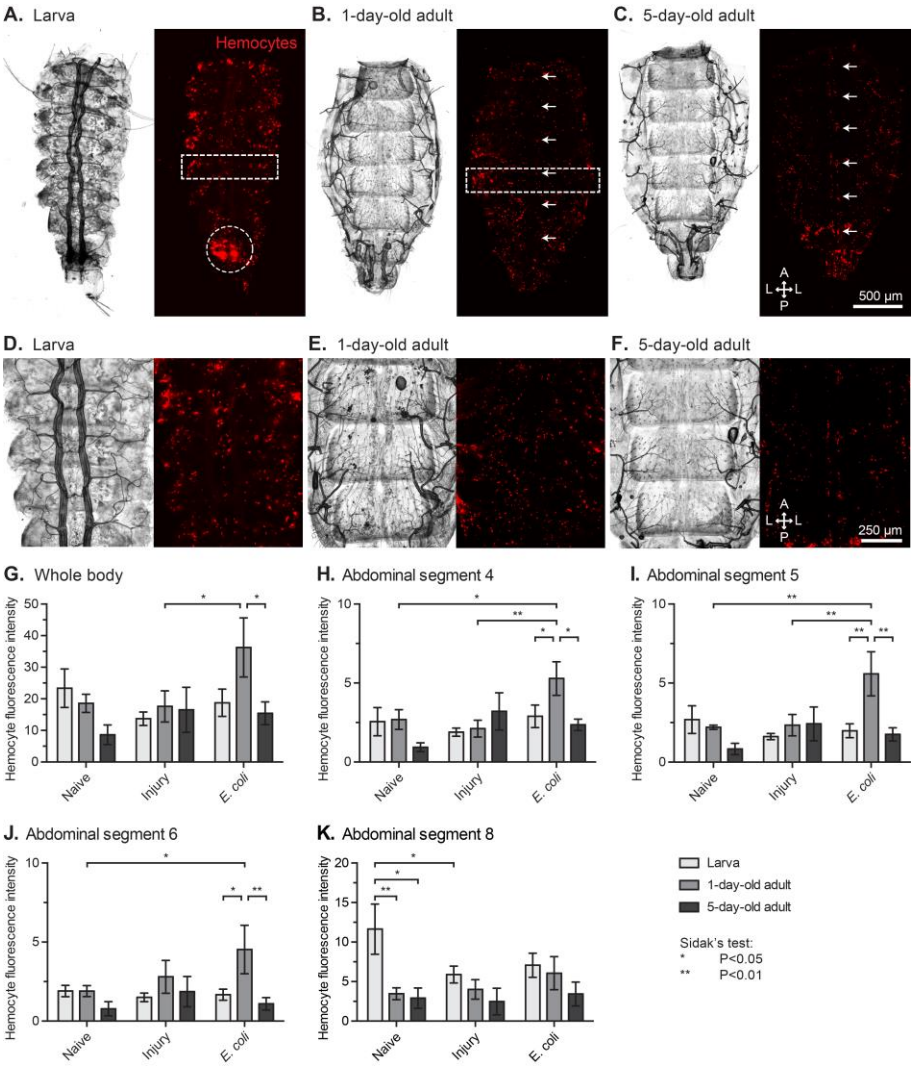

Figure 4. Sessile hemocytes differ in spatial arrangement and circulation-dependent aggregation across life stages and in response to infection. (A-F) Dissected larva (A, D), 1-day-old adult (B, E) and 5-day-old adult (C, F) dorsal and lateral abdomens viewed under bright-field and fluorescence illumination at 24 h post-infection with *E. coli*. D-F show higher magnification images of segments 4, 5, and 6. Hemocytes were stained with CM-DiI (red). Larvae showed segmentally arranged hemocytes (box in A, D) as well as a high concentration of hemocytes in the 8th abdominal segment (circle in A). One-day-old adults showed an abundance of segmental hemocytes (box in B, E), including periostial hemocytes (arrows in B, E). Five-day-old adults displayed a similar arrangement except that segmental hemocytes were more dispersed, and periostial hemocytes were more distinct (arrows in C, F). Directional arrows: A, anterior; P, posterior; L, lateral. (G-K) Total fluorescence intensity of CM-DiI-stained hemocytes from the dorsal and lateral abdomen for abdominal segments 2-8 combined (G) or from abdominal segments 4 (H), 5 (I), 6 (J), and 8 (K) alone in naïve, injured, and infected larvae, 1-day-old adults and 5-day-old adults at 24 h post-treatment. Quantitative data were analyzed by two-way ANOVA, followed by Šidák's *post hoc* test. In G-K, whiskers denote the SEM. Data for abdominal segments 2, 3, and 7 is presented in Fig. 5 and data for hemocyte counts in abdominal segments 4, 5, and 6 (D-F) is presented in Fig. 6.

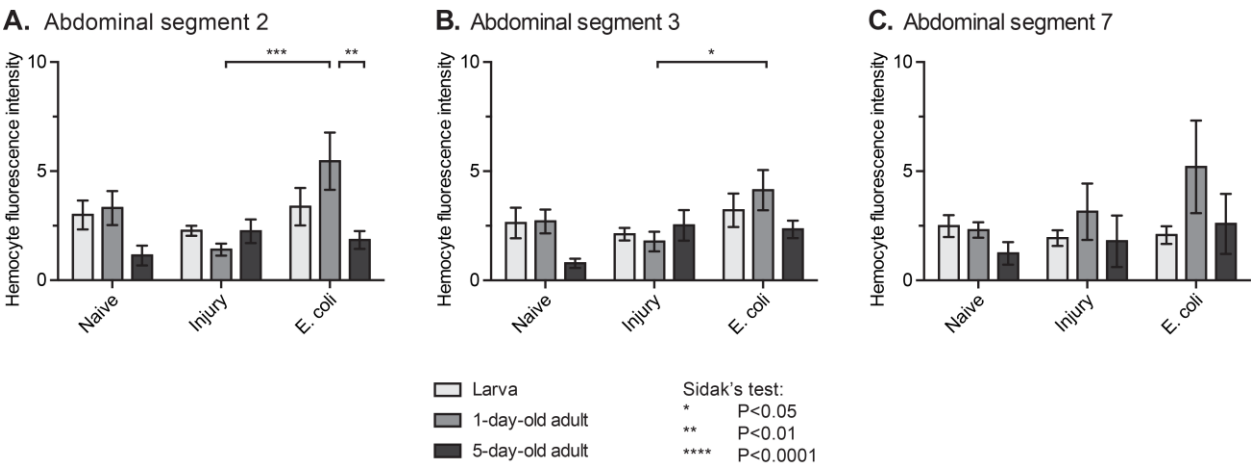

Figure 5. Sessile hemocytes of segments 2, 3, and 7 in response to infection. Fluorescence intensity of CM-DiI-stained hemocytes in abdominal segments 2 (A), 3 (B), and 7 (C) of naïve, injured, and *E. coli*-infected larvae, 1-day-old adults and 5-day-old adults at 24 h post-treatment. Quantitative data were analyzed by two-way ANOVA, followed by Šidák's *post hoc* test. Whiskers denote the SEM. Data for abdominal segments 4, 5, 6 and 8 is presented in Fig. 4.

To explore in greater detail the abundance of sessile hemocytes on the dorsal and lateral abdominal wall, we counted the number of hemocytes in segments 4, 5, and 6 and divided them by their anatomical location. We found that the infection-induced increase in sessile hemocytes in 1-day-old adults was due to an increase in the number of tracheal, cuticular, and periostial hemocytes relative to larvae and 5-day-old adults (Fig. 6; Šidák's $P \leq 0.0001$ for all comparisons). Together, these results show that sessile hemocytes are numerous in larvae and adults, and that they increase in number after infection in newly-emerged adults. This infection-induced increase is particularly evident in the mid abdominal segments, which in adults is a region where there is high immune activity (for example, at the periostial regions) and high hemolymph flow (King and Hillyer, 2012; Sigle and Hillyer, 2016). Furthermore, these findings confirm that the primary location of sessile hemocyte aggregation in larvae is at the tracheal tufts

of the eighth abdominal segment, which are structures that surround the posterior openings of the larval heart (League and Hillyer, 2016).

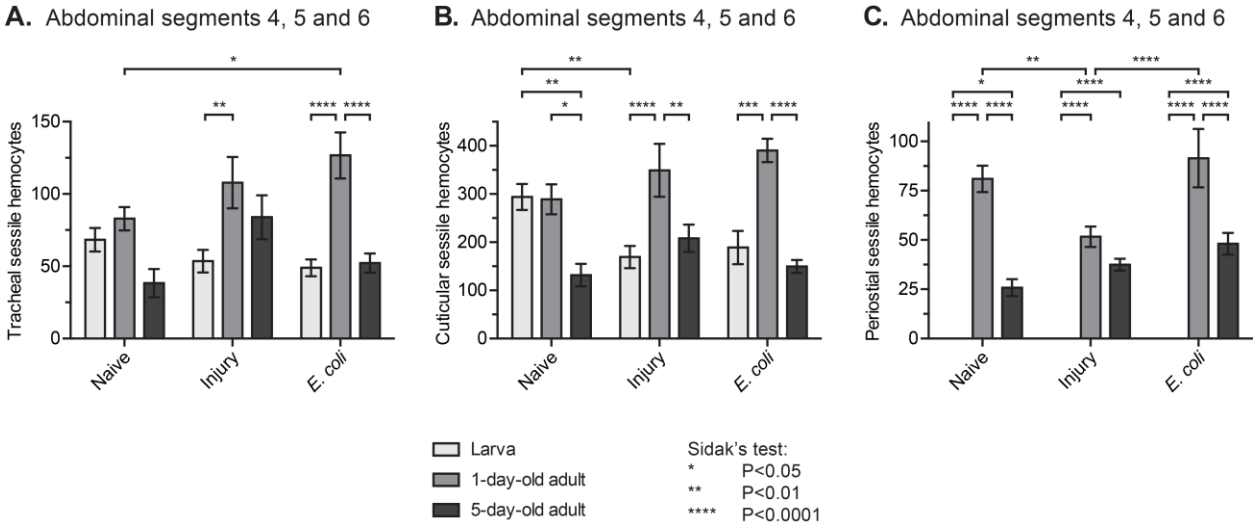

Figure 6. The distribution of sessile hemocytes in the trachea, cuticle, and periostial regions of abdominal segments 4, 5, and 6 varies with life stage and with infection state. Total number of CM-DiI-stained hemocytes attached to the trachea (A), cuticle (B, integument) and periostial regions of the heart (C) in abdominal segments 4, 5, and 6 of naïve, injured, and *E. coli*-infected larvae, 1-day-old adults and 5-day-old adults at 24 h post-treatment. Data were analyzed by two-way ANOVA, followed by Šidák's *post hoc* test. Whiskers denote the SEM.

The phagocytic activity of individual hemocytes is higher in adult mosquitoes compared to larvae

Our initial hypothesis postulated that changes in the abundance of hemocytes underscored the increased resistance of larvae and newly-emerged adults to a bacterial infection. However, differences in immune proficiency may also arise from differences in the frequency or degree to which hemocytes engage in phagocytosis. To test phagocytic activity across life stages, larvae and adults were infected with GFP-*E. coli* and the phagocytic activity of circulating hemocytes was quantified 1 h later. The phagocytic index, defined as the percentage of hemocytes that engage in phagocytosis following an immune challenge (Coggins et al., 2012;

Hillyer et al., 2005), differed significantly between larvae, 1-day-old adults, and 5-day-old adults (Fig. 7A; Kruskal-Wallis test $P<0.0001$). Specifically, 60%, 75%, and 85% of larval, 1-day-old adult, and 5-day-old adult hemocytes phagocytosed bacteria at 1 h post-challenge, respectively (Dunn's $P\leq0.0156$ for all comparisons). Phagocytic capacity, defined as the number of bacteria internalized by individual hemocytes, also differed significantly (Fig. 7B; Kruskal-Wallis $P<0.0001$), with larval, 1-day-old adult, and 5-day-old adult hemocytes containing an average of 2, 6, and 7 bacteria per cell, respectively (Fig. 7B; Dunn's $P<0.0001$ for all comparisons). When only hemocytes that phagocytosed bacteria were included in the analysis, a nearly identical pattern was observed (Fig. 7C; Kruskal-Wallis $P<0.0001$; Dunn's $P\leq0.0086$ for all comparisons). Interestingly, in addition to differences in levels of phagocytosis, following infection many larval hemocytes displayed a fibroblast-like morphology with numerous filopodial extensions, which is different from the rounded morphology that is most often observed in adult hemocytes (Fig. 7D-F). Together, these data show that, upon an identical bacterial challenge, the phagocytic burden of individual circulating hemocytes is higher in adults than it is in larvae (Fig. 7), although larvae contain more circulating hemocytes than adults (Fig. 3).

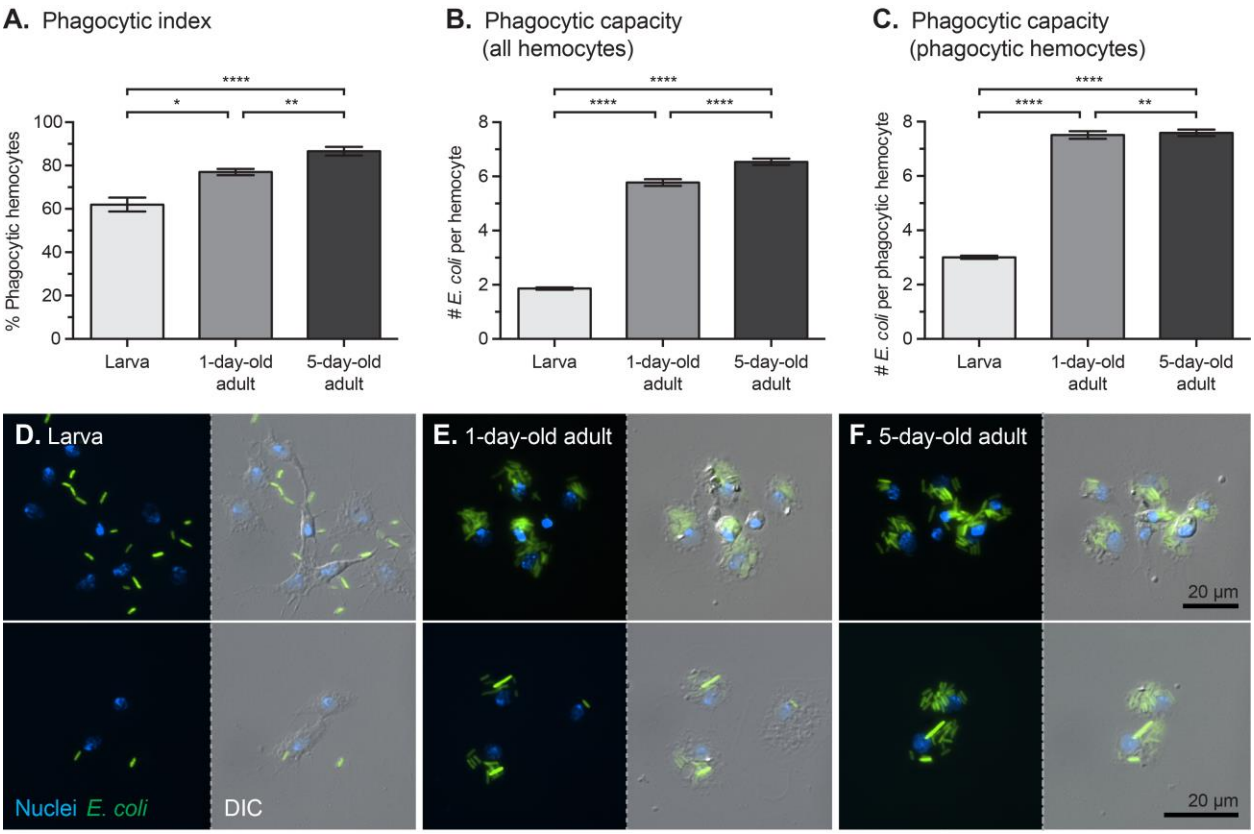

Figure 7. Hemocytes from adults carry higher phagocytic burdens and spread differently than hemocytes from larvae. (A) Percentage of larval and adult hemocytes that phagocytosed bacteria at 1 h post-infection with *E. coli* (phagocytic index). (B-C) Number of bacteria in individual larval or adult hemocytes at 1 h post-infection (phagocytic capacity). Data were analyzed for all hemocytes observed (B), and for only the hemocytes that had engaged in phagocytosis (C). Data were analyzed by the Kruskal-Wallis test, followed by Dunn's *post hoc* test (*, $P<0.05$; **, $P<0.01$; ****, $P<0.0001$). In A-C, whiskers denote the SEM. (D-F) Larval and adult hemocytes viewed under both fluorescence and DIC illumination. Phagocytosed GFP-*E. coli* (green) is contained within hemocytes whose nuclei have been stained with Hoechst 33342 (blue). Many larval hemocytes display fibroblast-like morphology (D), whereas hemocytes from newly-emerged adults (E) and older adults (F) display a more rounded spreading morphology.

Hemolymph from immune stimulated larvae has stronger antibacterial activity than hemolymph from adults

In response to infection, mosquitoes produce humoral immune factors that lyse pathogens (Bartholomay, 2014; Clayton et al., 2014; Hillyer, 2010; Severo and Levashina, 2014; Yassine and Osta, 2010) . To test whether the enhanced immunity we observed in mosquito larvae is

correlated with enhanced humoral antimicrobial activity in their hemolymph, we employed a zone of inhibition assay to measure the general antibacterial activity of hemolymph.

At 24 h following immune stimulation with heat-killed *E. coli*, the antibacterial activity of hemolymph differed significantly between larvae, 1-day-old, and 5-day-old adults (Fig. 8A-B; two-way ANOVA $P<0.0001$), and this was due to the significantly higher antibacterial activity of larval hemolymph compared to both adult groups (Šidák's $P<0.0001$ for both comparisons). Furthermore, this difference in antibacterial activity was due to an induced response, rather than a constitutive response, as the antibacterial activity in the hemolymph of naïve and injured individuals did not differ between larvae and adults, with the exception of when injured larvae were compared to 1-day-old adults (Šidák's $P=0.0387$). To test whether this finding was unique to immune stimulation with Gram (-) *E. coli*, we repeated the experiment by stimulating mosquitoes with heat-killed Gram (+) *M. luteus* (Fig. 8C-D) and heat-killed Gram (-) *Enterobacter* sp. isolate Ag1 (Fig. 8E-F), a bacterial strain that naturally colonizes the midgut of *A. gambiae* and is a core adult bacterial symbiont taxa (Jiang et al., 2012; Wang et al., 2011a). In both sets of experiments, antibacterial activity of hemolymph was significantly higher in larvae compared to adults (Fig. 8D, F; two-way ANOVA $P<0.0001$ for both bacteria; Šidák's $P\leq0.0252$ for all comparisons). This resulted from an induced response, as the antibacterial activity of hemolymph from naïve and injured mosquitoes did not differ between larvae and adults (Šidák's $P\geq0.2856$ for all comparisons). In sum, these experiments show that the strength of humoral antibacterial activity of hemolymph is stronger in larvae compared to adults.

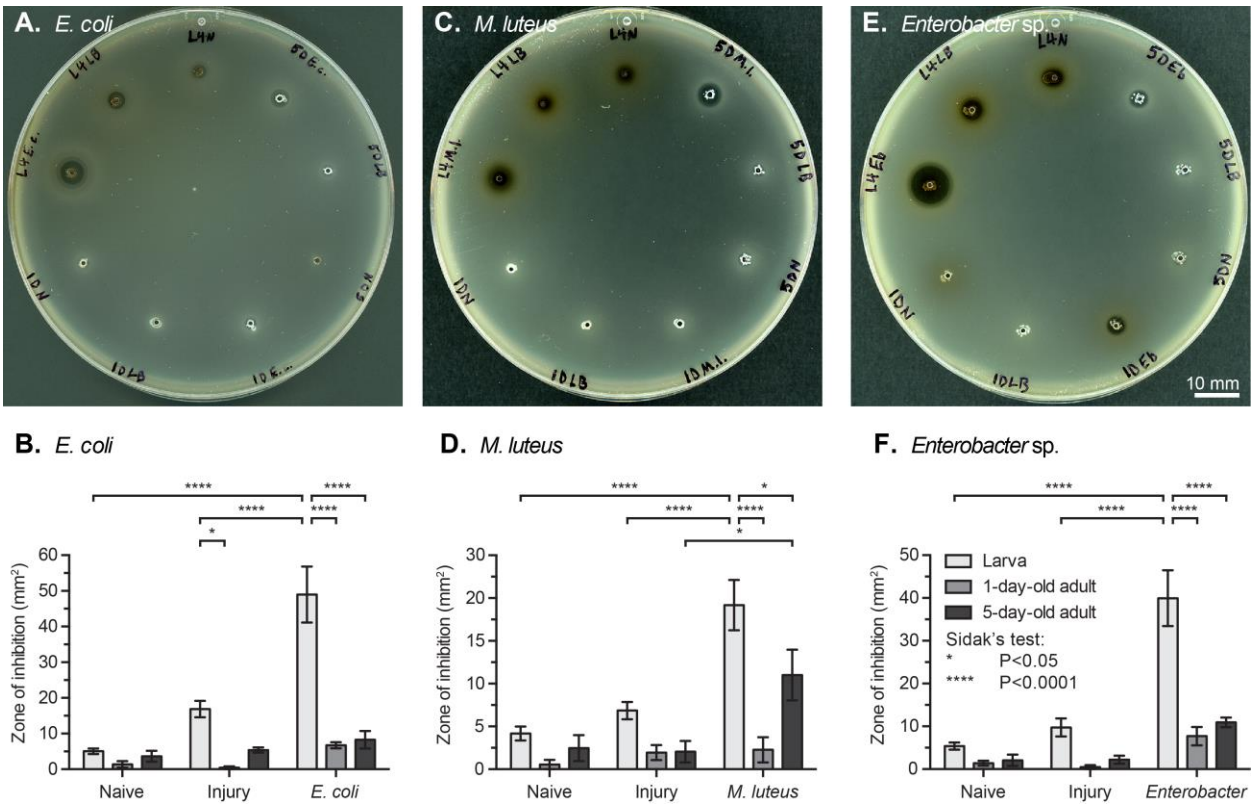

Figure 8. Larvae display stronger antibacterial humoral immunity compared to adults. (A-B) Zone of inhibition plating assay (A), including quantitative measurement of the zones of inhibition (B), showing the extent of hemolymph lytic activity in mosquitoes that were naïve, injured, or challenged with heat-killed *E. coli* 24 h earlier. (C-F) Similar experiment except using heat-killed *M. luteus* (C, D) or heat-killed *Enterobacter* sp. (E, F) as the challenge agent. Abbreviations in panels A, C, and E: L4, 4th instar larvae; 1D, 1-day-old adult; 5D, 5-day-old adult; N, naïve; LB, injured; E.c., *E. coli*; M.l., *M. luteus*; Eb, *Enterobacter*. In B, D, and F, data were analyzed by two-way ANOVA, followed by Šidák's *post hoc* test. Whiskers denote the S.E.M.

Phenoloxidase activity is higher in larvae compared to adults

While conducting experiments measuring the antibacterial activity of hemolymph, we noticed that hemolymph, especially from larvae, had a tendency to darken rapidly after extraction, a phenomenon suggestive of the activation of phenoloxidase-mediated melanization. Because melanization is a major component of the humoral immune response of mosquitoes (Christensen et al., 2005), we tested the relative strength of melanization in larval and adult hemolymph using a phenoloxidase activity assay (Sidjanski et al., 1997; Thomas et al., 2011)

that relies on the conversion of L-DOPA to dopachrome by phenoloxidase, a rate limiting enzyme in the melanization pathway (Christensen et al., 2005; Zhao et al., 1995) .

Measurements of the absorbance of diluted hemolymph (1:500 final dilution) incubated with L-DOPA, taken every 5 min for 30 min, showed that phenoloxidase activity differs significantly between life stages (Fig. 9A, B; repeated measures two-way ANOVA $P<0.0001$). Specifically, the phenoloxidase activity of larval hemolymph was significantly higher at all time points measured when compared to 1-day-old and 5-day-old adults (Šidák's $P\leq0.0263$ for all 5 min comparisons and $P<0.0001$ for all 10-30 min comparisons). Phenoloxidase activity is a constitutive response, rather than an induced response, because no differences in phenoloxidase activity were detected between the hemolymph of naïve, injured, and infected larvae or 1-day-old adults ($P>0.9999$ for all comparisons). In 5-day-old mosquitoes, infection reduced the melanization activity of hemolymph, with statistically significant differences beginning at the 20-min time point, suggesting that at the time of hemolymph collection the enzymatic cascade was partially depleted by immune responses during the ongoing infection ($P\leq0.0335$ for all but two of six pairwise comparisons). No melanization activity was detected when L-DOPA was incubated in water in the absence of hemolymph, confirming that L-DOPA was not undergoing auto-oxidation (Fig. 9A; Fig. 10; $P>0.9999$ for all comparisons).

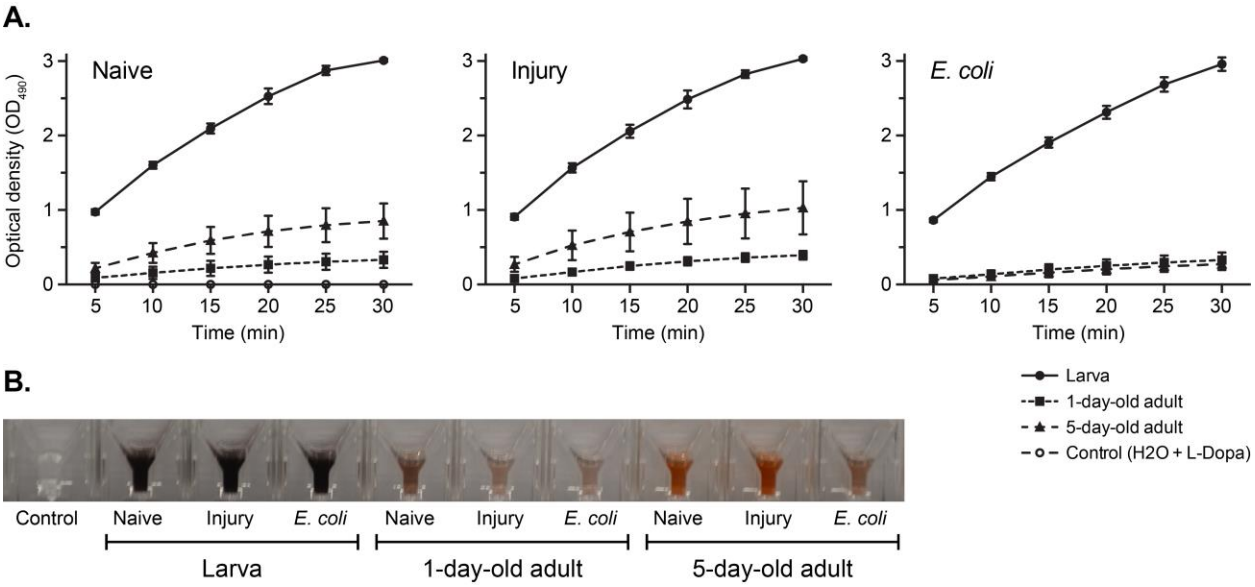

Figure 9. Larval hemolymph has higher phenoloxidase activity than adult hemolymph. (A) Time course of optical density (OD_{490}) measurements of hemolymph from naïve, injured, and *E. coli*-infected larvae, 1-day-old adults, and 5-day-old adults that was diluted in water containing L-DOPA. Data were analyzed by two-way ANOVA, followed by Šidák's multiple comparisons *post hoc* test. Regardless of treatment and time point, larvae showed higher phenoloxidase activity than 1-day-old and 5-day-old adults (Šidák's $P \leq 0.0263$ for all comparisons). Whiskers denote the SEM. (B) Images of cuvette wells at the 30 min time point showing that melanization-induced darkening is more pronounced in the larval samples.

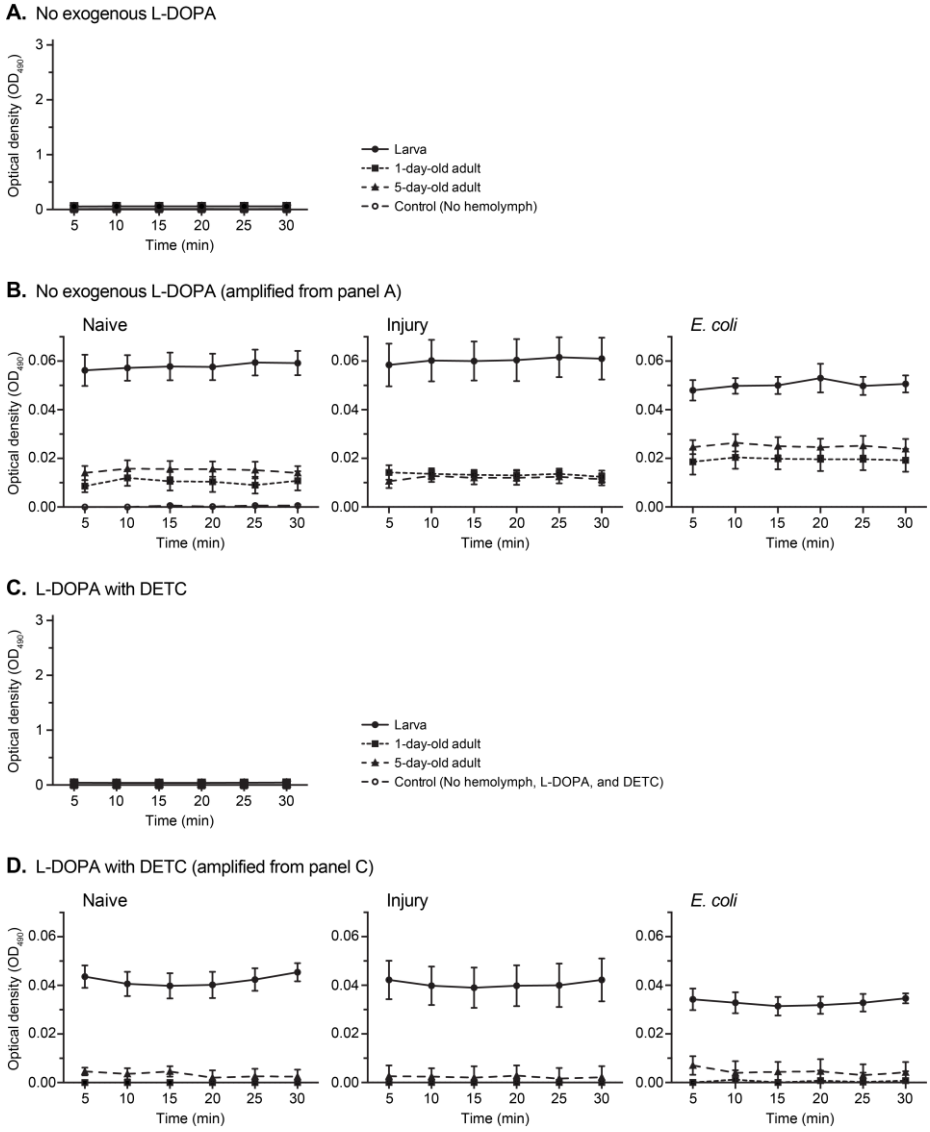

Figure 10. Phenoloxidase-based melanization of endogenous substrates is higher in larvae than in adults, and melanization of exogenous substrates is completely inhibited by DETC. (A-B) Time course of optical density (OD_{490}) measurements of hemolymph from naïve, injured, and *E. coli*-infected larvae, 1-day-old adults and 5-day-old adults diluted in water. The scale in panel A is amplified and separated by treatment in panel B. Larval hemolymph was significantly darker than adult hemolymph (Šidák's $P \leq 0.0086$ for all comparisons) and melanization levels did not change when comparing the initial and final readings of any age or treatment group (Šidák's $P \geq 0.1690$ for all comparisons). (C-D) Time course of optical density (OD_{490}) measurements of hemolymph from naïve, injured, and *E. coli*-infected larvae, 1-day-old adults and 5-day-old adults diluted in saturated L-DOPA with DETC, which is a phenoloxidase inhibitor. The scale in panel C is amplified and separated by treatment in panel D. Larval hemolymph was significantly darker than adult hemolymph (Šidák's $P \leq 0.0013$ for all comparisons) and melanization levels did not change from the initial to final readings of any age or treatment group ($P \geq 0.5840$ for all comparisons). Data were analyzed by two-way ANOVA, followed by Šidák's *post hoc* test. Whiskers denote the SEM.

To quantify the melanization of endogenous substrates in diluted hemolymph, as opposed to the conversion of exogenous L-DOPA as in the above experiment, we repeated the experiment by diluting hemolymph samples in water alone, without L-DOPA. As expected, because of the absence of exogenous substrate, the absorbance values in all samples were very low (Fig. 10A). Nevertheless, larval hemolymph was significantly darker than adult hemolymph (Fig. 10B; Šidák's $P \leq 0.0086$ for all comparisons), and no change in melanization occurred when comparing the initial and final readings, indicating that by the initial reading all endogenous substrates had been consumed in melanization reactions ($P \geq 0.1690$ for all comparisons).

Finally, to ensure that the darkening of hemolymph did not occur because of the activity of enzymes other than phenoloxidase, including iron-based peroxidase and catalase (Christensen et al., 2005), we mixed diluted hemolymph with a solution containing both L-DOPA and diethyldithiocarbamate (DETC), a copper-specific chelator that inhibits copper-based phenoloxidase (Ajamhassani et al., 2012; Christensen et al., 2005; Feng et al., 2008; Ryazanova et al., 2012). Although larval hemolymph was again significantly darker than adult hemolymph because of the rapid melanization of endogenous substrates soon after hemolymph collection (Fig. 10C, D; Šidák's $P \leq 0.0013$ for all comparisons), melanization levels did not change following the addition of the solution of L-DOPA and DETC ($P \geq 0.5840$ for all comparisons), confirming that the melanization activity of hemolymph is driven by the activity of phenoloxidase. Together, these findings demonstrate that larval hemolymph contains greater melanization potential than adult hemolymph, and that this is due to the activity of phenoloxidase.

Infection-induced transcriptional upregulation of immunity-related genes is higher in larvae than in adults

To determine whether larvae and differently aged adults differ with respect to the expression of immunity genes, relative mRNA fold change was assayed by qPCR at 24 h post-treatment in naïve, injured, and *E. coli*-infected larvae, 1-day-old adults, and 5-day-old adults (Fig. 11; Appendix A and B). A broad range of immune responses was surveyed by measuring the transcription of 24 immunity genes representing four major categories of immune function: (1) pathogen recognition, specifically *CTL4* (Osta et al., 2004; Pinto et al., 2009; Schnitger et al., 2009), *FREP13* (Christophides et al., 2002; Dong and Dimopoulos, 2009), *GNBPB4* (Warr et al., 2008), *TEP1* (Levashina et al., 2001; Moita et al., 2005), *Eater*, *Nimrod*, and *Draper* (Estévez-Lao and Hillyer, 2014), and *SCRBQ2* (Dimopoulos et al., 2002; González-Lázaro et al., 2009); (2) signal modulation, specifically *CLIPB15* (Christophides et al., 2002; Pinto et al., 2009; Volz et al., 2005) and *SRPN6* (Abraham et al., 2005; Pinto et al., 2008); (3) signal transduction, specifically Toll pathway members *MYD88* and *CACTUS* (Christophides et al., 2002; Ramirez and Dimopoulos, 2010; Xi et al., 2008), Imd pathway members *CASPL1* and *CASPAR* (Garver et al., 2012), and Jak/Stat pathway members *AGSTAT-A* and *PIAS* (Dong et al., 2012; Gupta et al., 2009; Souza-Neto et al., 2009); and (4) effector responses, specifically *CECA* (Christophides et al., 2002; Kim et al., 2004; Vizioli et al., 2000), *GAM1* (Christophides et al., 2002; Vizioli et al., 2001a), *DEF1* (Blandin et al., 2002; Christophides et al., 2002; Dimopoulos et al., 1997; Richman et al., 1996; Vizioli et al., 2001b), *PPO1* (Ahmed et al., 1999; Baton et al., 2009; Christophides et al., 2002; Müller et al., 1999), *PPO6* (Baton et al., 2009; Müller et al., 1999), *LYSC1* (Kajla et al., 2010; Kajla et al., 2011; Li et al., 2005; Li and Paskewitz, 2006), *NOS* (Hillyer and Estévez-Lao, 2010), and *DUOX* (Kumar et al., 2003; Kumar et al., 2010; Molina-

Cruz et al., 2008; Oliveira et al., 2011). In addition, the expression of two genes involved in the ecdysteroid biosynthetic pathway, *CYP302A1* and *CYP315A1* (Pondeville et al., 2008; Sieglaff et al., 2005), was measured, as ecdysone peaks in the late larval and pupal stages, and ecdysone induces the transcriptional upregulation of phenoloxidase genes in an *A. gambiae* hemocyte-like cell line (Ahmed et al., 1999; Müller et al., 1999). *RPS7* was used as the reference gene, and *RPS17* was used as a control (Coggins et al., 2012).

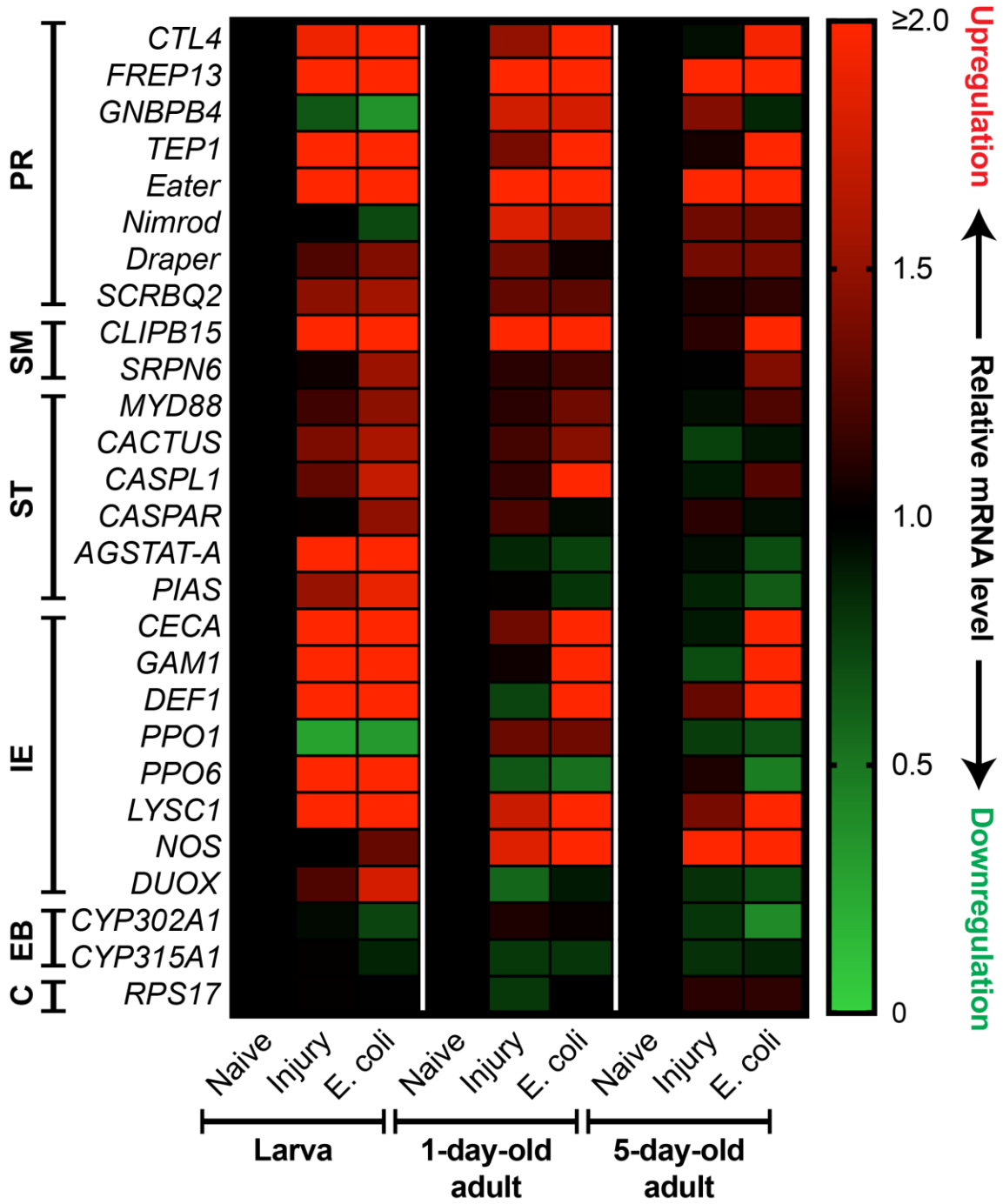

Figure 11. Infection-induced transcriptional regulation of immunity-related genes is higher in larvae than in adults. Heat map showing the average relative mRNA fold change of immunity-related genes in naïve, injured, and *E. coli*-infected larvae, 1-day-old adults, and 5-day-old adults. Data are normalized against naïve individuals of the same age. Red color indicates upregulation, green indicates downregulation, and black indicates no regulation (see scale on right). For detailed graphs for each gene, see Appendix B. Abbreviations for gene categories: PR, pathogen recognition; SM, signal modulation; ST, signal transduction; IE, immune effectors; EB, ecdysteroid biosynthesis; C, control.

In larvae, 17 immunity genes were either strongly (greater than 2-fold; 11) or weakly (between 1.5 and 2-fold; 6) upregulated by infection relative to naïve larvae, whereas in 1-day-old and 5-day-old adults, only 13 (11 strongly and 2 weakly) and 10 (9 strongly and 1 weakly) immunity genes were upregulated by infection, respectively, relative to naïve adults of their respective age (Fig 11; Appendix B). Transcription of ecdysteroid biosynthesis genes and, as expected, *RPS17* was not regulated by infection in any age group. In general, larvae and adults showed a similar level of induction of some pathogen recognition and signal modulation genes, as well as some immune effector genes, such as cecropin (*CECA*), gambicin (*GAM1*), defensin (*DEF1*) and lysozyme (*LYSC1*).

When comparing the levels of induction, larvae showed greater than 2-fold higher induction (that is, the fold change of the larval group divided by the fold change of the adult group was >2) of *AGSTAT-A*, *PIAS*, *PPO6*, and dual oxidase (*DUOX*) relative to both adult groups. Both adult groups showed greater than 2-fold higher induction of nitric oxide synthase (*NOS*) and a fibrinogen-related protein gene (*FREP13*, also known as *FBN9*) relative to larvae, and 1-day-old adults showed greater than 2-fold higher induction of a CLIP domain serine protease (*CLIPB15*) relative to larvae, despite *FREP13* and *CLIPB15* being greater than 2-fold upregulated in both life stages (Fig. 11; Appendix B).

In addition to differences in the level of induction of specific immunity genes across life stages, some genes were only upregulated in a single life stage. For example, infection in larvae, but not adults, induced the upregulation of Jak/Stat essential pathway genes *AGSTAT-A* and *PIAS*, as well as the immune effectors *PPO6* and *DUOX*. Conversely, infection in adults, but not larvae, strongly induced the upregulation of *NOS*. Interestingly, although the Gram (-) binding protein gene, *GNBPB4*, was transcriptionally downregulated in larvae following infection, when

all the data was instead normalized against naïve 5-day-old adults, basal expression of *GNBPB4* in naïve larvae was 470- and 710-fold higher than in naïve 1-day-old and 5-day-old adults, respectively. A similar finding was made with respect to one of the phenoloxidase genes assayed, *PPO1*, which was expressed 170- and 110-fold higher in naïve larvae relative to naïve 1-day-old and 5-day-old adults, respectively. Collectively, these data show that induction of immunity genes differs with life stage and adult age, with infection-induced expression being highest in larvae and declining shortly after eclosion and as adults age.

Discussion

Mosquitoes are susceptible to infections during all stages of their life cycle, and in response have evolved a robust innate immune system (Hillyer, 2010). Because the adult stage is responsible for the transmission of disease-causing pathogens such as malaria (Clayton et al., 2014; Severo and Levashina, 2014), the vast majority of research on mosquito immunology has focused on that life stage, and in particular, on the adult females that feed on blood. In contrast to this, research on the immune system of the larvae of other insects, such as *Manduca sexta*, *Bombyx mori*, and *Drosophila melanogaster* has proven invaluable for uncovering fundamental aspects of the cellular and humoral immune response of insects, and animals in general (Honti et al., 2014; Jiang et al., 2010; Lemaitre and Hoffmann, 2007). Nevertheless, lacking in Insecta are comparative studies that examine differences in immunity across the different life stages of a given species. As noted by Fellous and Lazzaro in 2011, "Almost all studies of the immune system of animals with metamorphosis have focused on either larval or on adult immunity, implicitly assuming that these traits are either perfectly correlated or evolutionarily independent" (Fellous and Lazzaro, 2011). Because mosquito larvae live in aquatic environments rife with microorganisms and survival through the larval stages is required to reach sexual maturity, at the

onset of this study we hypothesized that larvae have evolved more proficient means of neutralizing infections than adults. To compare larval and adult immunity in *A. gambiae*, we measured a broad range of immune parameters that were previously unexamined in larvae, and show that immune activity is strongest in larvae and wanes in the adult life stage, which is indicative of immune senescence (Table 1). Furthermore, because immunity phenotypes differ between life stages that are separated by metamorphosis, these findings suggest that adaptive decoupling, or the independent evolution of larval and adult traits made possible by metamorphosis (Moran, 1994), has occurred in *A. gambiae*.

Table 1. Mosquito immunity rapidly declines after metamorphosis and with adult age. Summary of the comparative immune data arising from experiments performed on larvae, 1-day-old adults, and 5-day-old adults. High, medium, and low responses are relative designations assigned by comparing each group to the other two groups and ranking them based on the strength of the response.

	Larva	1-day-old adult	5-day-old adult
Bacterial killing	High	High	Low
Number of circulating hemocytes (increase after infection)	High (Yes)	Medium (No)	Low (No)
Number of sessile hemocytes (increase after infection)	Medium (No)	High (Yes)	Low (No)
Phagocytic burden	Low	High	High
Antimicrobial activity of hemolymph	High	Low	Low
Phenoloxidase activity of hemolymph	High	Low	Medium
Immune gene induction	High	Medium	Low
Genes transcriptionally upregulated >2-fold (strongly)	*CTL4, FREP13, TEP1, Eater, CLIPB15, AGSTAT-A, CECA, GAM1, DEF1, PPO6, LYSC1*	*CTL4, FREP13, TEP1, Eater, CLIPB15, CASPL1, CECA, GAM1, DEF1, LYSC1, NOS*	*FREP13, TEP1, Eater, CLIPB15, CECA, GAM1, DEF1, LYSC1, NOS*
Genes transcriptionally upregulated 1.5-2-fold (weakly)	*SCRBQ2, SRPN6, CACTUS, CASPL1, PIAS, DUOX*	*GNBPB4, Nimrod*	*CTL4*

Evidence for adaptive decoupling has been found in a broad range of animals with complex life cycles, including amphibians, fish, marine invertebrates, and insects (Aguirre et al., 2014; Anderson et al., 2016; Ebenman, 1992; Fellous and Lazzaro, 2011; Moran, 1994; Parichy, 1998; Phillips, 1998; Quigley et al., 2004; Stoks and Córdoba-Aguilar, 2012). Several lines of evidence suggest that adaptive decoupling of immune responses has also occurred in the mosquito lineage. First, we have shown that the strength and composition of the mosquito

immune response differs between immature larvae, newly-emerged adults, and reproductively active older adults. Second, we have previously shown (King and Hillyer, 2012; League and Hillyer, 2016; Sigle and Hillyer, 2016), and recapitulate here, that the mosquito circulatory and immune systems display stage-specific functional integration, enabling functionally analogous, yet anatomically disparate immune strategies in larvae and adults. Third, mosquitoes have complex life cycles with ecologically distinct larval and adult stages that are subject to different selection pressures due to differences in pathogen exposure and reproductive status. Thus, we expect that a decoupling of key traits between these life stages, which are separated by metamorphosis, is advantageous to both stages in responding independently to differing selection pressures and in the performance of different fitness tasks (for example, food consumption and growth in larvae and reproduction in adults). Taken together, these arguments suggest that adaptive decoupling has occurred in mosquitoes, enabling the independent evolution of key larval and adult immune traits.

Our data show that larvae kill bacteria at a higher rate, possess more circulating hemocytes, have higher lytic and melanization activity in their hemolymph, and have higher infection-induced expression of immunity genes than adults, thus strongly supporting our hypothesis that mosquito larvae invest more in immunity than adults. In our view this is not surprising; larvae inhabit bacteria-rich pools and display higher gut microbial diversity than adults (Rani et al., 2009; Wang et al., 2011a), suggesting that mosquitoes are exposed to a higher density and diversity of bacteria as larvae than as adults, and require more robust immune responses as larvae, as has been hypothesized previously (Cornet et al., 2013). Thus, given the vastly different ecologies between larvae and adults, coupled with the fact that evolutionary pressures are strongest on younger individuals that have yet to reach their reproductive potential

(Hamilton, 1966; Koella et al., 2009), we hypothesize that the stronger selection pressures at work in the larval stage compared to the adult stage have over time caused larvae to invest more greatly in immunity than adults.

Our findings on immune proficiency in larvae and adults is also indicative of immune senescence, as immunity in larvae is stronger than in adults, and immunity continues to weaken after metamorphosis, with 5-day-old adults mounting weaker immune responses than adults that were 4 days younger. This finding is consistent with well-attested evolutionary theories of senescence, which state that greater selection pressures are at work in the larval stage to ensure survival to the reproductively mature adult life stage (Hamilton, 1966; Monaghan et al., 2008). According to the "Disposable Soma" theory of aging, this occurs in part due to immune trade-offs that would not be in play at the larval stage, particularly those related to reproduction (Kirkwood, 1977). For example, resistance to pathogens in adult mosquitoes has been associated with reproductive costs (Ahmed et al., 2002; Ahmed and Hurd, 2006; Ferdig et al., 1993; Yan et al., 1997). Furthermore, numerous studies have document age-associated declines in immune functions in mosquitoes (Castillo et al., 2006; Christensen et al., 1986; Chun et al., 1995; Cornet et al., 2013; Estevez-Lao and Hillyer, 2014; Hillyer et al., 2005; King and Hillyer, 2013; Li et al., 1992; Pigeault et al., 2015; Schwartz and Koella, 2002), fruit flies (Felix et al., 2012; Horn et al., 2014; Mackenzie et al., 2011), butterflies (Prasai and Karlsson, 2012; Stoehr, 2007), bees (Doums et al., 2002; Laughton et al., 2011; Moret and Schmid-Hempel, 2009; Schmid et al., 2008; Wilson-Rich et al., 2008), and other insects (Adamo et al., 2001; Eleftherianos et al., 2008; Kaaya and Darji, 1988; Kurtz, 2002; Rolff, 2001). However, unlike these earlier studies, which focused almost exclusively on adults, our findings show that this trend extends into the earlier larval life stage. This suggests that mosquito adults employ a "live fast, die young" life history

strategy (Travers et al., 2015), whereby immunity declines and mortality increases after adults reach reproductive maturity and selection for their survival wanes (Hamilton, 1966).

The age-dependent decrease in immune proficiency correlates with age-related changes in the number of circulating hemocytes present in the hemocoel. We found that mosquito larvae contain more circulating hemocytes than adult mosquitoes, and that the number of larval hemocytes increases in response to infection. This is consistent with earlier studies conducted in *Anopheles gambiae* and *Aedes aegypti* adults that showed that immune stimulation or blood feeding increases the number of circulating hemocytes (Baton et al., 2009; Bryant and Michel, 2014; Bryant and Michel, 2016; Castillo et al., 2011; Castillo et al., 2006; Christensen et al., 1989; Coggins et al., 2012; Foley, 1978), and that the number of circulating hemocytes declines with adult age (Castillo et al., 2006; Hillyer et al., 2005; King and Hillyer, 2013; Pigeault et al., 2015). Hemocytes are the first cellular responders to infection, phagocytosing pathogens within minutes of infection (Hillyer et al., 2003a; Hillyer et al., 2003b; King and Hillyer, 2012; League and Hillyer, 2016; Nazario-Toole and Wu, 2017; Sigle and Hillyer, 2016), and producing factors that limit both bacteria and *Plasmodium* infection (Bartholomay et al., 2007; Baton et al., 2009; Pinto et al., 2009; Smith et al., 2016). Thus, developmental changes in hemocyte profiles in part explain the higher bacteria killing efficiency of larvae relative to adults.

Although sessile hemocytes were abundant in both larvae and adults, the spatial arrangement of sessile hemocytes differed as adults aged, with newly-emerged adults displaying a pronounced segmental arrangement of hemocytes, which is more akin to what is observed in larvae than what is observed in 5-day-old adults (King and Hillyer, 2013; League and Hillyer, 2016). Furthermore, whereas hemocytes in adults aggregate at the periostial regions of the heart, hemocytes in larvae aggregate in the tracheal tufts of the 8th abdominal segment, where the sole

incurrent openings into the heart is located. These differences are due to the stage-specific functional integration of the immune and circulatory systems, as hemocytes aggregate in the areas of highest hemolymph flow (King and Hillyer, 2012; King and Hillyer, 2013; League and Hillyer, 2016; Sigle and Hillyer, 2016). Overall, these data show that sessile hemocyte populations undergo developmentally-related changes in spatial configuration and infection-induced abundance.

The finding that larvae have more circulating hemocytes than adults may account for the seemingly counterintuitive finding that larvae show lower phagocytic indices and capacities than adults. This is because larvae have more hemocytes available to phagocytose pathogens than adults, and based on our finding on the lytic and melanization activity of hemolymph, they also have a greater recourse to other means of pathogen clearance. Thus, an accumulation of phagocytic events in adults may signify a greater need for this immune mechanism, or lower phagocytic turnover rates, which has also been observed in aging fruit fly adults (Horn et al., 2014). Interestingly, these differences in phagocytosis are accompanied by changes in hemocyte morphology. Larval hemocytes tended to have a fibroblast-like spread morphology, which has been observed in other insect hemocytes (Ribeiro and Brehélin, 2006; Wang et al., 2011b), as opposed to the more rounded spread morphology typical of mosquito adult hemocytes (Castillo et al., 2006; Hillyer and Christensen, 2002; Hillyer et al., 2003a; Hillyer et al., 2003b; King and Hillyer, 2012; King and Hillyer, 2013).

In addition to stage-specific differences in hemocyte biology, we detected profound differences in the melanization activity of hemolymph. Melanization is commonly used in the immune response against bacteria, malaria, and filarial worms (Bartholomay, 2014; Christensen et al., 2005; Hillyer, 2016), and we found that mosquito larvae display a far greater capacity for

phenoloxidase-mediated humoral melanization than adults. This finding is consistent with our recent observations of rapid and extensive melanin deposits in the abdomen of larvae following a bacterial infection (League and Hillyer, 2016), as well as with the decline in phenoloxidase activity that occurs with adult age in *Aedes aegypti* (Li et al., 1992), and across life stage and with adult age in *Culex pipiens* (Cornet et al., 2013). In addition to enhancing humoral immunity, larvae may increase the melanization activity of hemolymph in preparation for cuticle tanning during and immediately after ecdysis, and for the rapid melanization of wounds in the more perilous aquatic environment of larvae.

Finally, we show that immunity gene induction is generally stronger in larvae compared to adults, with the difference being exacerbated as adults age, and that larvae and adults differentially regulate the expression of some immunity genes. The higher rate of *E. coli* killing in larvae is consistent with the expression of immune effector genes such as the Gram (-) binding protein gene, *GNBPB4*, which was expressed 470- and 710-fold higher in naïve larvae compared to naïve 1-day-old and 5-day-old adults, respectively, as well as the higher expression of the phenoloxidase gene *PPO1*, which was expressed 170- and 110-fold higher in larvae relative to naïve 1-day-old and 5-day-old adults, respectively. The higher rate of melanization we observed in larval hemolymph is also consistent with the higher *PPO6* gene induction we observed in larvae, and supports our previous finding of higher infection-induced melanization in the abdomen of larvae when compared adults (League and Hillyer, 2016). Furthermore, the higher melanization activity in the hemolymph of larvae is also consistent with the high level of dual oxidase (*DUOX*) gene induction detected in this life stage, as increased reactive oxygen species levels have been correlated with increased melanization (Kumar et al., 2003). In addition to the immune effector genes *PPO6* and *DUOX*, we also found that the Jak/Stat essential pathway

member *AGSTAT-A* and, to a lesser extent, the negative regulator of this pathway, *PIAS*, were induced in response to *E. coli* infection in larvae and not in adults, showing that the same infection results in stage-specific induction of signaling pathway genes. The upregulation of Imd pathway member in larvae and 1-day-old adults is consistent with this pathway's role in combating Gram (-) bacterial infections, however the cause for Jak/Stat pathways involvement in the larval response alone is unknown, though it may have to do with its function in mosquito development (Souza-Neto et al., 2009) as this pathway is involved in *Drosophila* development (Arbouzova and Zeidler, 2006). Adults, and not larvae, showed distinct upregulation of nitric oxide synthase, an important component of the adult immune response (Hillyer and Estévez-Lao, 2010; Luckhart et al., 1998), as well as higher upregulation of the pathogen recognition gene *FREP13* and the signal modulation gene *CLIPB15*. These differences in immunity gene induction across life stages could result from changes in the tissues expressing these genes during metamorphosis, as has been hypothesized previously (Dimopoulos et al., 1997; Fellous and Lazzaro, 2011). More broadly, however, these differences in immune gene regulation in larvae and adults are suggestive of adaptive decoupling, which would permit the independent regulation of larval and adult immune gene expression (Fellous and Lazzaro, 2011; Moran, 1994).

Studying larval immunity is crucial to our general understanding of mosquito biology, disease transmission, and vector control for several reasons. First, because mosquitoes are holometabolous insects, studying the larval immune system could yield important insights into how immune responses change over the course of development (League and Hillyer, 2016). Second, larval environmental factors, including food availability, temperature, population density, competition, and chemical insecticide exposure (Alto, 2011; Kim and Muturi, 2013;

Moller-Jacobs et al., 2014; Mourya et al., 2004; Murdock et al., 2012; Muturi, 2013; Muturi et al., 2011; Telang et al., 2012; Yadav et al., 2005), as well as exposure to bacterial and fungal pesticides (Bukhari et al., 2011; Capone et al., 2013; Federici et al., 2003; Federici et al., 2007; Kala and Gunasekaran, 1999; Mahapatra et al., 1999; Otieno-Ayayo et al., 2008; Paily et al., 2012), have all been shown to impact adult vector competence. Third, many of the most widespread and effective mosquito control methods directly target the larval stages (Fillinger and Lindsay, 2011; Floore, 2006; Tusting et al., 2013), and resistance to insecticides evolves more rapidly in larvae compared to adults, likely due to the stronger selection pressures at work in the larval stage (Koella et al., 2009). The present study highlights both continuities and discontinuities between the larval and adult immune systems, and shows that mosquito larvae possess an enhanced immune system compared to adults. Hence, understanding the larval immune system of *Anopheles gambiae*, a major vector of malaria in Sub Saharan Africa, could prove critical to the development and implementation of novel pest and disease control methods that are tailored to each life stage.

CHAPTER V

CONCLUSION AND FUTURE DIRECTIONS

Overview

As holometabolous insects, mosquitoes undergo dramatic changes in their morphology, ecology, and behavior as they develop from aquatic larvae to terrestrial and aerial adults. However, perhaps due to the imminent threat posed to human health by the adult life stage, most studies of the mosquito immune system have focused exclusively on adult females and have not addressed immunity in larvae. As noted by Fellous and Lazzaro "Almost all studies of the immune system of animals with metamorphosis have focused on either larval or on adult immunity, implicitly assuming that these traits are either perfectly correlated or evolutionarily independent" (Fellous and Lazzaro, 2011). In contrast to this "either-or" assumption, we suggest adopting a holistic, "both-and" approach to the study of mosquito immunity by examining this system throughout the complex lifecycle of the organism. The work presented in this dissertation adopts just such an approach by using a comparative approach to analyze circulatory and immune processes in both the larva and adult life stages to show that: (1) the larval and adult circulatory systems are functionally distinct; (2) the larval circulatory and immune systems are functionally integrated in a manner that is functionally analogous but spatially distinct from what is seen in adults; and (3) larvae mount more robust cellular and humoral immune responses compared to adults, especially as they age.

Larval and Adult Circulatory Physiology

Our investigation into the larval circulatory system, done side-by-side with adults, shows how this system changes, and remains stable, across metamorphosis. Overall, this study showed that the larval heart, though in most respects anatomically similar to the adult heart in location and structure, differs functionally from the adult heart in two important ways: (1) the larval heart does not undergo heartbeat directional reversals, but instead beats in the anterograde direction only; and (2) the larval heart does not accept hemolymph through the abdominal ostia, but instead through incurrent openings at the posterior terminus of the heart, which in adults serve an exclusively excurrent function during periods of retrograde flow (Andereck et al., 2010; Glenn et al., 2010).

The first finding from this study suggests that heartbeat directional reversals begin at the onset of, during, or shortly after pupal metamorphosis, though the exact timing of this transition has not been determined. Furthermore, the precise cause of heartbeat directional reversals is still unknown, though evidence from studies in other insects suggests that it may be due to new innervation of the heart that occurs during metamorphosis or differences in the activities of myotropic hormones (Davis et al., 2001; Dulcis et al., 2001; Dulcis and Levine, 2003; Dulcis and Levine, 2004; Dulcis and Levine, 2005; Kuwasawa et al., 1999). Larvae provide a helpful system for studying the potential causes that trigger the onset of retrograde heartbeats in adults, as their constant anterograde heart contractions provides a natural negative control environment into which cardiomyotropic neuropeptides or other stimuli, such as those which have been tested on the mosquito adult heart, could be added to test whether they have an impact on heartbeat directionality (Chen and Hillyer, 2013; Estévez-Lao et al., 2013; Hillyer et al., 2014; Hillyer et al., 2012). The presence of heart innervations in the larval and pupal stages could also be

examined, as previous work from our lab has detected such innervations in the mosquito adult heart using antibody-based immunohistochemical staining methods (Estévez-Lao et al., 2013). Discovering the causes behind the developmental onset of heartbeat reversals would not only shed light as to why they are absent in larvae, but could also lead to a means of manipulating their occurrence in adults to better understand their biological significance.

The second finding regarding hemolymph flow patterns in larvae show that the larval heart accepts hemolymph via posterior incurrent openings, but does not accept hemolymph through the ostia, though the precise reason for this is still unknown. We note that ostia are present in larvae yet remain in the closed position, and hence are unable to accept hemolymph. On a mechanistic level, one potential explanation for this is that the larval ostia are unable to open because they lack sufficient support from the nearby alary muscles, which are underdeveloped in larvae compared to adults (Glenn et al., 2010; League et al., 2015). Another possibility is that the ostia themselves are not fully developed, and hence would be non-functional regardless of the degree of alary muscle support, though we were unable to detect structural differences between larval and adult ostia using our imaging methods. However, on a broader evolutionary level, our data on hemolymph flow and ostia function in larvae suggests that their heart structure, function, and resultant hemolymph flow patterns are adapted to maintain proper hemolymph pressure and volume throughout their more uniformly-shaped hemocoel and to meet demands associated with their unique feeding and swimming behaviors. In adults, however, the heart has adapted to contract bidirectionally and accept hemolymph through abdominal and thoraco-abdominal ostia during anterograde and retrograde contraction periods, respectively, to accommodate the hemolymph distribution needs of their more

compartmentalized body plan as well as to meet the demands of processes unique to their life stage, such as flight, blood feeding, and reproduction.

The method for measuring ostia usage I developed for use in larvae has already been used in adults to show which ostia experience the highest levels of hemolymph flow (Sigle and Hillyer, 2016). The findings from that study suggest that immune activity along the heart, including pathogen sequestration and recruitment of hemocytes to the periostial regions, is at least partially dependent upon hemolymph circulation patterns. This is further confirmed by our finding that neither hemocytes nor pathogens aggregate near the larval ostia, which do not experience incurrent hemolymph flow (League and Hillyer, 2016; League et al., 2015). The work described here could also serve as a foundation for the construction of more exhaustive hemolymph flow maps throughout the hemocoel, as this has yet to be done in either larvae or adults. Finally, the descriptions of the larval aorta detailed in this study are currently aiding ongoing attempts in our lab to characterize the aorta of adults, which to date has proven an elusive structure to describe due to its fragility and position within the thorax (Glenn et al., 2010). Taken together, these comparative analyses lend credence to the notion that neither life stage can be fully understood in isolation from the other.

Functional Integration of the Larval Circulatory and Immune Systems

A principal location where immune responses occur in adult mosquitoes is the surface of the heart, which is the region of the body with the highest hemolymph flow (King and Hillyer, 2012; Sigle and Hillyer, 2016). The work on the coordinated function of the larval circulatory and immune systems presented in Chapter III represents the first detailed description of circulation-dependent immunity at the larval tracheal tufts, which are respiratory structures that are located at the sole entry point of hemolymph into the larval heart. These findings also

provide the first detailed description of the tracheal tufts in any mosquito species as well as the first time these structures have been assigned a central role in hemocyte-mediated immunity in any insect.

The tracheal tufts had previously been described in detail in the larvae of only one lepidopteran species, *Calpodes ethlius*, where they were said to function as a sort of "lung" for hemocyte oxygenation (Locke, 1997). Although tracheal tufts had been previously linked to parasitoid wasp egg oxygenation in another lepidopteran (Rao et al., 2009), and had been noted in passing in some dipteran larvae (Dell, 1905; Imms, 1907; Vaney, 1902), including mosquitoes (Christophers, 1960; Imms, 1907; Jones, 1954; Wigglesworth, 1949), until now their role in immunity had gone unstudied. We found that the tracheal tufts are the principal locations where larvae sequester bacterial pathogens that have entered the hemocoel. Furthermore, we found that, unlike the periostial hemocyte aggregation response that occurs on the heart of infected adults (King and Hillyer, 2012; Sigle and Hillyer, 2016), additional hemocytes do not aggregate at the tracheal tufts in response to infection. It remains unclear why pathogens, but not additional hemocytes, aggregate at the tracheal tufts during infection, particularly given the high rates of hemolymph flow in this region. We propose that the need to recruit additional hemocytes to the site of pathogen aggregation is unnecessary due to high number of hemocytes already bound to the tracheal tufts. However, the absence of infection-induced hemocyte recruitment at the tufts may also have to do with the signaling mechanisms underlying the periostial hemocyte aggregation response in adults, which may involve an immune factor that is not expressed in hemocytes at the larval stage. To test this, hemocyte aggregation candidates arising from ongoing work in our lab could potentially be validated by their absence or reduced expression in larval tissues.

The effects of varying oxygen levels on the functioning of the tracheal tufts was not a focus of this study, but such experiments could be performed to test whether these structures are indeed necessary for the oxygenation of hemocytes, as has been previously suggested in other insects (Hilken et al., 2003; Locke, 1997). However, this is not expected to be the case for mosquito larvae because hemocytes persist in adults in the absence of comparable tracheal structures, arguing against their function as hemocyte lungs in larvae. Rather, because hemocytes cover these thin trachea, and such trachea serve not only as the sole site of pathogen sequestration at the region of highest hemolymph flow into the heart but also as sites of potential pathogen invasion into the hemocoel from the external environment (Bukhari et al., 2010; Clark et al., 1968; Engelhard et al., 1994; Franz et al., 2015; King and Hillyer, 2013; Lacey et al., 1988; Miranpuri and Khachatourians, 1991; Romoser et al., 2004; Scholte et al., 2004), it is more likely that hemocytes associate with the tracheal tufts solely for the purpose of immune surveillance.

Although not associated with tracheal tufts in *Drosophila* (dissections in our lab confirmed that these structures are absent in fruit fly larvae), eighth abdominal segment hemocytes comprise a major blood cell compartment in *Drosophila* and serve an important role in larval immunity and hematopoiesis (Honti et al., 2014; Kurucz et al., 2007; Márkus et al., 2009; Shrestha and Gateff, 1982a; Stofanko et al., 2008). However, despite the observation in some insects that eighth segment hemocytes, and sessile hemocytes in general, serve a hematopoietic function (Arvy, 1953; Arvy, 1954; Ghosh et al., 2015; Lanot et al., 2001; Márkus et al., 2009), this function has thus far not been supported in mosquito larvae. In fact, a hematopoietic organ has not been documented in mosquito larvae (Strand, 2008) and their eighth segment sessile hemocytes, unlike those of *Drosophila*, have not been implicated as a

hematopoietic compartment for specialized larval immune responses (Márkus et al., 2009). Future studies in mosquitoes investigating developmental hematopoiesis may either help explain the apparent absence of a hematopoietic organ in mosquito larvae, or actually discover one, as well as determine whether the eighth segment hemocytes of mosquito larvae have a hematopoietic function. One possible explanation for the apparent lack of a larval hematopoietic organ is that it is unnecessary because larval circulating hemocytes are capable of replicating, as is true in the larvae of other insects (Arnold and Hinks, 1976; Feir and McClain, 1968; Gardiner and Strand, 2000; Kiuchi et al., 2008) as well as in mosquito adults (King and Hillyer, 2013). This could be tested by treating larvae with chemicals that interfere with mitosis such as taxol or colchicine, thus enriching the number of potentially dividing cells, and directly visualizing mitosis, if present, by labelling hemocytes with anti-tubulin antibodies (King and Hillyer, 2013).

Larval and Adult Cellular and Humoral Immune Responses

Larval and adult immune responses have seldom been compared in tandem and many of the immune measurements detailed in Chapter IV represent the first of their kind in the larval life stage. This may in part be due to the technical difficulties of working with small, soft-bodied larvae, but it is mainly due to the fact that it is the female adult, and not the larva, that vectors human pathogens. However, our findings suggest that studies of the adult immune system should be accompanied by complementary studies in larvae. Such an approach assumes neither that larval and adult immunity are exactly the same (complete evolutionary coupling), therefore rendering the study of both redundant, nor that they are completely different (complete evolutionary decoupling), therefore rendering the study of one irrelevant to the other (Fellous and Lazzaro, 2011). Our comparative investigation of the larval and adult immune systems

suggests that the truth lies somewhere in between these extremes, with both continuities and discontinuities existing between larval and adult immunity.

Similar to what we observed in the functional integration of the circulatory and immune systems in larvae and adults, all of the cellular and humoral immune parameters we measured are functional at both stages, though to varying degrees and with some developmental differences. We note an overall increased ability of larvae to kill *E. coli in vivo*, however, no other pathogens were investigated in this assay. Future studies could use this assay with other bacteria to see how typical this pattern is, although our other immune assays would suggest that this would be true for a broad range of pathogens. For example, the zone of inhibition assay included immune challenges with several types of bacteria and found that in each instance, the larval humoral antibacterial immune response was stronger compared to adults.

We also noted decreases of hemocyte numbers with age, and increases with infection, at least in the larvae (adults showed a similar, albeit non-significant trend). Although the precise source of these hemocytes remains unknown, they most likely arise from hemocyte replication in response to infection, and not from the release of sessile hemocytes into circulation upon infection (King and Hillyer, 2013). We have not observed sessile hemocytes in larvae entering circulation en masse upon infection, as occurs in response to parasitoid wasp infections in *Drosophila* larvae (Márkus et al., 2009), although modest levels of interchange between sessile and circulating hemocyte populations have been observed in adult mosquitoes (Sigle and Hillyer, 2016).

Furthermore, our comparison of immunity gene expression between life stages and adult ages shows that larvae and adults differentially express some immunity genes and that larvae generally display stronger levels of immune gene induction than adults, especially as they age.

On an evolutionary level, the differences in the strength of adult immunity gene expression are no doubt related to processes involved in senesce (Kirkwood, 1977), and the stronger immune gene induction observed in larvae likely result from the stronger evolutionary pressures at work on younger individuals to ensure their survival to reproductive maturity (Hamilton, 1966). However, the proximate causes behind both the cis- and trans-stadial (that is, within and between stage) differences we observed in immunity gene expression remain unknown. We examined the expression of ecdysone biosynthetic pathway genes in larvae and adults, as ecdysone is high in the larval stages and is known to regulate some immune functions (Ahmed et al., 1999; Müller et al., 1999). However, we found that these genes were not regulated by infection in any of our larval or adult groups, nor was their expression elevated in one stage compared to the other. Future studies could further probe into the reasons underlying these differences in immunity gene expression between life stages by examining whether larvae and adults differ in tissue-specific immunity gene expression due to metamorphosis (Dimopoulos et al., 1997) as well as how the differences we observed with *E. coli* infections vary with different bacterial insults. Furthermore, by employing RNA sequencing technology, as is currently being done in our lab to identify factors involved in periostial hemocyte aggregation on the heart of adults, we could obtain a broader look at the whole transcriptome in larvae and adults after infection and identify novel factors that may explain the differences we observed in their gene expression.

Concluding Thoughts

The work presented in this dissertation shows that the larval and adult circulatory and immune systems differ in important ways, thus necessitating their continued study in both life stages. Although all of the basic immune functions examined thus far are present in both life stages, there are distinct differences in the potency, composition, and regulation of these

responses, suggesting a decoupling of immunity in larvae and adults made possible by metamorphosis, the process that separates the two life stages and enables their independent evolution (Fellous and Lazzaro, 2011; Moran, 1994). However, this decoupling is clearly only partial, as some of the immune parameters we measured were similar between larvae and adults. Furthermore, it is also known that the fitness of adult mosquitoes is partially dependent upon rearing conditions and a number of stressors experienced during the larval stages (Alto, 2011; Bukhari et al., 2011; Capone et al., 2013; Favia et al., 2007; Federici et al., 2003; Federici et al., 2007; Kala and Gunasekaran, 1999; Kim and Muturi, 2013; Mahapatra et al., 1999; Moller-Jacobs et al., 2014; Mourya et al., 2004; Muturi, 2013; Muturi et al., 2011; Otieno-Ayayo et al., 2008; Paily et al., 2012; Telang et al., 2012; Yadav et al., 2005), thus limiting the degree to which these two stages could evolve independently. Thus, studying the larval immune system is useful not only in uncovering how it differs, but also how it is similar to that of adults, and therefore the extent to which it has diverged between the life stages. Such findings could have broad implications for epidemiological studies in mosquito adults as well as the implementation of control measures in the field.

Lastly, there are good reasons to believe that infections in the larval life stage could affect subsequent adult-acquired infections. Although insects do not possess an adaptive immune response, the innate immune systems of some insects display memory-like qualities, referred to as “immune priming” (Schmid-Hempel, 2005). Current studies in our lab are underway to determine whether transstadial immune priming can occur with bacterial insults in *A. gambiae*, as there is evidence that this occurs in mosquitoes (Bargielowski and Koella, 2009; Moreno-García et al., 2015) as well as other insects (Cisarovsky et al., 2012; Jacot et al., 2005; Thomas and Rudolf, 2010). In further support of this notion, we already know that immune priming

occurs within the adult life stage, as mosquitoes that have been pre-challenged with bacteria or *Plasmodium* prior to infection, or reinfection, with *Plasmodium* show increased parasite resistance (Lowenberger et al., 1999; Ramirez et al., 2015; Rodrigues et al., 2010). However, such resistance often comes at a price, as resistance to pathogens in mosquitoes has been associated with reproductive costs (Ahmed et al., 2002; Ahmed and Hurd, 2006; Ferdig et al., 1993; Yan et al., 1997) and altered developmental timelines (Koella and Boëte, 2002). Indeed, some authors have proposed taking advantage of certain insecticides that induce rapid resistance in larvae due to the trade-offs they cause in adult mosquitoes, which have the effect of lowering their ability to transmit malaria (Koella et al., 2009).

Given these ties between larval and adult immunity, future studies must take these observations further and delve into the cellular and molecular mechanisms that lie beneath them. This can only be accomplished by viewing the mosquito as a complex series of life stages that are both distinct, yet inseparable from each another. As a major vector of *Plasmodium* in sub-Saharan Africa, *A. gambiae* must be studied from new and compelling angles in order to discover novel pest control strategies for this seemingly uncontrollable pest. Investigating immunity at the larval stage provides just such an angle, and could very well lead to the veritable metamorphosis of our understanding of mosquito immunity as a whole.

REFERENCES

1. **Abraham, E. G. and Jacobs-Lorena, M.** (2004). Mosquito midgut barriers to malaria parasite development. *Insect Biochem Mol Biol* **34**, 667-71.
2. **Abraham, E. G., Pinto, S. B., Ghosh, A., Vanlandingham, D. L., Budd, A., Higgs, S., Kafatos, F. C., Jacobs-Lorena, M. and Michel, K.** (2005). An immune-responsive serpin, SRPN6, mediates mosquito defense against malaria parasites. *Proc Natl Acad Sci U S A* **102**, 16327-32.
3. **Adamo, S. A., Jensen, M. and Younger, M.** (2001). Changes in lifetime immunocompetence in male and female *Gryllus texensis* (formerly *G. integer*): trade-offs between immunity and reproduction. *Animal Behaviour* **62**, 417-425.
4. **Ahmed, A., Martín, D., Manetti, A. G., Han, S. J., Lee, W. J., Mathiopoulos, K. D., Müller, H. M., Kafatos, F. C., Raikhel, A. and Brey, P. T.** (1999). Genomic structure and ecdysone regulation of the prophenoloxidase 1 gene in the malaria vector Anopheles gambiae. *Proc Natl Acad Sci U S A* **96**, 14795-800.
5. **Ahmed, A. M., Baggott, S. L., Maingon, R. and Hurd, H.** (2002). The costs of mounting an immune response are reflected in the reproductive fitness of the mosquito Anopheles gambiae. In *Oikos*, vol. 97, pp. 371-377.
6. **Ahmed, A. M. and Hurd, H.** (2006). Immune stimulation and malaria infection impose reproductive costs in Anopheles gambiae via follicular apoptosis. *Microbes Infect* **8**, 308-15.
7. **Ajamhassani, M., Sendi, J. J., Farsi, M. J. and Zibaee, A.** (2012). Purification and characterization of phenoloxidase from the hemolymph of *Hyphantria cunea* (Lepidoptera: Arctiidae). *Invertebrate Survival Journal* **9**, 64-71.
8. **Akbar, M. A., Tracy, C., Kahr, W. H. and Krämer, H.** (2011). The full-of-bacteria gene is required for phagosome maturation during immune defense in *Drosophila*. *J Cell Biol* **192**, 383-90.
9. **Akhouayri, I. G., Habtewold, T. and Christophides, G. K.** (2013). Melanotic pathology and vertical transmission of the gut commensal *Elizabethkingia meningoseptica* in the major malaria vector *Anopheles gambiae*. *PLoS One* **8**, e77619.
10. **Alto, B. W.** (2011). Interspecific larval competition between invasive Aedes japonicus and native Aedes triseriatus (Diptera: Culicidae) and adult longevity. *J Med Entomol* **48**, 232-42.
11. **Andereck, J. W., King, J. G. and Hillyer, J. F.** (2010). Contraction of the ventral abdomen potentiates extracardiac retrograde hemolymph propulsion in the mosquito hemocoel. *PLoS One* **5**, e12943.
12. **Arnold, J. W. and Hinks, C. F.** (1976). Haemopoiesis in Lepidoptera. 1. The multiplication of circulating haemocytes. *Canadian Journal of Zoology* **54**, 1003-1012.
13. **Arvy, L.** (1953). Contribution à l'étude de la leucopoïèse chez quelques diptères. *Bull. Soc. Zool. Fr.* **78**, 158-169.
14. **Arvy, L.** (1954). Données sur la leucopoièse chez *Musca domestica*, L. *Proc. Roy. Ent. Soc., London* **29**, 39-41.
15. **Babcock, D. T., Brock, A. R., Fish, G. S., Wang, Y., Perrin, L., Krasnow, M. A. and Galko, M. J.** (2008). Circulating blood cells function as a surveillance system for damaged tissue in *Drosophila* larvae. *Proc Natl Acad Sci U S A* **105**, 10017-22.

16. **Bao, Y. Y., Xue, J., Wu, W. J., Wang, Y., Lv, Z. Y. and Zhang, C. X.** (2011). An immune-induced reeler protein is involved in the *Bombyx mori* melanization cascade. *Insect Biochem Mol Biol* **41**, 696-706.
17. **Bargielowski, I. and Koella, J. C.** (2009). A possible mechanism for the suppression of Plasmodium berghei development in the mosquito Anopheles gambiae by the microsporidian Vavraia culicis. *PLoS One* **4**, e4676.
18. **Bartholomay, L. C.** (2014). Infection barriers and responses in mosquito-filarial worm interactions. *Current Opinion in Insect Science* **3**, 37-42.
19. **Baton, L. A., Robertson, A., Warr, E., Strand, M. R. and Dimopoulos, G.** (2009). Genome-wide transcriptomic profiling of Anopheles gambiae hemocytes reveals pathogen-specific signatures upon bacterial challenge and Plasmodium berghei infection. *BMC Genomics* **10**, 257.
20. **Biron, D. G., Agnew, P., Marché, L., Renault, L., Sidobre, C. and Michalakis, Y.** (2005). Proteome of Aedes aegypti larvae in response to infection by the intracellular parasite Vavraia culicis. *Int J Parasitol* **35**, 1385-97.
21. **Blair, C. D. and Olson, K. E.** (2014). Mosquito immune responses to arbovirus infections. *Curr Opin Insect Sci* **3**, 22-29.
22. **Blandin, S., Moita, L. F., Köcher, T., Wilm, M., Kafatos, F. C. and Levashina, E. A.** (2002). Reverse genetics in the mosquito Anopheles gambiae: targeted disruption of the Defensin gene. *EMBO Rep* **3**, 852-6.
23. **Boppana, S. and Hillyer, J. F.** (2014). Hemolymph circulation in insect sensory appendages: functional mechanics of antennal accessory pulsatile organs (auxiliary hearts) in the mosquito *Anopheles gambiae*. *J Exp Biol*.
24. **Brey, P. T., Lebrun, R. A., Papierok, B., Ohayon, H., Vennavalli, S. and Hafez, J.** (1988). Defense reactions by larvae of Aedes aegypti during infection by the aquatic fungus Lagenidium giganteum (Oomycete). *Cell Tissue Res* **253**, 245-50.
25. **Bryant, W. B. and Michel, K.** (2014). Blood feeding induces hemocyte proliferation and activation in the African malaria mosquito, Anopheles gambiae Giles. *J Exp Biol* **217**, 1238-45.
26. **Bryant, W. B. and Michel, K.** (2016). Anopheles gambiae hemocytes exhibit transient states of activation. *Dev Comp Immunol* **55**, 119-29.
27. **Bukhari, T., Middelman, A., Koenraadt, C. J., Takken, W. and Knols, B. G.** (2010). Factors affecting fungus-induced larval mortality in *Anopheles gambiae* and *Anopheles stephensi*. *Malar J* **9**, 22.
28. **Bukhari, T., Takken, W. and Koenraadt, C. J.** (2011). Development of *Metarhizium anisopliae* and *Beauveria bassiana* formulations for control of malaria mosquito larvae. *Parasit Vectors* **4**, 23.
29. **Capone, A., Ricci, I., Damiani, C., Mosca, M., Rossi, P., Scuppa, P., Crotti, E., Epis, S., Angeletti, M., Valzano, M. et al.** (2013). Interactions between *Asaia*, *Plasmodium* and *Anopheles*: new insights into mosquito symbiosis and implications in Malaria Symbiotic Control. *Parasit Vectors* **6**, 182.
30. **Castillo, J., Brown, M. R. and Strand, M. R.** (2011). Blood feeding and insulin-like peptide 3 stimulate proliferation of hemocytes in the mosquito Aedes aegypti. *PLoS Pathog* **7**, e1002274.

31. **Castillo, J. C., Robertson, A. E. and Strand, M. R.** (2006). Characterization of hemocytes from the mosquitoes Anopheles gambiae and Aedes aegypti. *Insect Biochem Mol Biol* **36**, 891-903.
32. **Chambers, M. C., Lightfield, K. L. and Schneider, D. S.** (2012). How the fly balances its ability to combat different pathogens. *PLoS Pathog* **8**, e1002970.
33. **Chapman, R. F., Douglas, A. E. and Siva-Jothy, M. T.** (2013). Circulatory system, blood, and the immune system. In *The insects: structure and function*, eds. S. J. Simpson and A. E. Douglas), pp. 107-131. Cambridge: Cambridge University Press.
34. **Chen, W. and Hillyer, J. F.** (2013). FlyNap (triethylamine) increases the heart rate of mosquitoes and eliminates the cardioacceleratory effect of the neuropeptide CCAP. *PLoS One* **8**, e70414.
35. **Cheng, G., Liu, Y., Wang, P. and Xiao, X.** (2016). Mosquito Defense Strategies against Viral Infection. *Trends Parasitol* **32**, 177-86.
36. **Christensen, B. M., Huff, B. M., Miranpuri, G. S., Harris, K. L. and Christensen, L. A.** (1989). Hemocyte population changes during the immune response of Aedes aegypti to inoculated microfilariae of Dirofilaria immitis. *J Parasitol* **75**, 119-23.
37. **Christensen, B. M., LaFond, M. M. and Christensen, L. A.** (1986). Defense reactions of mosquitoes to filarial worms: effect of host age on the immune response to Dirofilaria immitis microfilariae. *J Parasitol* **72**, 212-5.
38. **Christensen, B. M., Li, J., Chen, C. C. and Nappi, A. J.** (2005). Melanization immune responses in mosquito vectors. *Trends Parasitol* **21**, 192-9.
39. **Christophers, S. R.** (1960). *Aedes Aegypti* (L.) The Yellow Fever Mosquito: Its Life History, Bionomics and Structure. New York: Cambridge University Press.
40. **Christophides, G. K., Zdobnov, E., Barillas-Mury, C., Birney, E., Blandin, S., Blass, C., Brey, P. T., Collins, F. H., Danielli, A., Dimopoulos, G. et al.** (2002). Immunity-related genes and gene families in Anopheles gambiae. *Science* **298**, 159-65.
41. **Chun, J., Riehle, M. and Paskewitz, S. M.** (1995). Effect of mosquito age and reproductive status on melanization of sephadex beads in Plasmodium-refractory and -susceptible strains of Anopheles gambiae. *J Invertebr Pathol* **66**, 11-7.
42. **Cirimotich, C. M., Dong, Y., Garver, L. S., Sim, S. and Dimopoulos, G.** (2010). Mosquito immune defenses against Plasmodium infection. *Dev Comp Immunol* **34**, 387-95.
43. **Cisarovsky, G., Schmid-Hempel, P. and Sadd, B. M.** (2012). Robustness of the outcome of adult bumblebee infection with a trypanosome parasite after varied parasite exposures during larval development. *J Evol Biol* **25**, 1053-9.
44. **Clark, T. B., Kellen, W. R., Fukuda, T. and Lindegren, J. E.** (1968). Field and laboratory studies on the pathogenicity of the fungus *Beauveria bassiana* to three genera of mosquitoes. *J Invertebr Pathol* **11**, 1-7.
45. **Clayton, A. M., Dong, Y. and Dimopoulos, G.** (2014). The Anopheles innate immune system in the defense against malaria infection. *J Innate Immun* **6**, 169-81.
46. **Clements, A. N.** (1992). The Biology of Mosquitoes: Development, Nutrition and Reproduction, vol. 1, pp. 100-123. London: Chapman and Hall.
47. **Coggins, S. A., Estévez-Lao, T. Y. and Hillyer, J. F.** (2012). Increased survivorship following bacterial infection by the mosquito Aedes aegypti as compared to Anopheles gambiae correlates with increased transcriptional induction of antimicrobial peptides. *Dev Comp Immunol* **37**, 390-401.

48. **Cornet, S., Gandon, S. and Rivero, A.** (2013). Patterns of phenoloxidase activity in insecticide resistant and susceptible mosquitoes differ between laboratory-selected and wild-caught individuals. *Parasit Vectors* **6**, 315.
49. **Crossley, A. C. S.** (1964). An experimental analysis of the origins and physiology of haemocytes in the blue blow-fly *Calliphora erythrocephala*, (Meig). In *Journal of Experimental Zoology*, vol. 157, pp. 375-397.
50. **Curtis, N. J., Ringo, J. M. and Dowse, H. B.** (1999). Morphology of the pupal heart, adult heart, and associated tissues in the fruit fly, *Drosophila melanogaster*. *J Morphol* **240**, 225-35.
51. **Cuttell, L., Vaughan, A., Silva, E., Escaron, C. J., Lavine, M., Van Goethem, E., Eid, J. P., Quirin, M. and Franc, N. C.** (2008). Undertaker, a *Drosophila* Junctophilin, links Draper-mediated phagocytosis and calcium homeostasis. *Cell* **135**, 524-34.
52. **Dasari, S. and Cooper, R. L.** (2006). Direct influence of serotonin on the larval heart of *Drosophila melanogaster*. *J Comp Physiol B* **176**, 349-57.
53. **Davis, N. T., Dulcis, D. and Hildebrand, J. G.** (2001). Innervation of the heart and aorta of Manduca sexta. *J Comp Neurol* **440**, 245-60.
54. **Dell, J. A.** (1905). On the structure and life-history of *Psychoda sexpunctata*. *Trans. Ent. Soc. Lond.*, 293.
55. **Dimopoulos, G., Christophides, G. K., Meister, S., Schultz, J., White, K. P., Barillas-Mury, C. and Kafatos, F. C.** (2002). Genome expression analysis of Anopheles gambiae: responses to injury, bacterial challenge, and malaria infection. *Proc Natl Acad Sci U S A* **99**, 8814-9.
56. **Dimopoulos, G., Richman, A., Müller, H. M. and Kafatos, F. C.** (1997). Molecular immune responses of the mosquito Anopheles gambiae to bacteria and malaria parasites. *Proc Natl Acad Sci U S A* **94**, 11508-13.
57. **Dong, Y. and Dimopoulos, G.** (2009). Anopheles fibrinogen-related proteins provide expanded pattern recognition capacity against bacteria and malaria parasites. *J Biol Chem* **284**, 9835-44.
58. **Dong, Y., Morton, J. C., Ramirez, J. L., Souza-Neto, J. A. and Dimopoulos, G.** (2012). The entomopathogenic fungus Beauveria bassiana activate toll and JAK-STAT pathway-controlled effector genes and anti-dengue activity in Aedes aegypti. *Insect Biochem Mol Biol* **42**, 126-32.
59. **Doums, C., Moret, Y., Benelli, E. and Schmid-Hempel, P.** (2002). Senescence of immune defence in *Bombus* workers. *Ecological Entomology* **27**, 138-144.
60. **Dulcis, D., Davis, N. T. and Hildebrand, J. G.** (2001). Neuronal control of heart reversal in the hawkmoth *Manduca sexta*. *J Comp Physiol A* **187**, 837-49.
61. **Dulcis, D. and Levine, R. B.** (2003). Innervation of the heart of the adult fruit fly, Drosophila melanogaster. *J Comp Neurol* **465**, 560-78.
62. **Dulcis, D. and Levine, R. B.** (2004). Remodeling of a larval skeletal muscle motoneuron to drive the posterior cardiac pacemaker in the adult moth, Manduca sexta. *J Comp Neurol* **478**, 126-42.
63. **Dulcis, D. and Levine, R. B.** (2005). Glutamatergic innervation of the heart initiates retrograde contractions in adult Drosophila melanogaster. *J Neurosci* **25**, 271-80.
64. **Dulcis, D., Levine, R. B. and Ewer, J.** (2005). Role of the neuropeptide CCAP in Drosophila cardiac function. *J Neurobiol* **64**, 259-74.

65. **Eleftherianos, I., Baldwin, H., ffrench-Constant, R. H. and Reynolds, S. E.** (2008). Developmental modulation of immunity: changes within the feeding period of the fifth larval stage in the defence reactions of Manduca sexta to infection by Photorhabdus. *J Insect Physiol* **54**, 309-18.
66. **Elrod-Erickson, M., Mishra, S. and Schneider, D.** (2000). Interactions between the cellular and humoral immune responses in *Drosophila*. *Curr Biol* **10**, 781-4.
67. **Engelhard, E. K., Kam-Morgan, L. N., Washburn, J. O. and Volkman, L. E.** (1994). The insect tracheal system: a conduit for the systemic spread of *Autographa californica* M nuclear polyhedrosis virus. *Proc Natl Acad Sci U S A* **91**, 3224-7.
68. **Erickson, S. M., Xi, Z., Mayhew, G. F., Ramirez, J. L., Aliota, M. T., Christensen, B. M. and Dimopoulos, G.** (2009). Mosquito infection responses to developing filarial worms. *PLoS Negl Trop Dis* **3**, e529.
69. **Estevez-Lao, T. Y. and Hillyer, J. F.** (2014). Involvement of the Anopheles gambiae Nimrod gene family in mosquito immune responses. *Insect Biochem Mol Biol* **44**, 12-22.
70. **Estévez-Lao, T. Y., Boyce, D. S., Honegger, H. W. and Hillyer, J. F.** (2013). Cardioacceleratory function of the neurohormone CCAP in the mosquito *Anopheles gambiae*. *J Exp Biol* **216**, 601-13.
71. **Estévez-Lao, T. Y. and Hillyer, J. F.** (2014). Involvement of the Anopheles gambiae Nimrod gene family in mosquito immune responses. *Insect Biochem Mol Biol* **44**, 12-22.
72. **Favia, G., Ricci, I., Damiani, C., Raddadi, N., Crotti, E., Marzorati, M., Rizzi, A., Urso, R., Brusetti, L., Borin, S. et al.** (2007). Bacteria of the genus *Asaia* stably associate with *Anopheles stephensi*, an Asian malarial mosquito vector. *Proc Natl Acad Sci U S A* **104**, 9047-51.
73. **Federici, B. A., Park, H. W., Bideshi, D. K., Wirth, M. C. and Johnson, J. J.** (2003). Recombinant bacteria for mosquito control. *J Exp Biol* **206**, 3877-85.
74. **Federici, B. A., Park, H. W., Bideshi, D. K., Wirth, M. C., Johnson, J. J., Sakano, Y. and Tang, M.** (2007). Developing recombinant bacteria for control of mosquito larvae. *J Am Mosq Control Assoc* **23**, 164-75.
75. **Feir, D. and McClain, E.** (1968). Induced changes in the mitotic activity of hemocytes of the large milkweed bug, *Oncopeltus fasciatus*. *Annals of the Entomological Society of America* **61**, 416-421.
76. **Felix, T. M., Hughes, K. A., Stone, E. A., Drnevich, J. M. and Leips, J.** (2012). Age-specific variation in immune response in Drosophila melanogaster has a genetic basis. *Genetics* **191**, 989-1002.
77. **Fellous, S. and Lazzaro, B. P.** (2011). Potential for evolutionary coupling and decoupling of larval and adult immune gene expression. *Mol Ecol* **20**, 1558-67.
78. **Feng, C., Song, Q., Lü, W. and Lu, J.** (2008). Purification and characterization of hemolymph prophenoloxidase from Ostrinia furnacalis (Lepidoptera: Pyralidae) larvae. *Comp Biochem Physiol B Biochem Mol Biol* **151**, 139-46.
79. **Ferdig, M. T., Beerntsen, B. T., Spray, F. J., Li, J. and Christensen, B. M.** (1993). Reproductive costs associated with resistance in a mosquito-filarial worm system. *Am J Trop Med Hyg* **49**, 756-62.
80. **Fillinger, U. and Lindsay, S. W.** (2011). Larval source management for malaria control in Africa: myths and reality. *Malar J* **10**, 353.

81. **Foley, D. A.** (1978). Innate Cellular Defense by Mosquito Hemocytes. In *Invertebrate Models for Biomedical Research*, eds. L. A. Bulla Jr. and T. C. Cheng), pp. 113-144. New York: Springer US.
82. **Franz, A. W., Kantor, A. M., Passarelli, A. L. and Clem, R. J.** (2015). Tissue Barriers to Arbovirus Infection in Mosquitoes. *Viruses* **7**, 3741-67.
83. **Gardiner, E. M. and Strand, M. R.** (2000). Hematopoiesis in larval Pseudoplusia includens and Spodoptera frugiperda. *Arch Insect Biochem Physiol* **43**, 147-64.
84. **Garver, L. S., Bahia, A. C., Das, S., Souza-Neto, J. A., Shiao, J., Dong, Y. and Dimopoulos, G.** (2012). Anopheles Imd pathway factors and effectors in infection intensity-dependent anti-Plasmodium action. *PLoS Pathog* **8**, e1002737.
85. **Gerould, J. H.** (1924). Periodic reversal of heart-beat in a chrysalis. *Science* **60**, 570-2.
86. **Gerould, J. H.** (1933). Orders of insects with heart-beat reversal. *Biological Bulletin* **64**, 424-431.
87. **Ghosh, S., Singh, A., Mandal, S. and Mandal, L.** (2015). Active hematopoietic hubs in *Drosophila* adults generate hemocytes and contribute to immune response. *Dev Cell* **33**, 478-88.
88. **Glenn, J. D., King, J. G. and Hillyer, J. F.** (2010). Structural mechanics of the mosquito heart and its function in bidirectional hemolymph transport. *J Exp Biol* **213**, 541-50.
89. **González-Lázaro, M., Dinglasan, R. R., Hernández-Hernández, F. e. L., Rodríguez, M. H., Laclaustra, M., Jacobs-Lorena, M. and Flores-Romo, L.** (2009). Anopheles gambiae Croquemort SCRBQ2, expression profile in the mosquito and its potential interaction with the malaria parasite Plasmodium berghei. *Insect Biochem Mol Biol* **39**, 395-402.
90. **Gorman, M. J. and Paskewitz, S. M.** (2000). Persistence of infection in mosquitoes injected with bacteria. *J Invertebr Pathol* **75**, 296-7.
91. **Gupta, L., Molina-Cruz, A., Kumar, S., Rodrigues, J., Dixit, R., Zamora, R. E. and Barillas-Mury, C.** (2009). The STAT pathway mediates late-phase immunity against Plasmodium in the mosquito Anopheles gambiae. *Cell Host Microbe* **5**, 498-507.
92. **Haine, E. R., Pollitt, L. C., Moret, Y., Siva-Jothy, M. T. and Rolff, J.** (2008). Temporal patterns in immune responses to a range of microbial insults (Tenebrio molitor). *J Insect Physiol* **54**, 1090-7.
93. **Hamilton, W. D.** (1966). The moulding of senescence by natural selection. *J Theor Biol* **12**, 12-45.
94. **Harrison, J. F., Woods, H. A. and Roberts, S. P.** (2012). Ecological and environmental physiology of insects. New York: Oxford University Press.
95. **Hernández-Martínez, S., Lanz-Mendoza, H., Martínez-Barnetche, J. and Rodríguez, M. H.** (2013). Antimicrobial properties of *Anopheles albimanus* pericardial cells. *Cell Tissue Res* **351**, 127-37.
96. **Hilken, G., Brockmann, C. and Nevermann, L.** (2003). Hemocytes of the centipede Scutigera coleoptrata (Chilopoda, Notostigmophora) with notes on their interactions with the tracheae. *J Morphol* **257**, 181-9.
97. **Hillyer, J. F.** (2009). Transcription in mosquito hemocytes in response to pathogen exposure. *J Biol* **8**, 51.

98. **Hillyer, J. F.** (2010). Mosquito immunity. *Adv Exp Med Biol* **708**, 218-38.
99. **Hillyer, J. F.** (2015). Integrated Immune and Cardiovascular Function in Pancrustacea: Lessons from the Insects. *Integr Comp Biol* **55**, 843-55.
100. **Hillyer, J. F.** (2016). Insect immunology and hematopoiesis. *Dev Comp Immunol* **58**, 102-18.
101. **Hillyer, J. F., Barreau, C. and Vernick, K. D.** (2007). Efficiency of salivary gland invasion by malaria sporozoites is controlled by rapid sporozoite destruction in the mosquito haemocoel. *Int J Parasitol* **37**, 673-81.
102. **Hillyer, J. F. and Christensen, B. M.** (2002). Characterization of hemocytes from the yellow fever mosquito, *Aedes aegypti*. *Histochem Cell Biol* **117**, 431-40.
103. **Hillyer, J. F. and Estévez-Lao, T. Y.** (2010). Nitric oxide is an essential component of the hemocyte-mediated mosquito immune response against bacteria. *Dev Comp Immunol* **34**, 141-9.
104. **Hillyer, J. F., Estévez-Lao, T. Y. and de la Parte, L. E.** (2014). Myotropic effects of FMRFamide containing peptides on the heart of the mosquito Anopheles gambiae. *Gen Comp Endocrinol* **202**, 15-25.
105. **Hillyer, J. F., Estévez-Lao, T. Y., Funkhouser, L. J. and Aluoch, V. A.** (2012). *Anopheles gambiae* corazonin: gene structure, expression and effect on mosquito heart physiology. *Insect Mol Biol* **21**, 343-55.
106. **Hillyer, J. F., Schmidt, S. L. and Christensen, B. M.** (2003a). Hemocyte-mediated phagocytosis and melanization in the mosquito *Armigeres subalbatus* following immune challenge by bacteria. *Cell Tissue Res* **313**, 117-27.
107. **Hillyer, J. F., Schmidt, S. L. and Christensen, B. M.** (2003b). Rapid phagocytosis and melanization of bacteria and *Plasmodium* sporozoites by hemocytes of the mosquito *Aedes aegypti*. *J Parasitol* **89**, 62-9.
108. **Hillyer, J. F., Schmidt, S. L. and Christensen, B. M.** (2004). The antibacterial innate immune response by the mosquito *Aedes aegypti* is mediated by hemocytes and independent of Gram type and pathogenicity. *Microbes Infect* **6**, 448-59.
109. **Hillyer, J. F., Schmidt, S. L., Fuchs, J. F., Boyle, J. P. and Christensen, B. M.** (2005). Age-associated mortality in immune challenged mosquitoes (Aedes aegypti) correlates with a decrease in haemocyte numbers. *Cell Microbiol* **7**, 39-51.
110. **Hillyer, J. F. and Strand, M. R.** (2014). Mosquito hemocyte-mediated immune responses. *Curr Opin Insect Sci* **3**, 14-21.
111. **Honti, V., Csordás, G., Kurucz, É., Márkus, R. and Andó, I.** (2014). The cell-mediated immunity of Drosophila melanogaster: hemocyte lineages, immune compartments, microanatomy and regulation. *Dev Comp Immunol* **42**, 47-56.
112. **Horn, L., Leips, J. and Starz-Gaiano, M.** (2014). Phagocytic ability declines with age in adult *Drosophila* hemocytes. *Aging Cell*.
113. **Hurd, H., Taylor, P. J., Adams, D., Underhill, A. and Eggleston, P.** (2005). Evaluating the costs of mosquito resistance to malaria parasites. *Evolution* **59**, 2560-72.
114. **Imms, A. D.** (1907). On the Larval and Pupal Stages of *Anopheles maculipennis*, Meigen. *J Hyg (Lond)* **7**, 291-318.3.
115. **Jacot, A., Scheuber, H., Kurtz, J. and Brinkhof, M. W.** (2005). Juvenile immune system activation induces a costly upregulation of adult immunity in field crickets Gryllus campestris. *Proc Biol Sci* **272**, 63-9.

116. **Jiang, H., Vilcinskas, A. and Kanost, M. R.** (2010). Immunity in lepidopteran insects. *Adv Exp Med Biol* **708**, 181-204.
117. **Jiang, J., Alvarez, C., Kukutla, P., Yu, W. and Xu, J.** (2012). Draft genome sequences of Enterobacter sp. isolate Ag1 from the midgut of the malaria mosquito Anopheles gambiae. *J Bacteriol* **194**, 5481.
118. **Jones, J. C.** (1954). The heart and associated tissues of *Anopheles quadrimaculatus* say (Diptera: Culicidae). In *Journal of Morphology*, vol. 94, pp. 71-123.
119. **Jones, J. C.** (1977). The circulatory system of insects. Springfield IL: Charles C. Thomas.
120. **Kaaya, G. P. and Darji, N.** (1988). The humoral defense system in tsetse: differences in response due to age, sex and antigen types. *Dev Comp Immunol* **12**, 255-68.
121. **Kajla, M. K., Andreeva, O., Gilbreath, T. M. and Paskewitz, S. M.** (2010). Characterization of expression, activity and role in antibacterial immunity of Anopheles gambiae lysozyme c-1. *Comp Biochem Physiol B Biochem Mol Biol* **155**, 201-9.
122. **Kajla, M. K., Shi, L., Li, B., Luckhart, S., Li, J. and Paskewitz, S. M.** (2011). A new role for an old antimicrobial: lysozyme c-1 can function to protect malaria parasites in Anopheles mosquitoes. *PLoS One* **6**, e19649.
123. **Kala, M. K. and Gunasekaran, K.** (1999). Effect of bacillus thuringiensis ssp. israelensis on the development of Plasmodium gallinaceum in Aedes aegypti (Diptera: Culicidae). *Ann Trop Med Parasitol* **93**, 89-95.
124. **Kim, C. H. and Muturi, E. J.** (2013). Effect of larval density and Sindbis virus infection on immune responses in Aedes aegypti. *J Insect Physiol* **59**, 604-10.
125. **Kim, W., Koo, H., Richman, A. M., Seeley, D., Vizioli, J., Klocko, A. D. and O'Brochta, D. A.** (2004). Ectopic expression of a cecropin transgene in the human malaria vector mosquito Anopheles gambiae (Diptera: Culicidae): effects on susceptibility to Plasmodium. *J Med Entomol* **41**, 447-55.
126. **King, J. G. and Hillyer, J. F.** (2012). Infection-induced interaction between the mosquito circulatory and immune systems. *PLoS Pathog* **8**, e1003058.
127. **King, J. G. and Hillyer, J. F.** (2013). Spatial and temporal in vivo analysis of circulating and sessile immune cells in mosquitoes: hemocyte mitosis following infection. *BMC Biol* **11**, 55.
128. **Kirkwood, T. B.** (1977). Evolution of ageing. *Nature* **270**, 301-4.
129. **Kiuchi, T., Aoki, F. and Nagata, M.** (2008). Effects of high temperature on the hemocyte cell cycle in silkworm larvae. *J Insect Physiol* **54**, 454-61.
130. **Klowden, A. J.** (2013). Circulatory systems. In *Physiological systems in insects*, pp. 365-413. Boston: Academic Press.
131. **Kocks, C., Cho, J. H., Nehme, N., Ulvila, J., Pearson, A. M., Meister, M., Strom, C., Conto, S. L., Hetru, C., Stuart, L. M. et al.** (2005). Eater, a transmembrane protein mediating phagocytosis of bacterial pathogens in *Drosophila*. *Cell* **123**, 335-46.
132. **Koella, J. C. and Boëte, C.** (2002). A genetic correlation between age at pupation and melanization immune response of the yellow fever mosquito Aedes aegypti. *Evolution* **56**, 1074-9.
133. **Koella, J. C., Lynch, P. A., Thomas, M. B. and Read, A. F.** (2009). Towards evolution-proof malaria control with insecticides. Evolutionary Applications Volume 2, Issue 4. In *Evolutionary Applications*, vol. 2, pp. 469-480.

134. **Kumar, S., Christophides, G. K., Cantera, R., Charles, B., Han, Y. S., Meister, S., Dimopoulos, G., Kafatos, F. C. and Barillas-Mury, C.** (2003). The role of reactive oxygen species on Plasmodium melanotic encapsulation in Anopheles gambiae. *Proc Natl Acad Sci U S A* **100**, 14139-44.
135. **Kumar, S., Molina-Cruz, A., Gupta, L., Rodrigues, J. and Barillas-Mury, C.** (2010). A peroxidase/dual oxidase system modulates midgut epithelial immunity in Anopheles gambiae. *Science* **327**, 1644-8.
136. **Kurtz, J.** (2002). Phagocytosis by invertebrate hemocytes: causes of individual variation in Panorpa vulgaris scorpionflies. *Microsc Res Tech* **57**, 456-68.
137. **Kurucz, E., Váczi, B., Márkus, R., Laurinyecz, B., Vilmos, P., Zsámboki, J., Csorba, K., Gateff, E., Hultmark, D. and Andó, I.** (2007). Definition of Drosophila hemocyte subsets by cell-type specific antigens. *Acta Biol Hung* **58 Suppl**, 95-111.
138. **Kuwasawa, K., Ai, H. and Matsushita, T.** (1999). Cardiac reflexes and their neural pathways in lepidopterous insects. *Comparative Biochemistry and Physiology - Part A Molecular & Integrative Physiology* **124**, 581-586.
139. **Lacey, C. M., Lacey, L. A. and Roberts, D. R.** (1988). Route of invasion and histopathology of *Metarhizium anisopliae* in *Culex quinquefasciatus*. *J Invertebr Pathol* **52**, 108-18.
140. **Laird, M.** (1988). The natural history of larval mosquito habitats. London ; San Diego: Academic.
141. **Lanot, R., Zachary, D., Holder, F. and Meister, M.** (2001). Postembryonic hematopoiesis in *Drosophila*. *Dev Biol* **230**, 243-57.
142. **Laughton, A. M., Boots, M. and Siva-Jothy, M. T.** (2011). The ontogeny of immunity in the honey bee, Apis mellifera L. following an immune challenge. *J Insect Physiol* **57**, 1023-32.
143. **Lavine, M. D. and Strand, M. R.** (2002). Insect hemocytes and their role in immunity. *Insect Biochem Mol Biol* **32**, 1295-309.
144. **League, G. P. and Hillyer, J. F.** (2016). Functional integration of the circulatory, immune, and respiratory systems in mosquito larvae: pathogen killing in the hemocyte-rich tracheal tufts. *BMC Biol* **14**, 78.
145. **League, G. P., Onuh, O. C. and Hillyer, J. F.** (2015). Comparative structural and functional analysis of the larval and adult dorsal vessel and its role in hemolymph circulation in the mosquito *Anopheles gambiae*. *J Exp Biol* **218**, 370-80.
146. **Lehmacher, C., Abeln, B. and Paululat, A.** (2012). The ultrastructure of *Drosophila* heart cells. *Arthropod Struct Dev* **41**, 459-74.
147. **Lemaitre, B. and Hoffmann, J.** (2007). The host defense of Drosophila melanogaster. *Annu Rev Immunol* **25**, 697-743.
148. **Levashina, E. A.** (2004). Immune responses in Anopheles gambiae. *Insect Biochem Mol Biol* **34**, 673-8.
149. **Levashina, E. A., Moita, L. F., Blandin, S., Vriend, G., Lagueux, M. and Kafatos, F. C.** (2001). Conserved role of a complement-like protein in phagocytosis revealed by dsRNA knockout in cultured cells of the mosquito, Anopheles gambiae. *Cell* **104**, 709-18.
150. **Leódido, A. C., Ramalho-Ortigão, M. and Martins, G. F.** (2013). The ultrastructure of the *Aedes aegypti* heart. *Arthropod Struct Dev* **42**, 539-50.

151. **Li, B., Calvo, E., Marinotti, O., James, A. A. and Paskewitz, S. M.** (2005). Characterization of the c-type lysozyme gene family in Anopheles gambiae. *Gene* **360**, 131-9.
152. **Li, B. and Paskewitz, S. M.** (2006). A role for lysozyme in melanization of Sephadex beads in Anopheles gambiae. *J Insect Physiol* **52**, 936-42.
153. **Li, J., Tracy, J. W. and Christensen, B. M.** (1992). Relationship of hemolymph phenol oxidase and mosquito age in Aedes aegypti. *J Invertebr Pathol* **60**, 188-91.
154. **Livak, K. J. and Schmittgen, T. D.** (2001). Analysis of relative gene expression data using real-time quantitative PCR and the 2(-Delta Delta C(T)) Method. *Methods* **25**, 402-8.
155. **Locke, M.** (1997). Caterpillars have evolved lungs for hemocyte gas exchange. *J Insect Physiol* **44**, 1-20.
156. **Lowenberger, C. A., Kamal, S., Chiles, J., Paskewitz, S., Bulet, P., Hoffmann, J. A. and Christensen, B. M.** (1999). Mosquito-Plasmodium interactions in response to immune activation of the vector. *Exp Parasitol* **91**, 59-69.
157. **Mackenzie, D. K., Bussière, L. F. and Tinsley, M. C.** (2011). Senescence of the cellular immune response in Drosophila melanogaster. *Exp Gerontol* **46**, 853-9.
158. **Mahapatra, N., Hazra, R. K., Rup, S., Acharya, A. S. and Dash, A. P.** (1999). Bacillus sphaericus interferes with the development of Brugia malayi in Aedes aegypti. *J Helminthol* **73**, 279-80.
159. **Makhijani, K., Alexander, B., Tanaka, T., Rulifson, E. and Brückner, K.** (2011). The peripheral nervous system supports blood cell homing and survival in the *Drosophila* larva. *Development* **138**, 5379-91.
160. **Martins, G. F., Ramalho-Ortigão, J. M. and Pimenta, P. F. P.** (2011). Morphological features of the heart of six mosquito species as revealed by scanning electron microscopy. *International Journal of Tropical Insect Science* **31**, 98-102.
161. **Matsushita, T., Kuwasawa, K., Uchimura, K., Ai, H. and Kurokawa, M.** (2002). Biogenic amines evoke heartbeat reversal in larvae of the sweet potato hornworm, *Agrius convolvuli*. *Comp Biochem Physiol A Mol Integr Physiol* **133**, 625-36.
162. **Meredith, J. M., Hurd, H., Lehane, M. J. and Eggleston, P.** (2008). The malaria vector mosquito Anopheles gambiae expresses a suite of larval-specific defensin genes. *Insect Mol Biol* **17**, 103-12.
163. **Michel, K., Budd, A., Pinto, S., Gibson, T. J. and Kafatos, F. C.** (2005). *Anopheles gambiae* SRPN2 facilitates midgut invasion by the malaria parasite *Plasmodium berghei*. *EMBO Rep* **6**, 891-7.
164. **Miller, T and A.** (1985). Structure and physiology of the circulatory system. In *Comprehensive Insect Physiology, Biochemistry, and Pharmacology.*, vol. 3, pp. 289-353: Pergamon, Oxford.
165. **Miller, T. A.** (1997). Control of circulation in insects. *Gen Pharmacol* **29**, 23-38.
166. **Miranpuri, G. S. and Khachatourians, G. G.** (1991). Infection sites of the entomopathogenic fungus *Beauveria bassiana* in the larvae of the mosquito *Aedes aegypti*. In *Entomologia Experimentalis et Applicata*, vol. 59, pp. 19-27.
167. **Moita, L. F., Wang-Sattler, R., Michel, K., Zimmermann, T., Blandin, S., Levashina, E. A. and Kafatos, F. C.** (2005). In vivo identification of novel regulators and conserved pathways of phagocytosis in A. gambiae. *Immunity* **23**, 65-73.

168. **Molina, M. R. and Cripps, R. M.** (2001). Ostia, the inflow tracts of the *Drosophila* heart, develop from a genetically distinct subset of cardial cells. *Mech Dev* **109**, 51-9.
169. **Molina-Cruz, A., DeJong, R. J., Charles, B., Gupta, L., Kumar, S., Jaramillo-Gutierrez, G. and Barillas-Mury, C.** (2008). Reactive oxygen species modulate Anopheles gambiae immunity against bacteria and Plasmodium. *J Biol Chem* **283**, 3217-23.
170. **Moller-Jacobs, L. L., Murdock, C. C. and Thomas, M. B.** (2014). Capacity of mosquitoes to transmit malaria depends on larval environment. *Parasit Vectors* **7**, 593.
171. **Moran, N. A.** (1994). Adaptation and Constraint in the Complex Life Cycles of Animals. *Annual Review of Ecology and Systematics* **25**, 573-600.
172. **Moreira, C. G., Jacinto, A. and Prag, S.** (2013). *Drosophila* integrin adhesion complexes are essential for hemocyte migration in vivo. *Biol Open* **2**, 795-801.
173. **Moreno-García, M., Vargas, V., Ramírez-Bello, I., Hernández-Martínez, G. and Lanz-Mendoza, H.** (2015). Bacterial Exposure at the Larval Stage Induced Sexual Immune Dimorphism and Priming in Adult Aedes aegypti Mosquitoes. *PLoS One* **10**, e0133240.
174. **Moret, Y. and Schmid-Hempel, P.** (2000). Survival for immunity: the price of immune system activation for bumblebee workers. *Science* **290**, 1166-8.
175. **Moret, Y. and Schmid-Hempel, P.** (2009). Immune responses of bumblebee workers as a function of individual and colony age: senescence versus plastic adjustment of the immune function. *Oikos* **118**, 371-378.
176. **Mourya, D. T., Yadav, P. and Mishra, A. C.** (2004). Effect of temperature stress on immature stages and susceptibility of Aedes aegypti mosquitoes to chikungunya virus. *Am J Trop Med Hyg* **70**, 346-50.
177. **Musselman, L. P., Fink, J. L., Narzinski, K., Ramachandran, P. V., Hathiramani, S. S., Cagan, R. L. and Baranski, T. J.** (2011). A high-sugar diet produces obesity and insulin resistance in wild-type Drosophila. *Dis Model Mech* **4**, 842-9.
178. **Muturi, E. J.** (2013). Larval rearing temperature influences the effect of malathion on Aedes aegypti life history traits and immune responses. *Chemosphere* **92**, 1111-6.
179. **Muturi, E. J., Kim, C. H., Alto, B. W., Berenbaum, M. R. and Schuler, M. A.** (2011). Larval environmental stress alters Aedes aegypti competence for Sindbis virus. *Trop Med Int Health* **16**, 955-64.
180. **Márkus, R., Laurinyecz, B., Kurucz, E., Honti, V., Bajusz, I., Sipos, B., Somogyi, K., Kronhamn, J., Hultmark, D. and Andó, I.** (2009). Sessile hemocytes as a hematopoietic compartment in *Drosophila melanogaster*. *Proc Natl Acad Sci U S A* **106**, 4805-9.
181. **Müller, H. M., Dimopoulos, G., Blass, C. and Kafatos, F. C.** (1999). A hemocyte-like cell line established from the malaria vector Anopheles gambiae expresses six prophenoloxidase genes. *J Biol Chem* **274**, 11727-35.
182. **Narita, R., Yamashita, H., Goto, A., Imai, H., Ichihara, S., Mori, H. and Kitagawa, Y.** (2004). Syndecan-dependent binding of *Drosophila* hemocytes to laminin alpha3/5 chain LG4-5 modules: potential role in sessile hemocyte islets formation. *FEBS Lett* **576**, 127-32.

183. **Nation, J. L.** (2008). Circulatory system. In *Insect Physiology and biochemistry*, pp. 339-365. Boca Raton: CRC Press.
184. **Neira Oviedo, M., Ribeiro, J. M. C., Heyland, A., VanEkeris, L., Moroz, T. and Linser, P. J.** (2009). The salivary transcriptome of Anopheles gambiae (Diptera: Culicidae) larvae: A microarray-based analysis. *Insect Biochem Mol Biol* **39**, 382-94.
185. **Oliveira, J. H., Gonçalves, R. L., Lara, F. A., Dias, F. A., Gandara, A. C., Menna-Barreto, R. F., Edwards, M. C., Laurindo, F. R., Silva-Neto, M. A., Sorgine, M. H. et al.** (2011). Blood meal-derived heme decreases ROS levels in the midgut of Aedes aegypti and allows proliferation of intestinal microbiota. *PLoS Pathog* **7**, e1001320.
186. **Osta, M. A., Christophides, G. K. and Kafatos, F. C.** (2004). Effects of mosquito genes on Plasmodium development. *Science* **303**, 2030-2.
187. **Otieno-Ayayo, Z. N., Zaritsky, A., Wirth, M. C., Manasherob, R., Khasdan, V., Cahan, R. and Ben-Dov, E.** (2008). Variations in the mosquito larvicidal activities of toxins from *Bacillus thuringiensis* ssp. *israelensis*. *Environ Microbiol* **10**, 2191-9.
188. **Paily, K. P., Geetha, I., Kumar, B. A. and Balaraman, K.** (2012). *Bacillus sphaericus* in the adults of *Culex quinquefasciatus* mosquitoes emerged from treated larvae and its effect on development of the filarial parasite, *Wuchereria bancrofti*. *Parasitol Res* **110**, 2229-35.
189. **Patterson, G. M.** (2016). Looking Backward, Looking Forward: The Long, Torturous Struggle with Mosquitoes. *Insects* **7**.
190. **Pereira, M. F., Rossi, C. C., de Queiroz, M. V., Martins, G. F., Isaac, C., Bossé, J. T., Li, Y., Wren, B. W., Terra, V. S., Cuccui, J. et al.** (2015). *Galleria mellonella* is an effective model to study *Actinobacillus pleuropneumoniae* infection. *Microbiology* **161**, 387-400.
191. **Piazza, N. and Wessells, R. J.** (2011). *Drosophila* models of cardiac disease. *Prog Mol Biol Transl Sci* **100**, 155-210.
192. **Pigeault, R., Nicot, A., Gandon, S. and Rivero, A.** (2015). Mosquito age and avian malaria infection. *Malar J* **14**, 383.
193. **Pinto, S. B., Kafatos, F. C. and Michel, K.** (2008). The parasite invasion marker SRPN6 reduces sporozoite numbers in salivary glands of Anopheles gambiae. *Cell Microbiol* **10**, 891-8.
194. **Pinto, S. B., Lombardo, F., Koutsos, A. C., Waterhouse, R. M., McKay, K., An, C., Ramakrishnan, C., Kafatos, F. C. and Michel, K.** (2009). Discovery of Plasmodium modulators by genome-wide analysis of circulating hemocytes in Anopheles gambiae. *Proc Natl Acad Sci U S A* **106**, 21270-5.
195. **Pompon, J. and Levashina, E. A.** (2015). A New Role of the Mosquito Complement-like Cascade in Male Fertility in Anopheles gambiae. *PLoS Biol* **13**, e1002255.
196. **Pondeville, E., Maria, A., Jacques, J. C., Bourgouin, C. and Dauphin-Villemant, C.** (2008). Anopheles gambiae males produce and transfer the vitellogenic steroid hormone 20-hydroxyecdysone to females during mating. *Proc Natl Acad Sci U S A* **105**, 19631-6.
197. **Prasai, K. and Karlsson, B.** (2012). Variation in immune defence in relation to age in the green-veined white butterfly (Pieris napi L.). *J Invertebr Pathol* **111**, 252-4.

198. **Ramirez, J. L., de Almeida Oliveira, G., Calvo, E., Dalli, J., Colas, R. A., Serhan, C. N., Ribeiro, J. M. and Barillas-Mury, C.** (2015). A mosquito lipoxin/lipocalin complex mediates innate immune priming in Anopheles gambiae. *Nat Commun* **6**, 7403.
199. **Ramirez, J. L. and Dimopoulos, G.** (2010). The Toll immune signaling pathway control conserved anti-dengue defenses across diverse Ae. aegypti strains and against multiple dengue virus serotypes. *Dev Comp Immunol* **34**, 625-9.
200. **Ramirez, J. L., Garver, L. S. and Dimopoulos, G.** (2009). Challenges and approaches for mosquito targeted malaria control. *Curr Mol Med* **9**, 116-30.
201. **Rani, A., Sharma, A., Rajagopal, R., Adak, T. and Bhatnagar, R. K.** (2009). Bacterial diversity analysis of larvae and adult midgut microflora using culture-dependent and culture-independent methods in lab-reared and field-collected Anopheles stephensi-an Asian malarial vector. *BMC Microbiol* **9**, 96.
202. **Rao, A., Henderson, R. E. and Bradleigh Vinson, S.** (2009). The probable significance of tracheal tufts in the 8th abdominal segment of *Heliothis virescens* (F.) on the development of its parasitoid, *Toxoneuron nigriceps* (Viereck). *J Insect Physiol* **55**, 769-73.
203. **Raschke, E. W.** (1887). Die Larve von *Cluex nemorosus*. *Zool. Anz.* **10**, 18.
204. **Richman, A. M., Bulet, P., Hetru, C., Barillas-Mury, C., Hoffmann, J. A. and Kafalos, F. C.** (1996). Inducible immune factors of the vector mosquito Anopheles gambiae: biochemical purification of a defensin antibacterial peptide and molecular cloning of preprodefensin cDNA. *Insect Mol Biol* **5**, 203-10.
205. **Rodrigues, J., Brayner, F. A., Alves, L. C., Dixit, R. and Barillas-Mury, C.** (2010). Hemocyte differentiation mediates innate immune memory in Anopheles gambiae mosquitoes. *Science* **329**, 1353-5.
206. **Rolff, J.** (2001). Effects of age and gender on immune function of dragonflies (Odonta, Lestidae) from a wild population. *Canadian Journal of Zoology* **79**, 2176-2180.
207. **Romoser, W. S., Wasieloski, L. P., Pushko, P., Kondig, J. P., Lerdthusnee, K., Neira, M. and Ludwig, G. V.** (2004). Evidence for arbovirus dissemination conduits from the mosquito (Diptera: Culicidae) midgut. *J Med Entomol* **41**, 467-75.
208. **Rono, M. K., Whitten, M. M., Oulad-Abdelghani, M., Levashina, E. A. and Marois, E.** (2010). The major yolk protein vitellogenin interferes with the anti-plasmodium response in the malaria mosquito Anopheles gambiae. *PLoS Biol* **8**, e1000434.
209. **Ryazanova, A. D., Alekseev, A. A. and Slepneva, I. A.** (2012). The phenylthiourea is a competitive inhibitor of the enzymatic oxidation of DOPA by phenoloxidase. *J Enzyme Inhib Med Chem* **27**, 78-83.
210. **Schmid, M. R., Brockmann, A., Pirk, C. W., Stanley, D. W. and Tautz, J.** (2008). Adult honeybees (Apis mellifera L.) abandon hemocytic, but not phenoloxidase-based immunity. *J Insect Physiol* **54**, 439-44.
211. **Schmid-Hempel, P.** (2005). Evolutionary ecology of insect immune defenses. *Annu Rev Entomol* **50**, 529-51.
212. **Schneider, C. A., Rasband, W. S. and Eliceiri, K. W.** (2012). NIH Image to ImageJ: 25 years of image analysis. *Nat Methods* **9**, 671-5.

213. **Schnitger, A. K., Kafatos, F. C. and Osta, M. A.** (2007). The melanization reaction is not required for survival of *Anopheles gambiae* mosquitoes after bacterial infections. *J Biol Chem* **282**, 21884-8.
214. **Schnitger, A. K., Yassine, H., Kafatos, F. C. and Osta, M. A.** (2009). Two C-type lectins cooperate to defend Anopheles gambiae against Gram-negative bacteria. *J Biol Chem* **284**, 17616-24.
215. **Scholte, E.-J., Knols, B. G. J., Samson, R. A. and Takken, W.** (2004). Entomopathogenic fungi for mosquito control: A review. *Journal of Insect Science* **4**.
216. **Schwartz, A. and Koella, J. C.** (2002). Melanization of plasmodium falciparum and C-25 sephadex beads by field-caught Anopheles gambiae (Diptera: Culicidae) from southern Tanzania. *J Med Entomol* **39**, 84-8.
217. **Severo, M. S. and Levashina, E. A.** (2014). Mosquito defenses against Plasmodium parasites. *Current Opinion in Insect Science* **3**, 30-36.
218. **Shin, S. W., Kokoza, V., Bian, G., Cheon, H. M., Kim, Y. J. and Raikhel, A. S.** (2005). REL1, a homologue of Drosophila dorsal, regulates toll antifungal immune pathway in the female mosquito Aedes aegypti. *J Biol Chem* **280**, 16499-507.
219. **Shiratsuchi, A., Mori, T., Sakurai, K., Nagaosa, K., Sekimizu, K., Lee, B. L. and Nakanishi, Y.** (2012). Independent recognition of *Staphylococcus aureus* by two receptors for phagocytosis in *Drosophila*. *J Biol Chem* **287**, 21663-72.
220. **Shrestha, R. and Gateff, E.** (1982a). Ultrastructure and Cytochemistry of the Cell Types in the Larval Hematopoietic Organs and Hemolymph of Drosophila Melanogaster. In *Development, Growth & Differentiation*, vol. 24, pp. 65-82.
221. **Shrestha, R. and Gateff, E.** (1982b). Ultrastructure and Cytochemistry of the Cell Types in the Larval Hematopoietic Organs and Hemolymph of *Drosophila Melanogaster*. In *Development, Growth & Differentiation*, vol. 24, pp. 65-82.
222. **Sidjanski, S., Mathews, G. V. and Vanderberg, J. P.** (1997). Electrophoretic separation and identification of phenoloxidases in hemolymph and midgut of adult Anopheles stephensi mosquitoes. *J Parasitol* **83**, 686-91.
223. **Sieglaff, D. H., Duncan, K. A. and Brown, M. R.** (2005). Expression of genes encoding proteins involved in ecdysteroidogenesis in the female mosquito, Aedes aegypti. *Insect Biochem Mol Biol* **35**, 471-90.
224. **Sigle, L. T. and Hillyer, J. F.** (2016). Mosquito hemocytes preferentially aggregate and phagocytose pathogens in the periostial regions of the heart that experience the most hemolymph flow. *Dev Comp Immunol* **55**, 90-101.
225. **Sim, S., Jupatanakul, N. and Dimopoulos, G.** (2014). Mosquito immunity against arboviruses. *Viruses* **6**, 4479-504.
226. **Sláma, K. and Farkas, R.** (2005). Heartbeat patterns during the postembryonic development of *Drosophila melanogaster*. *J Insect Physiol* **51**, 489-503.
227. **Smits, A. W., Burggren, W. W. and Oliveras, D.** (2000). Developmental changes in *in vivo* cardiac performance in the moth *Manduca sexta*. *J Exp Biol* **203**, 369-78.
228. **Souza-Neto, J. A., Sim, S. and Dimopoulos, G.** (2009). An evolutionary conserved function of the JAK-STAT pathway in anti-dengue defense. *Proc Natl Acad Sci U S A* **106**, 17841-6.

229. **Stoehr, A. M.** (2007). Inter- and intra-sexual variation in immune defence in the cabbage white butterfly, *Pieris rapae* L. (Lepidoptera: Pieridae). *Ecological Entomology* **32**, 188-193.
230. **Stofanko, M., Kwon, S. Y. and Badenhorst, P.** (2008). A misexpression screen to identify regulators of *Drosophila* larval hemocyte development. *Genetics* **180**, 253-67.
231. **Stone, E. F., Fulton, B. O., Ayres, J. S., Pham, L. N., Ziauddin, J. and Shirasu-Hiza, M. M.** (2012). The circadian clock protein timeless regulates phagocytosis of bacteria in *Drosophila*. *PLoS Pathog* **8**, e1002445.
232. **Strand, M. R.** (2008). The insect cellular immune response. In *Insect Science*, vol. 15, pp. 1-14.
233. **Suwanchaichinda, C. and Kanost, M. R.** (2009). The serpin gene family in Anopheles gambiae. *Gene* **442**, 47-54.
234. **Telang, A., Qayum, A. A., Parker, A., Sacchetta, B. R. and Byrnes, G. R.** (2012). Larval nutritional stress affects vector immune traits in adult yellow fever mosquito Aedes aegypti (Stegomyia aegypti). *Med Vet Entomol* **26**, 271-81.
235. **Tepass, U., Fessler, L. I., Aziz, A. and Hartenstein, V.** (1994). Embryonic origin of hemocytes and their relationship to cell death in *Drosophila*. *Development* **120**, 1829-37.
236. **Thomas, A. M. and Rudolf, V. H. W.** (2010). Challenges of metamorphosis in invertebrate hosts: maintaining parasite resistance across life-history stages. *Ecological Entomology* **35**, 200-205.
237. **Thomas, P., Kenny, N., Eyles, D., Moreira, L. A., O'Neill, S. L. and Asgari, S.** (2011). Infection with the wMel and wMelPop strains of Wolbachia leads to higher levels of melanization in the hemolymph of Drosophila melanogaster, Drosophila simulans and Aedes aegypti. *Dev Comp Immunol* **35**, 360-5.
238. **Travers, L. M., Garcia-Gonzalez, F. and Simmons, L. W.** (2015). Live fast die young life history in females: evolutionary trade-off between early life mating and lifespan in female Drosophila melanogaster. *Sci Rep* **5**, 15469.
239. **Tusting, L. S., Thwing, J., Sinclair, D., Fillinger, U., Gimnig, J., Bonner, K. E., Bottomley, C. and Lindsay, S. W.** (2013). Mosquito larval source management for controlling malaria. *Cochrane Database Syst Rev* **8**, CD008923.
240. **Uchimura, K., Ai, H., Kuwasawa, K., Matsushita, T. and Kurokawa, M.** (2006). Excitatory neural control of posterograde heartbeat by the frontal ganglion in the last instar larva of a lepidopteran, Bombyx mori. *J Comp Physiol A Neuroethol Sens Neural Behav Physiol* **192**, 175-85.
241. **Ursic Bedoya, R. J., Mitzey, A. M., Obraztsova, M. and Lowenberger, C.** (2005). Molecular cloning and transcriptional activation of lysozyme-encoding cDNAs in the mosquito Aedes aegypti. *Insect Mol Biol* **14**, 89-94.
242. **Vaney, C.** (1902). Contributions à l'étude des Larves et des metamorphoses des Diptères. *Ann. de l'Univ. de Lyon* **1**, 138.
243. **Vizioli, J., Bulet, P., Charlet, M., Lowenberger, C., Blass, C., Müller, H. M., Dimopoulos, G., Hoffmann, J., Kafatos, F. C. and Richman, A.** (2000). Cloning and analysis of a cecropin gene from the malaria vector mosquito, Anopheles gambiae. *Insect Mol Biol* **9**, 75-84.

244. **Vizioli, J., Bulet, P., Hoffmann, J. A., Kafatos, F. C., Müller, H. M. and Dimopoulos, G.** (2001a). Gambicin: a novel immune responsive antimicrobial peptide from the malaria vector Anopheles gambiae. *Proc Natl Acad Sci U S A* **98**, 12630-5.

245. **Vizioli, J., Richman, A. M., Uttenweiler-Joseph, S., Blass, C. and Bulet, P.** (2001b). The defensin peptide of the malaria vector mosquito Anopheles gambiae: antimicrobial activities and expression in adult mosquitoes. *Insect Biochem Mol Biol* **31**, 241-8.

246. **Volz, J., Osta, M. A., Kafatos, F. C. and Müller, H. M.** (2005). The roles of two clip domain serine proteases in innate immune responses of the malaria vector Anopheles gambiae. *J Biol Chem* **280**, 40161-8.

247. **Wang, Y., Gilbreath, T. M., Kukutla, P., Yan, G. and Xu, J.** (2011a). Dynamic gut microbiome across life history of the malaria mosquito Anopheles gambiae in Kenya. *PLoS One* **6**, e24767.

248. **Wang, Z., Lu, A., Li, X., Shao, Q., Beerntsen, B. T., Liu, C., Ma, Y., Huang, Y., Zhu, H. and Ling, E.** (2011b). A systematic study on hemocyte identification and plasma prophenoloxidase from Culex pipiens quinquefasciatus at different developmental stages. *Exp Parasitol* **127**, 135-41.

249. **Warr, E., Das, S., Dong, Y. and Dimopoulos, G.** (2008). The Gram-negative bacteria-binding protein gene family: its role in the innate immune system of anopheles gambiae and in anti-Plasmodium defence. *Insect Mol Biol* **17**, 39-51.

250. **Wasserthal, L. T.** (1980). Oscillating haemolymph 'circulation' in the butterfly *Papilio machaon* L. revealed by contact thermography and photocell measurements. *Journal of Comparative Physiology* **139**, 145-163.

251. **Wasserthal, L. T.** (1981). Oscillating haemolymph 'circulation' and discontinuous tracheal ventilation in the giant silk moth *Attacus atlas* L. *Journal of comparative physiology* **145**, 1-15.

252. **Wasserthal, L. T.** (1999). Functional morphology of the heart and of a new cephalic pulsatile organ in the blowfly *Calliphora vicina* (Diptera: Calliphoridae) and their roles in hemolymph transport and tracheal ventilation. *International Journal of Insect Morphology and Embryology* **28**, 111-129.

253. **Wasserthal, L. T.** (2003). Circulation and thermoregulation. In *Lepidoptera, Moths and Butterflies: Morphology, Physiology, and Development*, vol. 2 (ed. N. Kristensen), pp. 205-228. New York: Walter De Gruyter.

254. **Wasserthal, L. T.** (2007). *Drosophila* flies combine periodic heartbeat reversal with a circulation in the anterior body mediated by a newly discovered anterior pair of ostial valves and 'venous' channels. *J Exp Biol* **210**, 3707-19.

255. **Wasserthal, L. T.** (2012). Influence of periodic heartbeat reversal and abdominal movements on hemocoelic and tracheal pressure in resting blowflies *Calliphora vicina*. *J Exp Biol* **215**, 362-73.

256. **Welman, A., Serrels, A., Brunton, V. G., Ditzel, M. and Frame, M. C.** (2010). Two-color photoactivatable probe for selective tracking of proteins and cells. *J Biol Chem* **285**, 11607-16.

257. **Whitten, M. M., Shiao, S. H. and Levashina, E. A.** (2006). Mosquito midguts and malaria: cell biology, compartmentalization and immunology. *Parasite Immunol* **28**, 121-30.

258. **Wigglesworth, V. B.** (1949). The physiology of mosquitoes. Philadelphia and London: Saunders.
259. **Wilson-Rich, N., Dres, S. T. and Starks, P. T.** (2008). The ontogeny of immunity: development of innate immune strength in the honey bee (Apis mellifera). *J Insect Physiol* **54**, 1392-9.
260. **Xi, Z., Ramirez, J. L. and Dimopoulos, G.** (2008). The Aedes aegypti toll pathway controls dengue virus infection. *PLoS Pathog* **4**, e1000098.
261. **Yadav, P., Barde, P. V., Gokhale, M. D., Vipat, V., Mishra, A. C., Pal, J. K. and Mourya, D. T.** (2005). Effect of temperature and insecticide stresses on Aedes aegypti larvae and their influence on the susceptibility of mosquitoes to dengue-2 virus. *Southeast Asian J Trop Med Public Health* **36**, 1139-44.
262. **Yan, G., Christensen, B. M. and Severson, D. W.** (1997). Comparisons of genetic variability and genome structure among mosquito strains selected for refractoriness to a malaria parasite. *J Hered* **88**, 187-94.
263. **Yassine, H., Kamareddine, L., Chamat, S., Christophides, G. K. and Osta, M. A.** (2014). A serine protease homolog negatively regulates TEP1 consumption in systemic infections of the malaria vector *Anopheles gambiae*. *J Innate Immun* **6**, 806-18.
264. **Yassine, H., Kamareddine, L. and Osta, M. A.** (2012). The mosquito melanization response is implicated in defense against the entomopathogenic fungus *Beauveria bassiana*. *PLoS Pathog* **8**, e1003029.
265. **Yassine, H. and Osta, M. A.** (2010). Anopheles gambiae innate immunity. *Cell Microbiol* **12**, 1-9.
266. **Zachary, D. and Hoffmann, J. A.** (1973). The haemocytes of *Calliphora erythrocephala* (Meig.) (Diptera). *Z Zellforsch Mikrosk Anat* **141**, 55-73.
267. **Zettervall, C. J., Anderl, I., Williams, M. J., Palmer, R., Kurucz, E., Ando, I. and Hultmark, D.** (2004). A directed screen for genes involved in *Drosophila* blood cell activation. *Proc Natl Acad Sci U S A* **101**, 14192-7.

Appendix A

Gene Names, VectorBase Gene IDs, and Primers Used for Quantitative RT-PCR

Protein	Gene	VectorBase ID *	Assembly	Forward primer (5'→3')	Reverse primer (5'→3')	Amplicon (bp)	
						Transcript	Genomic
Pathogen recognition							
C-type lectin 4	*CTL4*	AGAP005335	AgamP4	TACCCAAAACCTGTGCGTTT	CTTTTCTGCGATCGTGTCAG	207	273
Fibrinogen-related protein 13	*FREP13*	AGAP011197	AgamP3	TTGTGATGAAGGAGCACAGC	GTGGTTGGAGCAGATGGTTT	176	176
Gram (-) binding pr. 4	*GNBPB4*	AGAP002796	AgamP3	TCAAGGACGGCATCTTCTTC	TCGGGTTGAGGTAGTTCGTT	174	250
Thioester-containing protein 1	*TEP1*	AGAP010815	AgamP4	GACGTCCAAATACGGATCTCA	CTTTCAGGCATCACCCGTAT	184	0
Eater	*Eater*	AGAP012386	AgamP3	TGGAGTCGACGAGAGGTTTC	TCGGTACGCATAAACCATCA	124	199
Nimrod	*Nimrod*	AGAP009762	AgamP3	AACGAAGGGACACATTCCTG	CCGACTGAGAGATGGATTGG	121	179
Draper	*Draper*	AGAP007256	AgamP3	GTGACGAGCGTATGACGAAC	GCCGGTAGTACAGCAGCATT	132	1862
Croquemort	*SCRBQ2*	AGAP010133	AgamP3	AGGACGTGGCATTTTGTACC	TGGTTTGTTTTTCCACAGCA	177	281
Signal modulation							
CLIPB 15	*CLIPB15*	AGAP009844	AgamP3	CCGAACGATATCTGCATCCT	GCTCCACGTGCTTCTGTGTA	184	274
Serpin 6	*SRPN6*	AGAP009212	AgamP3	AGCGTATGCATCAGCGGTAT	TGGGCAGATCCTTCTGGTAG	195	279
Signal Transduction							
MyD88	*MYD88*	AGAP005252	AgamP4	ACCGCTGGTGTCTACCAATC	TTGCTCCCGCAGTAGAAACT	196	269
Cactus	*CACTUS*	AGAP007938	AgamP4	GGATGATTCCAGACGAGGAG	TCAGAAACTGCTGTGGAACG	204	318
Caspl1	*CASPL1*	AGAP011693	AgamP4	TGCTAGAAGCGCTGACCATA	GGGGCAAAAGTAGTCGATTG	217	217
Caspar	*CASPAR*	AGAP006473	AgamP4	CCGATCATCAATCAGCAGAA	GTGCAGATAGATCGCCAACA	204	647
Stat-A	*AGSTAT-A*	AGAP010423	AgamP4	CCTTGGAACAGGAAGAGCTG	ACGACCTACCCGTGCACTAA	218	218
Pias	*PIAS*	AGAP005031	AgamP4	ATCGACGTGCTCCCATCTAC	CCAGGAACCATCTTTGTGGA	205	294
Immune effectors							
Cecropin A	*CECA*	AGAP000693	AgamP3	GCTGAAGAAGCTGGGAAAGA	ATGTTAGCAGAGCCGTCGTC	158	247
Gambicin 1	*GAM1*	AGAP008645	AgamP3	TGCGAGATGTAAAAGCATCG	CAGCAGAGCTCCACTCAGAA	174	273
Defensin 1	*DEF1*	AGAP011294	AgamP3	GCAACGATCGTCTGTACCATT	GCTTGGCCCGATAGTTCTC	175	275
Phenoloxidase 1	*PPO1*	AGAP002825	AgamP4	CACCATCATGATCGAGAACG	GGAATTGTGACGGTGGATTC	207	296
Phenoloxidase 6	*PPO6*	AGAP004977	AgamP3	AGAGCCACTACCGGAAGGAT	TCGATGCTCTCAGCAATACG	174	242
Lysozyme C1	*LYSC1*	AGAP007347	AgamP3	ACGGCATCTTCCAGATCAAC	CATTGCAGTGGTTCTTCCAG	180	259
Nitric oxide synthase	*NOS*	AGAP008255	AgamP3	CAAGAGTGGGACCACATCAA	ACCCTTCTGGACCATCTCCT	129	210
Dual oxidase	*DUOX*	AGAP009978	AgamP3	TTTACCGGGCTAAAAGCAGT	ATTTGCGGCTCTTGTTCACT	175	251
Ecdysteroid biosynthesis							
CYP302A1	*CYP302A1*	AGAP005992	AgamP4	CATCCTGCCCACCGACCA	CCAAACGGAAGCACCAGGT	201	270
CYP315A1	*CYP315A1*	AGAP000284	AgamP4	CGAAGCGGAGTGCGTTGTT	CGTCTGTGCGTTTGCTATTC	202	274
Ribosomal genes							
Ribosomal pr. 17	*RPS17*	AGAP004887	AgamP3	GACGAAACCACTGCGTAACA	TGCTCCAGTGCTGAAACATC	153	264
Ribosomal pr. 7	*RPS7*	AGAP010592	AgamP3	GACGGATCCCAGCTGATAAA	GTTCTCTGGGAATTCGAACG	132	281

* VectorBase PEST strain genomic sequence (www.vectorbase.org)

Appendix B

Relative mRNA Expression Levels of Individual Immunity Genes

The following are graphs of the relative induction of individual immunity genes in naïve, injured, and *E. coli*-infected larvae, 1-day-old adults, and 5-day-old adults assayed in the qPCR analysis presented in Figure 11 of Chapter IV. Graphs show the average relative mRNA fold change of pathogen recognition (A), signal transduction (B), signal modulation (C), immune effector (D), ecdysteroid biosynthesis (E) and ribosomal (F) genes relative to the naïve group of a given life stage or adult age. Whiskers denote the SEM. Asterisks denote the significant regulation of mRNA levels relative to the naïve group as determined by the Kruskal-Wallis test, followed by Dunn's *post hoc* test (*, $P<0.05$; **, $P<0.01$; ***, $P<0.001$; ****, $P<0.0001$).

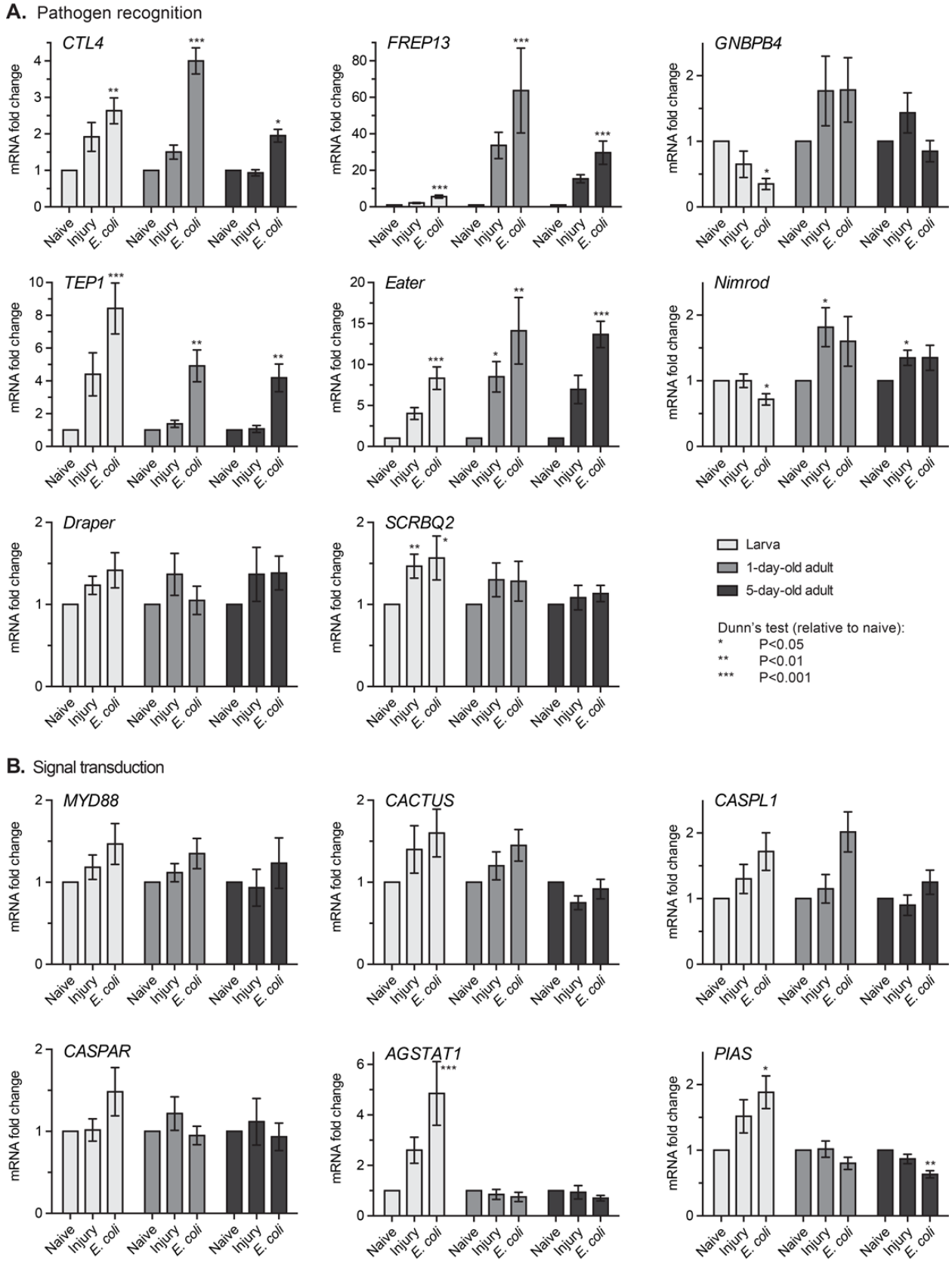
A. Pathogen recognition
CTL4
FREP13
GNBPB4
TEP1
Eater
Nimrod
Draper
SCRBQ2
mRNA fold change
Naive
Injury
E. coli
Larva
1-day-old adult
5-day-old adult
Dunn's test (relative to naive):
* P<0.05
** P<0.01
*** P<0.001
B. Signal transduction
MYD88
CACTUS
CASPL1
CASPAR
AGSTAT1
PIAS

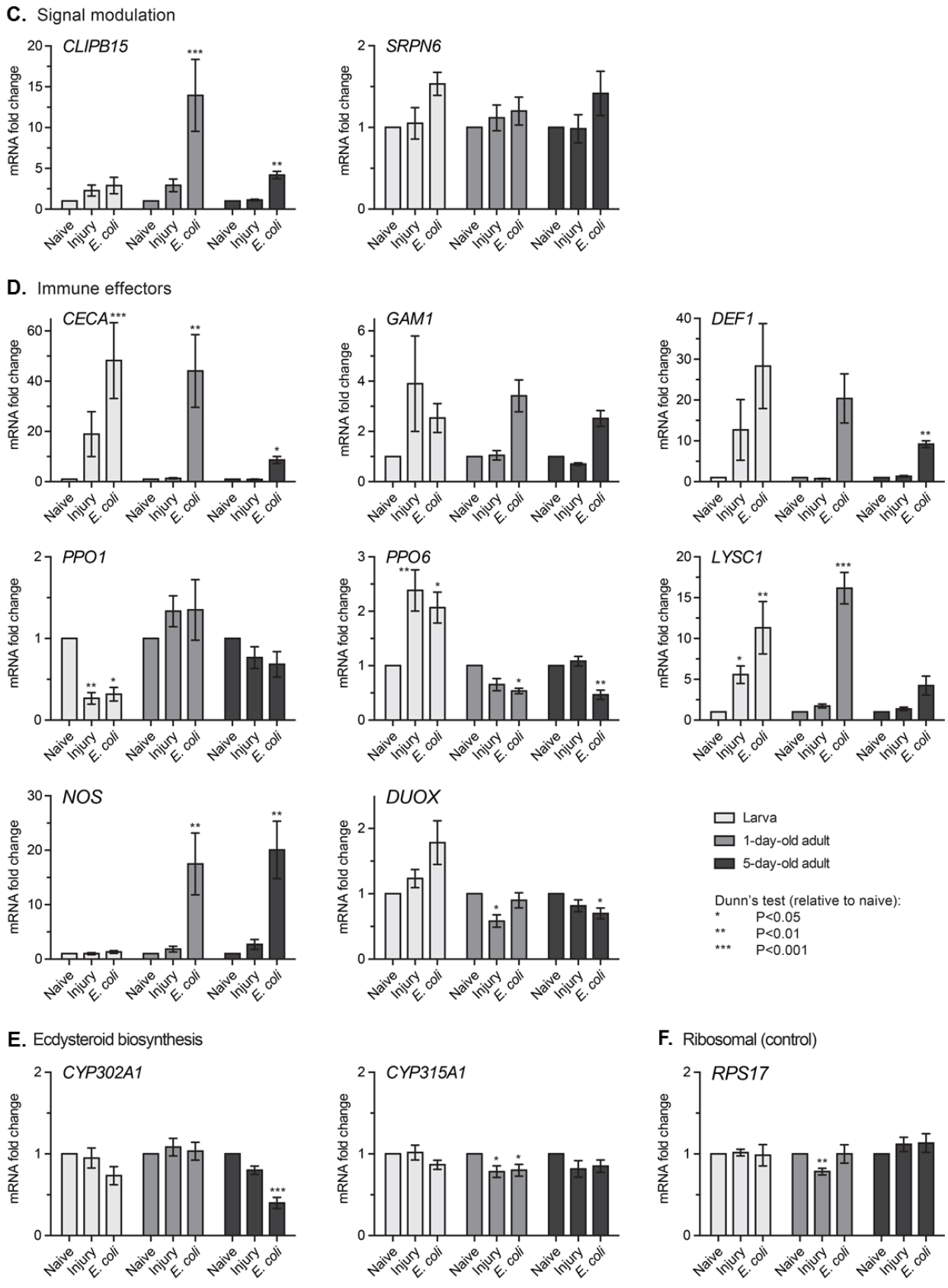
C. Signal modulation
CLIPB15
SRPN6
D. Immune effectors
CECA
GAM1
DEF1
PPO1
PPO6
LYSC1
NOS
DUOX
mRNA fold change
Naive
Injury
E. coli
Larva
1-day-old adult
5-day-old adult
Dunn's test (relative to naive):
* P<0.05
** P<0.01
*** P<0.001
E. Ecdysteroid biosynthesis
CYP302A1
CYP315A1
F. Ribosomal (control)
RPS17